The contribution of the reaction catalyzed by succinyl-CoA ligase to substrate-level phosphorylation

PhD Thesis

Gergely Kacsó

Semmelweis University
János Szentágothai Doctoral School of Neurosciences
Functional Neurosciences Program

Supervisor: Christos Chinopoulos, Ph.D

Official reviewers: Ferenc Gallyas Jr, D.Sc,
                             Tamás Kardon, PhD

Chairman of the final examination board: József Mandl D.Sc

Members of the final examination board: Erzsébet Ligeti, D.Sc.
                                           Olivér Ozohanics, Ph.D.,

Budapest
2018

TABLE OF CONTENTS

1. THE LIST OF ABBREVIATIONS

AcAc: acetoacetate

AcAc-CoA: acetoacetyl-coenzyme A

ADP: adenosine diphosphate

ALA: aminolaevulinic acid

ALAS: aminolaevulinic acid synthase

ANT: adenine nucleotide translocase

ATP: adenosine triphosphate

BAEP: brain auditory evoked potential

BCA: bicinchoninic acid

bp: base pair

BSA: bovine serum albumin

C: Coulomb

C10:   decanoyl carnitine

C10:1:   decenoyl carnitine

C12:   dodecanoyl carnitine (see also C6-1DS)

C14:   myristoyl carnitine

C14:1:   tetradecenoyl carnitine

C16:   palmitoyl carnitine

C16-OH: 3-hydroxyhexadecenoyl carnitine

C18:   stearoyl carnitine

C18:1:   oleyl carnitine

C18-OH: 3-hydroxystearoyl carnitine

C2:   acetyl carnitine

C3:   propionyl carnitine

C3-DC: malonyl carnitine

C4:   butyryl/isobutyryl carnitine

C4-DC: methylmalonyl/succinyl carnitine

C4-OH: 3-hydroxybutyryl carnitine

C5:   isovaleryl/2-methylbutyryl/pivaloyl carnitine

C5-DC: glutaryl carnitine

C5-OH: 3-hydroxy isovaleryl/2-methyl 3-hydroxybutyryl carnitine

C6-1DS:	dodecanoyl carnitine (see also C12)
cATR:	carboxyatractyloside
CoASH:	coenzyme A
complex I:	nicotinamide adenine dinucleotide-ubiquinone oxidoreductase
complex II:	succinate dehydrogenase
complex III:	ubiquinone-cytochrome c oxidoreductase
complex IV:	cytochrome c oxidase (also known as COX)
CoQ:	coenzyme Q, coenzyme Q10, ubiquinone, ubidecarenone,
COX:	cytochrome c oxidase (also known as complex IV)
Cox1:	cytochrome c oxidase subunit 1
CS:	citrate synthase
CSF:	cerebrospinal fluid
CT:	computed tomography
DCPIP:	dichlorophenolindophenol
dhz:	double heterozygote
DLD:	dihydrolipoyl dehydrogenase
DLST:	dihydrolipoyl succinyltrasferase
DNA:	deoxyribonucleic acid
DTNB:	5,5′-Dithiobis(2-nitrobenzoic acid)
EEG:	electroencephalogram
EGTA:	ethylene glycol-bis(2-aminoethyleter)-N,N,N',N'-tetraacetic acid
EMG:	electromyogram
E_{rev_ATPase}:	reversal potential of the adenine nucleotide translocase
E_{rev_ATPase}:	reversal potential of the F_oF_1-ATP synthase
ES cells:	embryonic stem cells
ETC:	electron transfer chain
F:	Faraday constant = $9.64 \cdot 10^4$ C·mol^{-1}
GABA T:	4-aminobutyrate-2-oxoglutarate transaminase
GABA:	4-aminobutyrate-2-oxoglutarate
GAD:	glutamate decarboxylase
GDH:	glutamate dehydrogenase
GDP:	guanosine diphosphate

glut:	glutamate
GSC:	glioma stem-like cells
GTP:	guanosine triphosphate
HEPES:	2-[4-(2-hydroxyethyl)piperazin-1-yl]ethanesulfonic acid
HIF-1α:	hypoxia-induced factor-1α
HVA:	homovanillic acid
Ile:	isoleucine
IMM:	inner mitochondrial membrane
Irg1:	immuneresponsive gene 1
K:	Kelvin, absolute temperature
KCN:	potassium-cyanide
K_M:	affinity constant
L-DOPA:	levodopa, L-3,4-dihydroxyphenylalanine
LED:	light-emitting diode
Lys:	lysine
mal:	malate
MCM:	methylmalonyl-coenzyme A mutase
MDC score:	mitochondrial disease criteria score
MDS:	mitochondrial deoxyribonucleic acid depletion syndrome
Met:	methionine
MMA:	methylmalonyl acid
MRI:	magnetic resonance imaging
mRNA:	messenger ribonucleic acid
MS/MS:	tandem mass spectrometry
mtDNA:	mitochondrial deoxyribonucleic acid
n:	coupling ratio
NAD^+:	nicotinamide adenine dinucleotide (oxidized form)
NADH:	nicotinamide adenine dinucleotide (reduced form)
OXCT1:	3-oxoacid CoA-transferase 1 (also known as SCOT)
PCR:	polymerase chain reaction
PDH:	pyruvate dehydrogenase
PEP:	phosphoenolpyruvate

PEPCK:	phosphoenolpyruvate-carboxykinase
PHD:	prolyl hydroxylase
P_i:	inorganic phosphate
PK:	pyruvate kinase
pmf:	protonmotive force/electrochemical gradient
pyr:	pyruvate
qPCR:	quantitative polymerase chain reaction
R:	universal gas constant = 8.31 $J \cdot mol^{-1} \cdot K^{-1}$
RC complex:	respiratory chain complex
RNA:	ribonucleic acid
ROS:	reactive oxygen species
rot:	rotenone
RPM:	revolutions per minute
RT-PCR:	reverse transcription polymerase chain reaction
SCOT:	succinyl-CoA:3-oxoacid-CoA transferase (also known as OXCT1)
SD:	standard deviation
SDH:	succinate dehydrogenase
SDS PAGE:	sodium dodecyl sulfate polyacrylamide gel electrophoresis
SEM:	standard error of the mean
SIDS:	sudden infant death syndrome
SSA:	succinate-semialdehyde
SSADH:	succinate-semialdehyde dehydrogenase
St2:	state 2 respiration
St3:	state 3 respiration
SUCL:	succinyl-coenzyme A ligase enzyme
SUCLA2:	human – gene, coding ATP-forming succinyl-CoA ligase β subunit
SUCLA2:	human – ATP-forming succinyl-CoA ligase β subunit
Sucla2:	mouse – gene, coding ATP-forming succinyl-CoA ligase β subunit
Sucla2:	mouse – ATP-forming succinyl-CoA ligase β subunit
SUCLG1:	human – gene, coding succinyl-CoA ligase invariant α subunit
SUCLG1:	human – succinyl-CoA ligase invariant α subunit
Suclg1:	mouse – gene, coding succinyl-CoA ligase invariant α subunit

Suclg1:	mouse – succinyl-CoA ligase invariant α subunit
SUCLG2:	human – gene, coding GTP-forming succinyl-CoA ligase β subunit
SUCLG2:	human – GTP-forming succinyl-CoA ligase β subunit
Suclg2:	mouse – gene, coding GTP-forming succinyl-CoA ligase β subunit
Suclg2:	mouse – GTP-forming succinyl-CoA ligase β subunit
T:	absolute temperature in Kelvin
t_a:	the timepoint of anoxia
Thr:	threonine
Val:	valine
VDAC:	voltage-dependent anion channels
WT:	wild type
α-Kg:	α-ketoglutarate
βOH:	β-hydroxybutyrate
ΔG:	change in Gibbs free energy (ΔG means equilibrium)
ΔpH:	transmembrane proton concentration difference
ΔΨm:	transmembrane potential

2. INTRODUCTION

Metabolism, a controlled cellular activity, consists of several processes that converts nutrients to cell-specific molecules, builds up or degrades macromolecules and biomolecules through thousands of enzymatic reactions. In living cells, the ability to generate, store and utilize chemical energy in the most efficient way is critical.

It is a fact found in all textbooks, that the primary power source (in other terms "the powerhouse") of cells are mitochondria. But while their primary role is to provide ATP for cells, they also take part in several other processes, e.g., Ca^{2+}-, ROS homeostasis, cellular death, and thermoregulation. Several other important biochemical pathways are also found here (oxidative phosphorylation, citric acid cycle, beta oxidation, heme synthesis, etc.) [1]. Additionally, in the last few decades it has been highlighted that impaired mitochondrial function is associated with several pathological conditions, such as excitotoxicity [2], ischemia/reperfusion-, neurodegenerative diseases [3], and oxidative stress [4] [5].

Energy limiting conditions lead to dysfunction of these organelles through losing inner mitochondrial membrane impermeability and/or losing mitochondrial membrane potential ($\Delta\Psi m$). A serious dysfunction accompanied by complete depolarization can lead to cytosolic ATP pool depletion [5-8]. The consequence of decreased ATP level can be the partial or complete demolition of the primary and secondary active transports e.g., Na^+/K^+ ATPase. It is not surprising that there has to be a rescue mechanism that is able to support to maintain the cellular ATP pool in those cells, where ATP synthesis through the oxidative phosphorylation is not satisfactory. A possible rescue mechanism revealed by our laboratory is the mitochondrial substrate-level phosphorylation catalyzed by succinyl-CoA ligase and other succinyl-CoA ligase supporting enzymes (see **Chapter 2.3**).

Mitochondrial diseases are collectively considered to be a primary cause of encephalomyopathies and other multisystem maladies [9-11]. A sizeable fraction of this pool of diseases are associated with mtDNA depletion [12]. Many animal models have been generated to model mtDNA depletion by explicitly deleting genes essential for

mtDNA replication [13-20], although only one study has addressed the role of succinyl-CoA ligase [21].

2.1 Mitochondrial ATP synthesis

It is well known that mitochondria are responsible for ATP synthesis. In 1961, Peter Mitchell proposed his Chemiosmotic theory, in which the electrochemical potential difference generated by the flow of electrons through respiratory complexes and the synthesis of ATP are coupled [22]. This process, called oxidative phosphorylation, is fundamental to bioenergetics. Respiratory complex I (NADH-ubiquinone oxidoreductase, EC 1.6.5.3), complex III (ubiquinone-cytochrome c oxidoreductase, EC 1.10.2.2), and complex IV (cytochrome c oxidase, EC 1.9.3.1) act as proton pumps, translocating protons from the matrix side of the inner mitochondrial membrane (IMM) to the intermembrane space, and generating a proton motive force (pmf) across the inner membrane. The membrane potential can change in a wide scale and in the literature different values are found e.g., -180 – -220 mV in [23] or -108 mV – -158 mV in [24] (see details below). The mitochondrial proton gradient drives the ATP synthase located in the IMM.

$F_o F_1$-ATP synthase [EC 3.6.3.14] is a reversible enzyme multicomplex which can both synthetize and hydrolyze ATP [25-31]. The directionality of the enzyme is governed by *pmf* (proton motive force) [32], which consists of membrane potential ($\Delta\Psi$m) and proton concentration gradients (ΔpH) across the IMM. However, as it will be proved later, in case of sufficiently high matrix inorganic phosphate (P_i) concentration the ΔpH is subtle (<0.15) [33-35], so the directionality of the enzyme rather depends on $\Delta\Psi$m. So, the $\Delta\Psi$m value at which the enzyme shifts its operational direction is called the reversal potential (E_{rev_ATPase}) and dictated by the concentration of participants [36]. E_{rev_ATPase} can be calculated at ΔG=0 by the following equation:

$$E_{rev\_ATPase} = -\left(\frac{316}{n}\right) - \left(\frac{2.3RT}{F \cdot n}\right) \cdot log\left[\left(\frac{[ATP^{4-}]free_{in} \cdot K_{M(ADP)}}{[ADP^{3-}]free_{in} \cdot K_{M(ATP)} \cdot [P^-]_{in}}\right)\right]$$

$$-\left(\frac{2.3RT}{F}\right) \cdot (pH_{out} - pH_{in}) \ and \ [P^-]_{in} = \frac{[P_{total}]_{in}}{(1 + 10^{pH_{in} - pK_{a2}})}$$

, where in and out means inside and outside of the mitochondrial matrix respectively; R is the universal gas constant 8.31 J·mol^{-1}·K^{-1}; T is the temperature (K); F is the Faraday constant 9.64 · 10^4 C·mol^{-1}; $K_{M(ADP)}$ and $K_{M(ATP)}$ are the true affinity constants of Mg^{2+}; [P$^-$] is the free phosphate concentration in mol; pK$_{a2}$=7.2 for phosphoric acid; and n is the coupling ratio (H$^+$/ATP). The latest parameter depends on the number of the c subunits of ATP synthase [37, 38].

Adenosine phosphates can be exchanged only through adenine nucleotide translocase (ANT) and by a minor fraction through the ATP-Mg/P$_i$ carrier [39]. ANT catalyzes a reversible reaction governed by mitochondrial membrane potential (ΔΨm). The membrane potential value at which ANT reverses its operation is E$_{rev\_ANT}$ calculated as follows:

$$E_{rev\_ANT} = \frac{2.3RT}{F} \cdot log \frac{[ADP^{3-}]free\ out \cdot [ATP^{4-}]free\ in}{[ADP^{3-}]free\ in \cdot [ATP^{4-}]free\ out}$$

where in and out means inside and outside of the mitochondrial matrix, respectively; R is the universal gas constant 8.31 J·mol^{-1}·K^{-1}; T is the temperature (K); F is the Faraday constant 9.64·10^4 C·mol^{-1}. In normal conditions when oxygen and nutrients are available, and ΔΨm is more negative than E$_{rev\_ATPase}$ and E$_{rev\_ANT}$, both enzymes operate in a so called "forward mode". F$_o$F$_1$-ATPase synthetizes ATP while ANT translocates ATP out of, and ADP into the matrix. The opposite status occurs when both operate in so-called "reverse mode", when F$_o$F$_1$-ATPase hydrolases ATP while ANT translocates ATP into, and ADP out of the matrix.

Having taken into account both equations (E$_{rev\_ATPase}$ and E$_{rev\_ANT}$), it turns out to be evident that alterations in [ATP^{4-}]$_{free\ in}$ and [ADP^{3-}]$_{free\ in}$ affect the reversal potentials inversely; a decrease in intramitochondrial [ATP]/[ADP] ratio shifts E$_{rev\_ATPase}$ towards more positive, while it shifts E$_{rev\_ANT}$ towards more negative, and *vice versa*. In other words, the greater the matrix [ATP] and, the greater the force for a forward-operating ANT (ATP outward/ADP inward) is, the <u>less</u> will the ANT seek to reverse. Also, the higher the matrix [ATP] is -which is the product of the forward-operating ATP synthase-, the <u>more</u> it will seek to reverse. There are some other parameters which are also

participating in the equations and may exhibit wild fluctuations. As such, cytosolic [ATP]/[ADP] ratio [40] coupling ratio [41, 42], phosphate concentration [43] $\Delta\Psi$m, and "$\Delta\Psi$m flickering", which could be greater than 100 mV [44-46]. Based on computational estimations and following circumstantial experimental works we know that there is a transient state when the F_oF_1-ATPase is already acting as a hydrolase, while the ANT is still operating in forward mode, translocating ATP from the matrix towards cytoplasm. Computer estimations were verified by experimental results in both isolated and *in situ* mitochondria. These results are showing that E_{rev_ATPase} is always more negative than E_{rev_ANT}, implying that progressively depolarizing mitochondria will first exhibit reversal of the F_oF_1-ATP synthase, followed by the reversal of ANT. The question arises at this point: what is the source of the matrix ATP? [6, 36].

2.2 Alternative mitochondrial ATP-producing biochemical pathways

As seen in the previous chapter, the main role in ATP synthesis is played by the mitochondrial F_oF_1 ATP synthase, nevertheless, it is controlled by membrane potential and oxygen availability.

In cells, other mechanisms can also act as ATP source independently from oxidative phosphorylation, e.g., the glycolysis in the cytoplasm. According to Otto Warburg's lasting theory -the Warburg effect-, most cancer cells produce predominantly ATP by a high rate of aerobic glycolysis [47].

In the mitochondrial matrix, there are two reactions capable of producing high-energy phosphate at substrate-level:

i. The mitochondrial form of the phosphoenolpyruvate carboxykinase (PEPCK) [EC 4.1.1.32]. It catalyzes a reversible reaction:

$$oxaloacetate + GTP \leftrightarrow phosphoenolpyruvate + GDP + CO_2$$
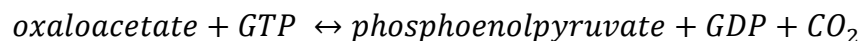
This enzyme participates in the pyruvate recycling pathway and is thought to take part in transferring phosphorylation potential from matrix to cytosol [48-50].

ii. GTP for the mitochondrial PEPCK may originate from the GTP-forming succinyl-CoA ligase [51]. It was considered earlier that the substrate-level phosphorylation catalyzed by

succinyl-CoA ligase might significantly contribute to the net ATP (or GTP) production [52].

As it was described in **Chapter 2.1,** while the F_oF_1-ATP synthase operates in reverse mode, ANT can operate in both reverse and forward modes. The reverse operation of the ANT would lead to the depletion of the cytosolic ATP pool and would further lead to cell death [5, 7, 53]. In case of the forward operation of the ANT (but a reverse operation of the F_oF_1-ATP synthase), ATP cannot originate from the cytosol. Thus, it should originate from the matrix and due to the lack of any other possible mechanism, the origin should be the succinyl-CoA ligase [6, 36, 48, 54].

2.3 Mitochondrial substrate-level phosphorylation and the SKDCC axis

As shown in **Chapter 2.1 and 2.2**, matrix substrate-level phosphorylation has a critical role in maintaining ANT operation in the forward mode, thereby preventing mitochondria from becoming cytosolic ATP consumers during respiratory arrest.

Furthermore, succinyl-CoA ligase does not require oxygen for ATP production and it is even activated during hypoxia [55]. Later, our research group showed that provision of succinyl-CoA by alfa-ketoglutarate dehydrogenase complex is essential for the maintenance of the substrate-level phosphorylation by supporting the succinyl-CoA ligase. Thus, substrate-level phosphorylation can prevent mitochondria -with a dysfunctional electron transport chain- to consume the extramitochondrial ATP pool. In order to prove this, experiments were performed in respiration-impaired isolated and *in situ* neuronal somal mitochondria from transgenic mice with a deficiency of either dihydrolipoyl succinyltransferase (E2 or DLST EC 2.3.1.61) or dihydrolipoyl dehydrogenase (E3 or DLD, EC 1.8.1.4) that exhibited 20-48% decrease in alpha-ketoglutarate dehydrogenase complex activity [56]. These results demonstrated the consumption of extramitochondrial ATP by mitochondria of $DLD^{+/-}$, $DLST^{+/-}$, or $DLD^{+/-}$/$DLST^{+/-}$ double transgenic mice provided with substrates supporting substrate-level phosphorylation (See later in **Chapter 4.4**), by clamping $\Delta\Psi m$ in a depolarized range due to targeted respiratory inhibition [56].

At this point the question arose: What provides NAD^+ for alpha-ketoglutarate dehydrogenase complex during anoxia, when complex I is not expected to oxidize NADH?

As it was shown, mitochondrial diaphorases and a finite pool of oxidizable quinones are the source of NAD^+ generated within the mitochondrial matrix during respiratory arrest caused by anoxia or poisons of the electron transport chain [57]. Using pharmacological tools, specific substrates, and by examining tissue from pigeon liver exhibiting no diaphorase activity it was shown in this work that mitochondrial diaphorases in mouse liver contribute up to 81% to the NAD^+ pool during respiratory inhibition. *In situ*, reoxidation of the reducible substrates for the diaphorases is mediated by complex III of the respiratory chain using cytochrome c and an unidentified cytosolic oxidant, i.e. possibly p66Shc [57] [58]. An extensive body of work in our laboratory on animal models has shown that substrate-level phosphorylation substantiated by succinyl-CoA ligase is part of an axis consisting of enzyme complexes termed 'SKDCC' axis. The pathway produces high-energy phosphates in the mitochondrial matrix in the absence of oxidative phosphorylation. The SKDCC axis is summarized in **Figure 1**. This rescue mechanism protects against cytosolic/nuclear ATP depletion in conditions involving impaired respiration, as it may occur in cancer.
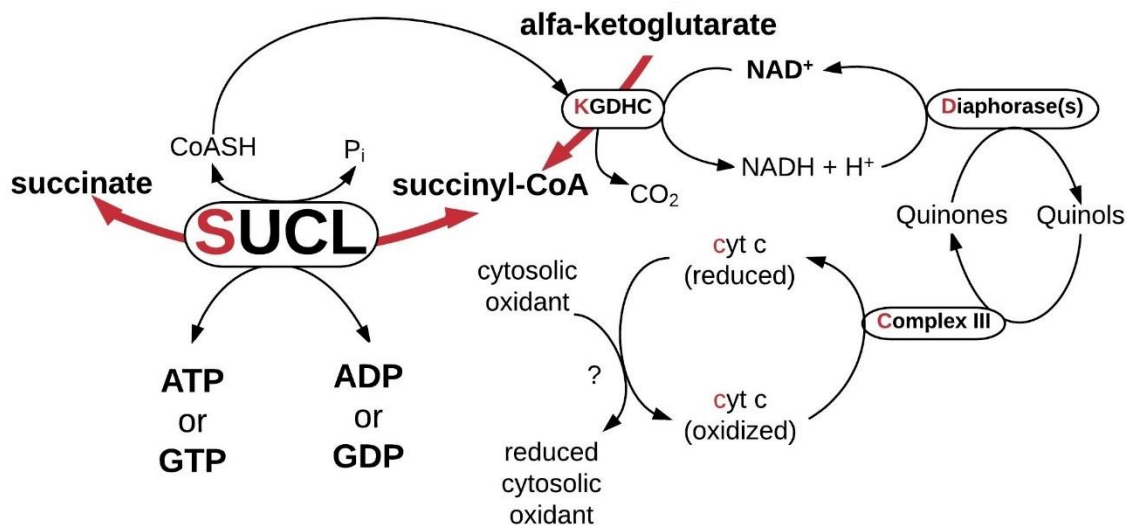
Figure 1 Illustration of the SKDCC axis
SKDCC stands for the initial letters (red) of the participant proteins: succinyl-CoA ligase, α-ketoglutarate dehydrogenase complex, diaphorases, complex III, cytochrome c. (adapted from [57]) Abbreviations: ADP: adenosine diphosphate, ATP: adenosine triphosphate, cyt c: cytochrome c, GDP: guanosine diphosphate, GTP: guanosine triphosphate, KGDHC: α-ketoglutarate dehydrogenase complex, P_i: inorganic phosphate, SUCL: succinyl-CoA ligase

2.4 Succinyl-CoA ligase

Succinyl-CoA ligase -also known as <u>succinyl coenzyme A synthetase</u> or <u>succinate thiokinase</u>- is a heterodimer enzyme incorporating the same α-subunit, but different β-subunits. The combination of the invariant α-subunit encoded by *SUCLG1* and the substrate-specific β-subunits encoded by *SUCLA2* and *SUCLG2* result in either ATP-forming (EC 6.2.1.5) or GTP-forming (EC 6.2.1.4) enzyme respectively (see **Figure 2.**) [59].
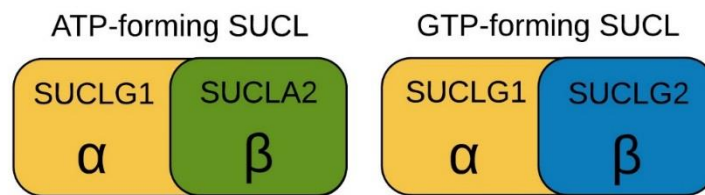
Figure 2 Different succinyl-CoA ligase enzyme compositions
Succinyl-CoA ligase is a heterodimer enzyme composed of invariant α-subunit encoded by *SUCLG1,* and substrate specific β-subunits encoded by *SUCLA2* and *SUCLG2* forming ATP and GTP, respectively.

ΔG is ~0.05 kJ/mol [60], therefore the reaction is reversible. Succinyl-CoA ligase is located in the mitochondrial matrix catalyzing the following reaction:

$$succinyl - CoA + P_i + ADP(or\ GDP) \leftrightarrow succinate + CoASH + ATP(or\ GTP)$$
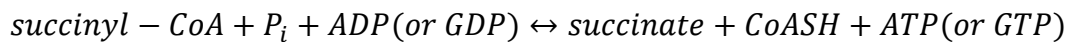
[61].

The catalytic mechanism of succinyl-CoA ligase has not been fully characterized. Representative catalytic mechanism and associated kinetic parameters that can explain data on the enzyme-catalyzed reaction kinetics have not been established (reviewed by Xin LI et al. in ref. [62]).

Generally, both GTP and ATP forming succinyl-CoA ligase are well represented in a variety of tissues, not only in humans but also in murine mitochondria. The GTP-forming subunit is rather expressed in anabolic tissues such as liver and kidney, the ATP-forming succinyl-CoA ligase is rather present in kidney, testis, and brain, whereas in cardiac tissue both ATP- and GTP-forming subunits are strongly expressed [61, 63-65]. In the human brain, SUCLA2 is exclusively expressed in neurons in the cerebral cortex and not in any other cell type [66], while *SUCLG2* encoded GTP-forming succinyl-CoA ligase is not found either in neurons or in astroglial cells, it can be found only in cells forming the microvasculature [67] (See **Figure 3**).
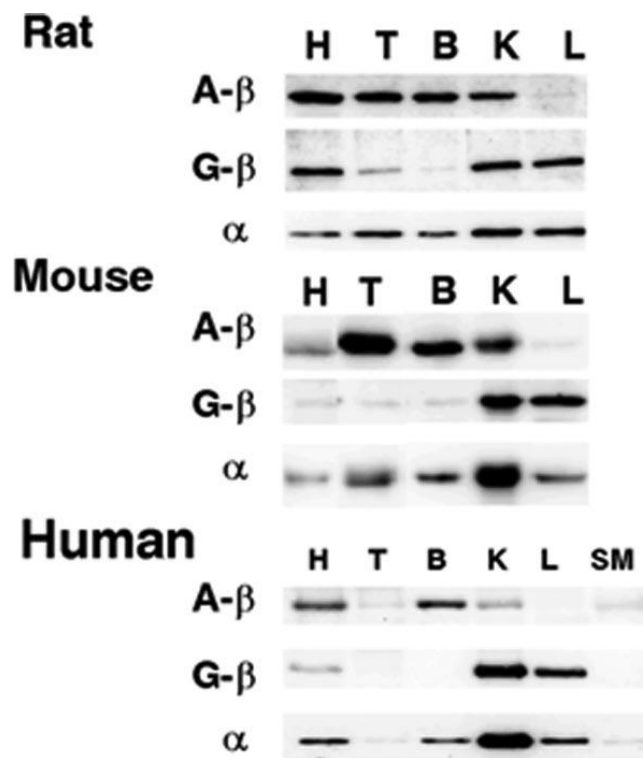
Figure 3 Western blots of succinyl-CoA ligase subunits in rat, mouse, and human.
The figure was adapted from Lambeth et al. 'Expression of two succinyl-CoA synthetases with different nucleotide specificities in mammalian tissues'.
Abbreviation on the figure: H – heart, T – testis, B – brain, K – kidney, L – liver, SM – skeletal muscle, A-β – ATP forming SUCL subunit, G-β – GTP-forming SUCL subunit, α – invariant SUCL α-subunit [63].

As it was described above, GTP also can form ATP due to a trans-phosphorylation by mitochondrial nucleotide diphosphate kinase [68]. While ATP is used by catabolic pathways, GTP is rather used for cellular anabolism [69], protein synthesis in mitochondria and also can support other GTP-binding regulatory proteins [70]. The GTP pool is outstanding in the mitochondrial matrix, since it is believed, that there is no mechanism for the export of GTP from the mitochondrial matrix to the cytosol in higher organisms [71]. Nevertheless, an atractyloside sensitive and insensitive guanine nucleotide transport mechanism was published by one group [72, 73], but it has not been confirmed yet.

Furthermore, there also exists another GTP using mechanism, i.e. the phosphoenolpyruvate (PEP) synthesis. PEP can be transported to the cytosol [74], where

it is used in gluconeogenesis for either GDP phosphorylation by cytosolic PEPCK or synthesis of ATP through the pyruvate kinase (PK, EC 2.7.1.40) reaction [63].

2.5 Succinyl-CoA ligase and surrounding enzymatic pathways
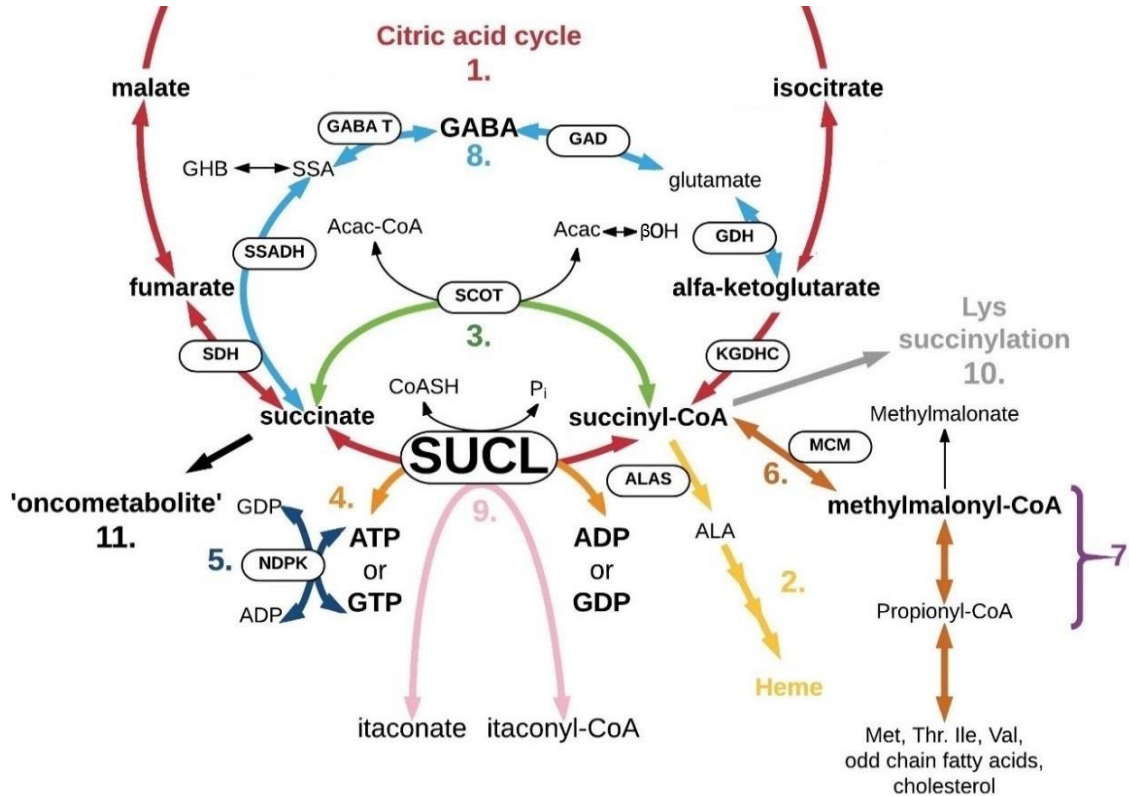
Figure 4 Succinyl-CoA ligase and surrounding enzymatic pathways
Succinate-CoA ligase is an intersection of several biochemical pathways, such as: citric acid cycle (1-red); Heme metabolism (2-yellow); in extrahepatic tissues, metabolism of ketone bodies (3-green); substrate-level phosphorylation (4-orange); succinyl-CoA ligase is associated with nucleoside-diphosphate kinase, therefore participate in maintaining mtDNA content (5-dark blue); through propionyl-CoA, succinyl-CoA is an entry point of several biomolecules (Met, Thr, Ile, Val, odd chain fatty acids, cholesterol) (6-brown); increases in propionyl-CoA and methylmalonyl-CoA may cause secondary metabolic aberrations due to their ability to inhibit steps in urea cycle, gluconeogenesis, and the glycine cleavage system (7-purple); in some particular cells in brain, succinate is the entry point of the GABA shunt (8-light blue); in cells of macrophage linage, succinyl-CoA ligase metabolizes the endogenously produced itaconate to itaconyl-CoA (9-pink); succinyl-CoA has been reported as a cofactor of lysine succinylation as a post-translational modification (10-grey); succinate has also been reported as an oncometabolite and a metabolic signal in inflammation (11-black); Abbreviations on figure: βOH: beta-hydroxybutyrate; AcAc: acetoacetate; AcAc-CoA: acetoacetyl-CoA; ADP: adenosine diphosphate; ALA: aminolaevulinic acid; ALAS: aminolaevulinic acid synthase; ATP: adenosine triphosphate; CoASH: coenzyme A; GABA T: 4-aminobutyrate-2-oxoglutarate transaminase; GABA: 4-aminobutyrate-2-oxoglutarate; GAD: glutamate decarboxylase; GDH: glutamate dehydrogenase; GDP: guanosine diphosphate; GHB: gamma hydroxybutyrate; GTP: guanosine triphosphate; Ile:

isoleucine; KGDHC: alpha-ketoglutarate dehydrogenase complex; Lys: lysine; MCM: methylmalonyl-CoA mutase; Met: methionine; NDPK: nucleotide diphosphate kinase; P_i: inorganic phosphate; SCOT: succinyl-CoA : 3-oxoacid-CoA transferase (also known as OXCT1); SDH: succinate dehydrogenase; SUCL: succinyl-CoA ligase; SSA: succinate-semialdehyde; SSADH: succinate-semialdehyde dehydrogenase; Thr: threonine; Val: valine

Succinyl-CoA ligase is at the intersection of several metabolic pathways (see **Figure 4**) [75]. The succinyl-CoA ligase enzyme itself has an important role in several functions, furthermore, there are several enzymatic reactions which may be affected by its performance or may affect the performance of the reaction through altering e.g., succinate, succinyl-CoA, inorganic phosphate, ADP, GDP, ATP, GTP, and/or CoA concentration in the matrix. In this chapter, most of these possible functions and reactions were summarized. These are the following:

a. Succinyl-CoA ligase is an enzyme of the **citric acid cycle**, one of the largest metabolic hub in mammalian cells [76]. As its name implies, it is a cycle, where every participating enzyme has a product which is a substrate of the following enzyme. This metabolic pathway has no end, but several entry points, where taken up fuels by mitochondria can fill up the cycle. When oxygen is available for cells, the cycle's primary role is to reduce NAD^+ and FAD^+ by dehydrogenases for the respiratory chain. NADH and $FADH_2$ oxidation lead to building up the electrochemical gradient of H^+-s across the inner mitochondrial membrane that is utilized by the F_oF_1-ATP synthase to produce ATP [48]. (see **Figure 4 - 1, red pathway**);

b. Succinyl-CoA ligase catalyzes a reversible reaction as mentioned above, thus succinyl-CoA ligase can proceed towards succinyl-CoA production. Due to the irreversible reaction catalyzed by alpha-ketoglutarate dehydrogenase complex [48, 56] it cannot be processed further than succinyl-CoA. In this case, succinyl-CoA may follow **heme metabolism** through aminolaevulinic-acid synthesis [77]. (see **Figure 4 - 2, yellow pathway**);

c. In extrahepatic tissues, 3-hydroxy butyrate (βOH) is changed back into acetoacetate (AcAc). In the next step it is activated to acetoacetyl-CoA by succinyl-CoA:3-oxoacid CoA transferase (SCOT or OXCT1, EC:2.8.3.5) Therefore, succinyl-CoA ligase is responsible also for maintaining the normal **ketone body homeostasis** through the regulation of the succinyl-CoA level within mitochondria [78]. This process is one of those that can mediate the by-pass of succinyl-CoA ligase (see **Figure 4 - 3, green pathway**);

d. Substrate-level phosphorylation is a definition of an enzyme reaction that results in a formation of an ATP or a GTP by the direct transfer of a phosphoryl (PO_3) group from a substrate to an ADP or GDP molecule respectively. In mitochondrial matrix, the major regulator of the ATP/ADP ratio is the F_oF_1-ATP synthase, however, this enzyme highly depends on the mitochondrial membrane potential (ΔΨm) [32].

There are two possible enzymatic transformations in mitochondria where GTP is utilized, and one of them is catalyzed by the reversible phosphoenolpyruvate carboxykinase (PEPCK, EC 4.1.1.32) (not shown in **Figure 4**). The reaction is the following [48]:

$$oxaloacetate + GTP \leftrightarrow phosphoenolpyruvate + GDP + CO_2$$
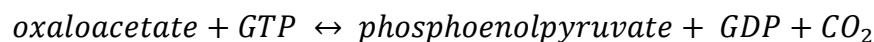
The PEPCK's mitochondrial isoform may operate rather as a GTPase linking hydrolysis of mitochondrial GTP made by succinyl-CoA ligase to an anaplerotic pathway resulting phosphoenolpyruvate (PEP) and also can contribute to glucose-stimulated insulin secretion in pancreas β cells [51].

The other reaction in the mitochondrial matrix, which is also capable for substrate-level phosphorylation, is succinyl-CoA ligase. As it was described above, the enzyme can form ATP and GTP as well. Nevertheless, GTP forming succinyl-CoA ligase also contributes to the ATP formation through the enzyme's concerted action with mitochondrial nucleotide diphosphate kinase (NDPK, EC 2.7.4.6) [79-81]. Thus, ATP can form GTP and *vice versa*.

Succinyl-CoA ligase as a mitochondrial substrate-level phosphorylation can yield high-energy phosphates in the absence of oxygen [36, 48, 56]. (see **Figure 4 – 4, orange pathway**)

e. Since succinyl-CoA ligase is associated with the nucleotide diphosphate kinase [80, 81], it has a major role in maintaining mtDNA content through the provision of phosphorylated deoxyribonucleotides. Mutation of succinyl-CoA ligase leads to mitochondrial DNA (mtDNA) depletion syndrome (MDS) [82], which is further explained **in Chapter 2.6.** (see **Figure 4 – 5**, dark-blue pathway)

f. The accumulation of succinyl-CoA due to the malfunction of succinyl-CoA ligase can be responsible for the alteration of different participants of the propionyl-methylmalonyl-CoA axis. **Succinyl-CoA is the entry point to the citric acid cycle for endpoint products of several biomolecules**, e.g., methionine, threonine, isoleucine, valine, propionate, odd-chain fatty acids and cholesterol. These main reaction steps in the catabolic propionyl-methylmalonyl-CoA axis are mediated by the sequential actions of propionyl-CoA carboxylase (EC 6.4.1.3) and methylmalonyl-CoA mutase (EC 5.4.99.2) [83] (see **Figure 4 – 6, brown pathway**)

g. In addition, increases in propionyl-CoA and methylmalonyl-CoA (partially shown on **Figure 4 – 7, purple pathway**) may cause secondary metabolic aberrations due to their ability to inhibit steps in urea cycle [84-86], gluconeogenesis and the glycine cleavage system [87, 88];

h. In specialized cells of the brain, **succinate is the entry point** to the citric acid cycle of the **'GABA shunt'** from succinate semialdehyde, a metabolite which is also in equilibrium with γ-hydroxybutyric acid [89-91]
GABA is found both in liver and brain, however, the hepatic tissue is not able to synthetize GABA, due to the relatively low glutamate decarboxylase (GAD, EC 4.1.1.15) activity, which is the key enzyme of the GABA synthesis. Unlike GABA

synthesis, GABA metabolism is possible in liver tissue, because of the presence of GABA transaminase (GABA-T, EC 2.6.1.19).

In tissues where succinyl semialdehyde dehydrogenase also can be found, GABA shunt also have an impact on succinyl-CoA ligase by leading to succinate production [92]. (See under *publications related to the present thesis* in **Chapter 11.**)

GABA shunt is also able to by-pass substrate-level phosphorylation (see **Figure 4 – 8, light-blue pathway**) and apparently produces less ATP from glutamate to succinate than the glutamate-α-ketoglutarate-succinyl-CoA-succinate pathway [75].

i. **Itaconic acid** (also known as 2-methylidenebutanedioic acid, methylenesuccinic acid) is a dicarboxylic acid. It has been identified in mammalian tissue specimens, such as *Mycobacterium tuberculosis*-infected lung tissue [93], glioblastomas [94], urine and serum samples [95]. It also has been shown that in human and mouse, macrophage lineage cells produce itaconic acid from cis-aconitate through an enzyme showing cis-aconitate decarboxylase activity. This enzyme is encoded by an *immuneresponsive gene 1* (*irg1*). In cells, where *irg1* can be activated, itaconate concentration is in millimolar range [96]. The role of itaconic acid in macrophages is to contribute to the antibacterial effect of these cells, since itaconate inhibits bacterial isocitrate lyase (EC 4.1.3.1), which is the key enzyme of bacterial glyoxylate shunt [97, 98] which renders bacteria able to grow on fatty acids and/or acetate [99]. More than a half decade ago it was described that itaconate is metabolized by succinyl-CoA ligase to itaconyl-CoA on a malonate sensitive manner, implying succinate dehydrogenase (EC 1.3.5.1) participation [100-103]. Considering substrate-level phosphorylation, itaconate:

- abolishes the process, resulting a "CoA trap" in the form of itaconyl-CoA;
- decreases ATP (or GTP) levels, since it diverts succinyl-CoA ligase towards thioesterification;
- inhibits SDH leading to a succinate build-up, which shifts succinyl-CoA ligase also towards thioesterification [104].

(See under *publications related to the present thesis* in **Chapter 11.**)

21

(see **Figure 4 – 9, pink pathway**)

j. According to a recent finding, succinyl-CoA might be the cofactor of enzyme-mediated **lysine succinylation** as an active form of succinate. This process is another way of protein post-translational modification, which can cause significant structural changes and is expected to have important cellular regulator functions [105] (see **Figure 4 – 10, grey pathway**).

k. In activated macrophages **succinate can stimulate dendric cells** through succinate receptor 1. Thus, succinate has an impact on cellular activation and immune response [106, 107].

l. Succinate can be named as 'oncometabolite' because **succinate links the dysfunction of the citric acid cycle to oncogenesis** through the activation of the hypoxia-inducible factor-1α (HIF-1α) [48, 108, 109]. Succinate can stabilize HIF-1α in tumors through succinate accumulation, which is itself can inhibit prolyl hydroxylase enzyme (PHD, EC 1.14.11.29) [108]. PHD is responsible for hydroxylation, thus the regulation of HIF1α causes its proteasomal-mediated degradation [110] (partially see **Figure 4 – 11, black pathway**).

m. In mitochondria, **inorganic phosphate** can act as a **signaling molecule** by activating oxidative phosphorylation through several points. Succinyl-CoA ligase has been identified as a new target of phosphate-induced activation of the oxidative phosphorylation and substrate-level phosphorylation under energy-limited circumstances [55].

2.6 Succinyl-CoA ligase mutations

As it was described in **Chapter 2.4,** succinyl-CoA ligase is encoded by three genes with different roles. *SUCLG1* encodes the invariant α subunit, *SUCLA2* and *SUCLG2* encode the β subunit forming ATP or GTP respectively.

To date, 51 patients have been reported with SUCLA2 deficiency [65, 111-121], 28 patients with SUCLG1 deficiency [112, 119, 122-132], and only 2 patients with SUCLG2

deficiency [122, 123]. Mitochondrial depletion syndrome (MDS), encephalomyopathy, lactic acidosis and methylmalonic aciduria are the most common features of succinyl-CoA ligase affecting diseases. In this chapter, the most typical symptoms, diagnostic aspects, metabolic alterations, and possible treatments are discussed highlighting the differences between subunit involvements.

Given the fact, that succinyl-CoA ligase plays a central role in the pathways mentioned beforehand, it is not surprising that this enzyme's deficiency leads to pleiotropic pathology, which is also influenced by the tissue-specific expression of its subunits. Significant clinical differences between mutations were hepatopathy found with *SUCLG1* cases but not in *SUCLA2* cases [112, 127, 132]. Hypertrophic cardiomyopathy was not reported in SUCLA2 patients (in one patient, a mild restrictive cardiomyopathy was found by echocardiography, but it resolved spontaneously [65]), but documented in several cases with *SUCLG1* mutations [112]. Since *SUCLG2* mutations have been described in the literature just twice recently, only few pieces of information are available about these patients. As it was reported, one of the patients had elevated methylmalonic acid and SIDS (sudden infant death syndrome), and the post-mortem blood spot analysis revealed a substantial elevation in C3 carnitine levels [122].

SUCLA2 mutant patients have significantly longer survival (median survival 20 years) than SUCLG1 deficient patients (median survival 20 months) significantly [112, 125], which is also true for missense mutations compared to loss-of-function (deletions, frameshift, nonsense) mutations [112].

2.6.1 Succinyl-CoA ligase deficiency

Succinyl-CoA ligase deficiency is a rare disease, however, it has a higher incidence of 1 in 1.700 in the Faroe Islands due to a founder effect. The carrier frequency of 1 in 33 [121] (frequency of the mutated allele is 2%, the estimated homozygote frequency is 1:2500 [111]). To date in Scandinavian population two founder mutations were identified as well [112]. Most of the mutation analyses have shown several novel mutations, including homozygous deletion of the entire *SUCLA2* gene, but other types also were found, such as one bp duplication, one bp deletion, three bp insertion, nonsense mutations, and a missense mutation [112, 131, 133, 134].

The median onset of symptoms was two months for patients with *SUCLA2* mutations and for *SUCLG1* patients it occurred at birth [111] with intrauterine growth retardation [132]. Both ATP- and GTP-forming subunit involving mutation caused the elevation of blood and urine methylmalonic acid, mtDNA depletion syndrome (MDS), lactic acidosis, and dystonia.

Hypertrophic cardiomyopathy and liver involvement were exclusively found in patients with *SUCLG1* mutations [132], whereas epilepsy was more frequent in patients with *SUCLA2* mutations compared to *SUCLG1* mutations [55].

According to MRI neuroimaging results, bilateral hyperdense lesions in basal ganglia (putamen, caudate nuclei) and a mild diffuse cerebral atrophy were found in both *SUCLA2* and *SUCLG1* cases as well [65, 91, 112, 131, 132]. Furthermore, EMG and nerve condition studies showed progressive axonal and demyelinating polyneuropathy especially of the lower limbs of *SUCLA2* patients [65]. Other symptoms are also typical as in Leigh-like encephalomyopathy [125, 131], such as diarrhea, emesis, dehydration, metabolic alterations (see details below), myopathy revealed by muscle echogram [65], severe muscle hypotonia [83, 133] with progressive areflexia [82], later on progressive dystonia [60, 121, 132, 133], dysphagia leading a failure to thrive [122, 133], and developmental delay. BAEP (brain auditory evoked potential) studies proved severe progressive sensorineural hearing loss [83, 111, 123, 133] in *SUCLA2* patients (Deafness in *SUCLG1* mutations hasn't been reported, due to the death during the first weeks, [18].) Interestingly liver failure [128, 131, 133] and hepatic encephalopathy [75] were also found in *SUCLG1* patients, however, almost none of the patients with *SUCLA2* mutation have been reported on so far suffered from cardiac, hepatic, gastrointestinal, or bone marrow involvement [131]. In *SUCLA2* patients with longer survival there was no speech development, but the children were able to understand sign language [65].

2.6.2 Metabolic alterations in succinyl-CoA ligase deficiencies

Regarding metabolic patterns or changes (see **Figure 5**), the accumulation of succinyl-CoA leads to an elevation in carnitine ester concentrations, especially C4-dicarboxylic carnitine [65, 111] and other elements of the succinyl-, methylmalonyl-, propionyl-CoA axis [65, 122, 123, 135, 136]. Since the end product of odd chain fatty acid oxidation is propionyl-CoA [83] which is also ending in here, it is evident that the elevation of the

intramitochondrial succinyl-CoA concentration blocks this metabolic pathway as well. Due to the fact that succinyl-CoA ligase deficiency causes an error in mtDNA maintenance, most succinyl-CoA ligase deficient patients had mtDNA depletion syndrome (MDS) resulting in a mitochondrial failure due to decreased respiratory complex activity [83, 125, 133, 136]. The most specific respiratory complex alterations are the combined complex I/IV; combined complex I/III/IV; isolated complex IV; isolated complex I deficiency (and also in [133]) and decreased RC complex activities were also found [112]. The insufficient succinyl-CoA ligase function leads to the accumulation of the TCA cycle intermediers, for example succinyl-CoA and citrate [65]. Since both citrate and succinyl-CoA [137] inhibit citrate synthase activity, as a secondary inhibitory affect the accumulating acetyl-CoA may inhibit the pyruvate dehydrogenase complex (PDH) [138]. It will direct the glycolysis towards lactic acid production causing -in most of the cases severe- lactic acidosis [65, 83, 111, 122, 123, 125, 132, 136]. The acidosis further enhanced by the succinyl-CoA ligase deficiency caused the accumulation of the citric acid cycle intermediers [65, 122, 132]. In one case a *SUCLA2* mutation accompanying PDH complex deficiency [136] was documented. The urinary excretion of L-leucine catabolism intermediers (3-hydroxyisovaleric acid and 3-methylglutaconic acid) were also found [65]. Isovaleric acid and isovaleryl-CoA are the direct precursors of 3-hydroxyisocvaleric acid. In case of the accumulation of isovaleric acid, the residual succinyl-CoA enzyme activity may be further decreased worsening the symptoms, since isovaleric acid has a succinyl-CoA ligase inhibitory effect [139]. (see also in **Figure 5**)
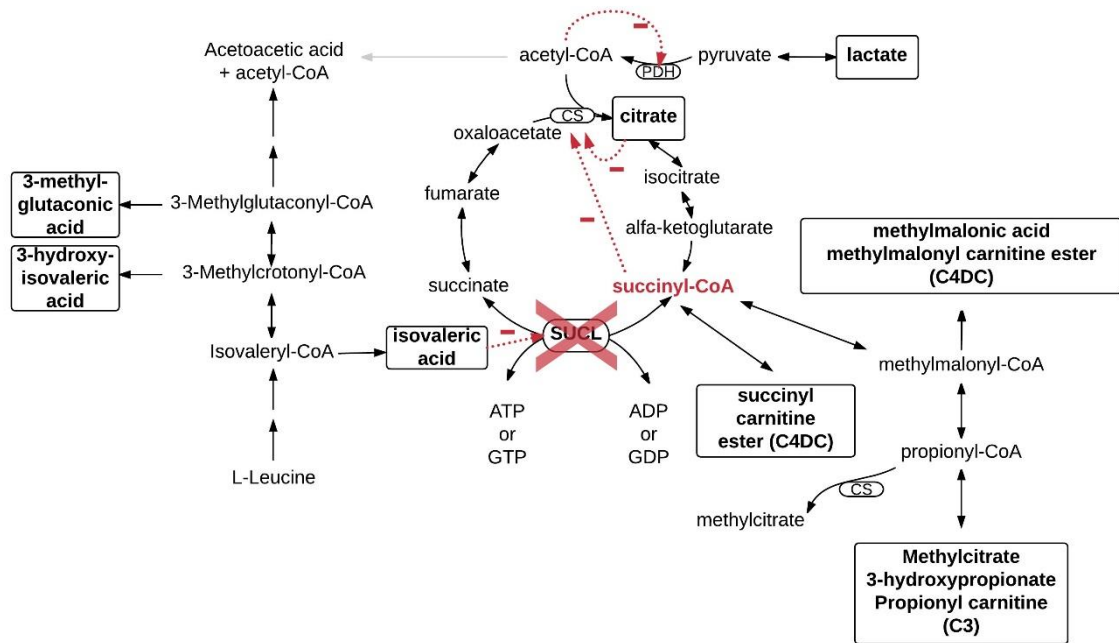
Figure 5 Schematic biochemical pathways demonstrating metabolic alterations in succinyl-CoA ligase deficiency caused by elevated succinyl-CoA (adapted from [65, 83]) Abbreviations: CS: citrate synthase; PDH: pyruvate dehydrogenase complex;

2.6.3 Diagnostic aspects of succinyl-CoA ligase deficiencies
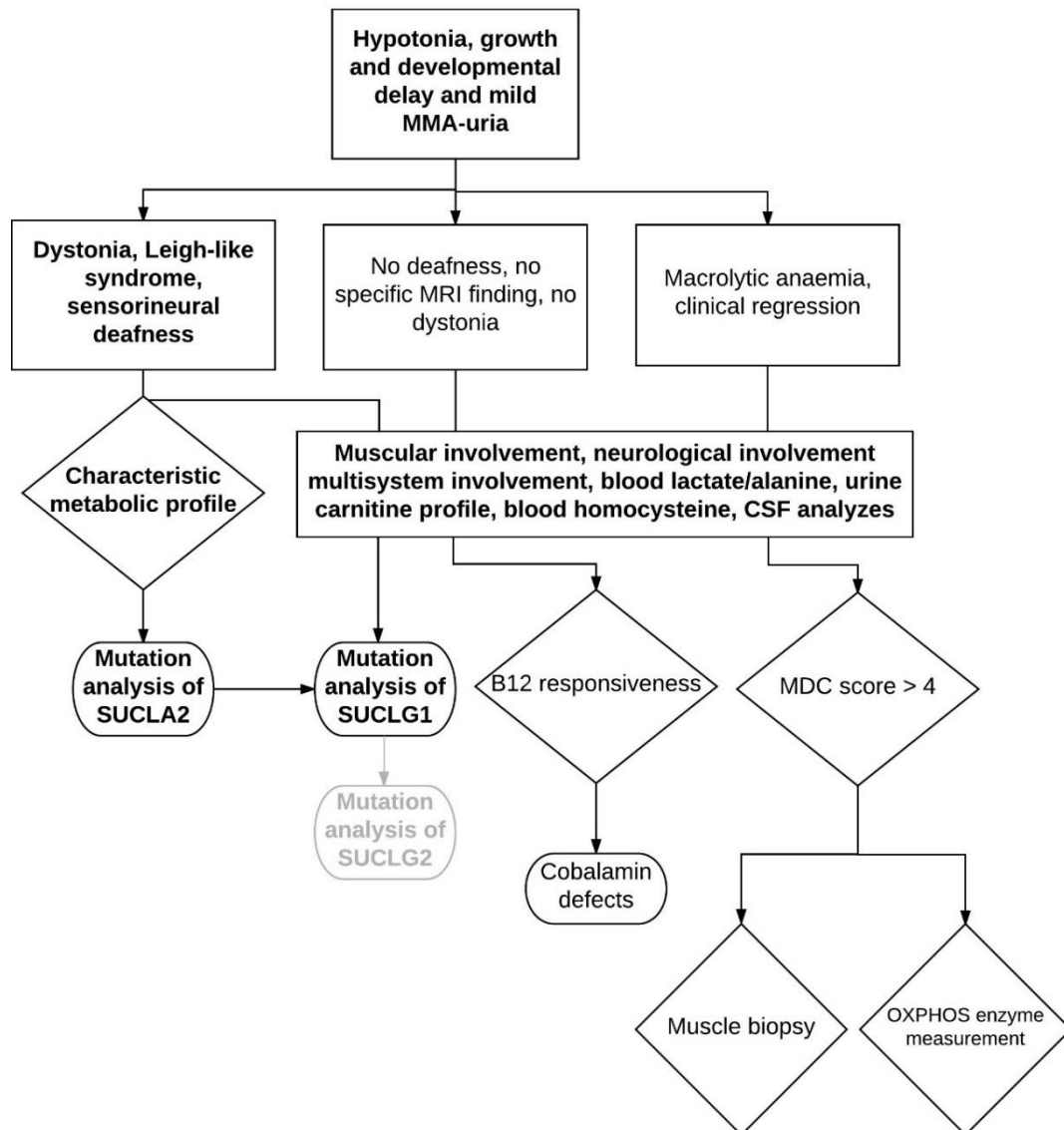
Figure 6 Diagnostic flowchart for patients with common MMA-uria, developmental delay and muscle hypotonia (adapted from [65, 140]) Characteristic metabolic profile in *SUCLA2* patients were increased e.g., lactic acid, methylmalonic acid, C4-DC carnitine, and 3-hydroxyisovaleric acid. Abbreviations: MDC: mitochondrial disease criteria; MMA: methylmalonic acid; CSF: cerebrospinal fluid; MRI: Magnetic resonance imaging;

As it has been described above there are only mild differences between *SUCLA2/SUCLG1* and *SUCLG2* mutations. As for diagnostic aspects, the common features are lactic acidaemia, elevated MMA concentration in blood and mildly in urine, and muscle dystonia should also be mentioned. As it can be seen in **Figure 6** not only the succinyl-CoA ligase affected differential diagnoses are difficult, but also other

mitochondrial diseases. Morava et al. suggested that late-onset hearing loss and absence of muscular and ocular involvement can be differential diagnostic clues in *SUCLA2* and *SUCLG1* mutations, since those rather favor *SUCLG1*. Unlike to this, in *SUCLG1* patients the mtDNA depletion in muscle is not a consistent finding, therefore cannot be used for diagnostic purposes [65].

Table 1 Most frequented elevated metabolite levels in *SUCLA2* and *SUCLG1* patients in blood and urine samples

Elevated metabolites in blood	References	Elevated metabolites in urine	References
methylmalonic acid	[65, 83, 112, 122, 123, 125, 133, 136]	methylmalonic acid	[65, 83, 112, 122, 131, 133]
creatinine	[65, 91]	creatinine	[65, 112, 133]
methylmalonyl/succinyl-carnitine (C4-DC)	[65, 111, 133]	methylmalonyl/succinyl-carnitine (C4-DC)	[65, 131]
propionyl-carnitine (C3)	[65, 122, 133]	propionyl-carnitine (C3)	[131]
butyryl carnitine (C4)	[133]	3-methylglutaconic acid	[65, 112]
propionyl-CoA	[83]	3-hydroxy-propionate	[65, 91]
pyruvate	[131, 133]	3-hydroxyisovaleric acid	[65, 112]
citric acid cycle intermedietes	[65, 122, 132]	citric acid	[65]
lactate	[56, 65, 83, 112, 122, 123, 125, 131]	methycitrate	[65, 112]
alanine	[65]	succinate	[65, 112]
		fumarate	[65, 82, 112, 131]
		α-ketoglutarate	[65, 112, 113]

Hereafter the thesis will focus on succinyl-CoA ligase affecting mutations. In all succinyl-CoA ligase diseases Leigh-like syndrome and accompanying symptoms were

typical, however muscular, cardiac, and liver involvement were described in *SUCLG1* patients (Only limited data have been available about the *SUCLG2* mutant patient). The summarization of metabolites which were elevated either in *SUCLA2* and *SUCLG1* patients can be found in **Table 1.**

Diagnostic results might come from metabolic investigations. There were several elevated metabolites identified such as lactic acid in all compartment, MMA in blood and mildly in urine, citric acid cycle intermediers, specified acyl-carnitines (C3/C4/C4DC) in all body fluids, etc. Furthermore 3-hydroxyisovaleric acid also should be listed as a biomarker of SUCLA2 and SUCLG1 deficiency. For final diagnosis, a direct sequence analysis of the *SUCLA2* and or *SUCLG1* gene is recommended in a suspected SUCLA2 or SUCLG1 deficiency.

2.6.4 Potential treatment of patients with succinyl-CoA ligase deficiency

Given the fact that succinyl-CoA ligase plays a role in several metabolic pathways and the deficiency of the enzyme causes severe metabolic and physiologic alterations, it is not surprising that the prognosis is bad and the number of tools for the treatment is limited. In children an individualized optimal dietary intake can increase the energy generating capacity of mitochondria, since it may be a possible way of therapy and could improve the quality of life [140]. Due to the fact that *SUCLA2* mutation-carrying patients have higher than normal total- and free acyl-carnitine levels, a carnitine supplementation might be beneficial. For the treatment of mild to moderate dystonia and early sign of extrapyramidal involvement accompanying mildly decreased CSF (cerebrospinal fluid) HVA (homovanillic acid) concentration (major end-product of the catecholamine metabolism) a low dose L-DOPA treatment (3-5mg/kg/day) was used with transient success. It resulted in an improvement of facial expressions and some cases increased hand mobility for 6-10 months. Baclofen (a central nervous system depressant) or clonazepam (tranquilizer of the benzodiazepine class) treatment also can be considered for dystonia [112]. Additional antioxidant, riboflavin and thiamine treatment were also documented as an effective supplementary. There were trials of applying B_{12} vitamin intramuscular, however, these treatments didn't show any improvement. It would be obvious to add succinate as anaplerosis, however, it would possibly worsen chronic encephalopathy due to an increase in methylmalonic acid concentration. Furthermore,

early cochlear implantation could help regarding the quality of life and increase the level of contact and vocalization dramatically [65]. The lactate acidosis was treated with bicarbonate and later citrate in one report [132].

3. OBJECTIVES

In the past several years our research group could demonstrate that mitochondrial substrate-level phosphorylation has a critical role in producing high energy phosphates in the absence of oxidative phosphorylation and in conditions where availability of oxygen and/or nutrients are limited e.g., in hypoxic tissue. It has also been shown that the provision of the succinyl-CoA by the alpha-ketoglutarate dehydrogenase complex is crucial for maintaining the function of the succinyl-CoA ligase, yielding ATP (or GTP) and preventing the ANT from reversing. The alpha-ketoglutarate dehydrogenase complex affecting mutations led to enzyme dysfunction, decreased amount of produced succinyl-CoA, and resulted in ATP consuming mitochondria with substrates supporting substrate-level phosphorylation (See **Chapter 4.4**). More recently it was shown that the NAD^+ supply for alpha-ketoglutarate dehydrogenase complex under anoxic conditions is also critical to maintain substrate-level phosphorylation. The revealed diaphorase enzyme system in mouse liver mitochondria adds up to 81 % to the NAD^+ pool during respiratory inhibition. As it was known from the literature, human succinyl-CoA ligase mutations confer a severe pathology.

Succinyl-CoA ligase plays a central role in several metabolic pathways as we have seen in **Chapter 2.5**. The enzyme deficiency resulted in mtDNA depletion in most of the cases and as a consequence of this respiratory complex failure. We proposed to investigate further the succinyl-CoA ligase deficiencies in order to contribute to the understanding of the succinyl-CoA ligase mutations related molecular pathology. See **Publications related to the present thesis** in **Chapter 11.** (Biochem J. 2016 Oct 15;473(20):3463-3485. Epub 2016 Aug 5.)

To achieve this, we generated transgenic mice lacking either one *Sucla2* or one *Suclg2* allele. Homozygous knockout mice for either gene were never born, suggesting that the complete absence of either gene is incompatible with life in mice, as also reported in [21]. We also quantitated the expression of succinyl-CoA ligase subunits in mitochondria isolated from brains, hearts, and livers of 3-, 6- and 12-month-old wild-type (WT) and heterozygote mice. In the tissues of *Sucla2* heterozygote mice we investigated respiration rates and membrane potential (ΔΨm) for an array of mitochondrial substrates and various metabolic states, complex I, II, II/III and IV activities, as well as substrate-level phosphorylation during respiratory inhibition or true anoxia. Substrate-level

phosphorylation was further investigated during submaximal inhibition of succinyl-CoA ligase by either itaconate or KM4549SC. We also compared mtDNA content, ATP-forming and GTP-forming succinyl-CoA ligase activities, and blood levels of 20 carnitine esters. Furthermore, we cross-bred *Sucla2+/−* with *Suclg2+/−* mice, yielding double heterozygote *Sucla2+/−/Suclg2+/−* mice, and investigated the expression of g1, g2 and a2 subunits, mtDNA content, blood carnitine esters and bioenergetic parameters.

Our aims for this thesis were:

1. **Setting up animal models for succinyl-CoA ligase deficiencies and investigating the impact of the mitochondrial substrate-level phosphorylation on the bioenergetics parameters.**
2. Advising the following questions:
   a. **How and to what extent do succinyl-CoA ligase mutations affect substrate-level phosphorylation?**
   b. **What happens if the SKDCC axis, the primary, central enzyme, the succinyl-CoA ligase itself was damaged?**
   c. **What would be the difference between ATP- or GTP-forming subunit affecting mutations?**
3. **Using this animal model revealing and elucidating the details of known symptoms, alterations in metabolites and mtDNA content in order to contribute to the better understanding of the succinyl-CoA ligase mutation and the function of the succinyl-CoA ligase enzyme.**
4. **Revealing a potential compensatory mechanism which is able to prevent phenotypic alterations in the heterozygous patients and animal model.**

4. METHODS

4.1 Animals

Mice were of either 129/SvEv (*Sucla2* heterozygote strain) or C57Bl/6N (*Suclg2* heterozygote strain) background. The animals used in our study were of both sex and 3, 6 or 12 months of age. Mice were housed in a room maintained at 20–22 °C on a 12-hour light–dark cycle with food and water available *ad libitum*. All experiments were approved by the Animal Care and Use Committee of the Semmelweis University (Egyetemi Állatkísérleti Bizottság) and the EU Directive 2010/63/EU for animal experiments.

Sucla2+/– heterozygous mice were generated by Texas A&M Institute for Genomic Medicine (TIGM) using a gene-trapping technique [141]. Mice (strain C57BL/6N) were cloned from an ES cell line (IST10208H1; TIGM). The ES cell clone contained a retroviral insertion in the *Sucla2* gene (intron 4) identified from the TIGM gene trap database and was microinjected into C57BL/6 albino host blastocysts to generate germline chimeras using standard procedures. The retroviral OmniBank Vector 76 contained a splice acceptor (see **Figure 7**) followed by a selectable neomycin resistance marker/LacZ reporter fusion (β-Geo) for identification of successful gene trap events further followed by a polyadenylation signal. Insertion of the retroviral vector into the *Sucla2* gene led to the splicing of the endogenous upstream exons into this cassette to produce a fusion that leads to termination of further transcription of the endogenous *Sucla2* exons downstream of the insertion. Chimeric males were bred to 129/SvEv females for germline transmission of the mutant *Sucla2* allele.

Suclg2 heterozygote mice [B6-Suclg2Gt(pU-21KBW)131Card] were generated at CARD, Kumamoto University, Japan also using a gene-trapping technique [142]. Mice (strain Albino B6) were cloned from an ES cell line (Ayu21-KBW131; Exchangeable Gene Trap Clones: EGTC). The ES cell clone contained a trap vector insertion in the *Suclg2* gene (first intron) identified from the EGTC database and was aggregated with morulae from ICR mice to generate germline chimeras using standard procedures. pU21-W (accession number: AB427140, 9333 bp) was a 'promoter trap' vector with three stop codons, which were arranged upstream of the ATG of the β-geo in all three frames (see **Figure 8**). Insertion of the trap vector into the *Suclg2* gene led to the splicing of the

endogenous upstream exons into this cassette to produce a fusion transcript that leads to termination of further transcription of the endogenous *Suclg2* exons downstream of the insertion. Chimeric males were bred to C57BL/6N females for germline transmission of the mutant *Suclg2* allele. To investigate the expression level of *Suclg2* mRNA of *Suclg2* heterozygote, the original ES cell line (Ayu21-KBW131: +/−) was compared with the parental strain (KAB6: +/+). mRNA was purified from parental ES cells (+/+) and 21-KBW131 (+/−). *Suclg2* expression levels of these cells were analyzed by real-time PCR using the TaqMan Gene Expression Assays, XS, *Suclg2* (AB, 4448892, FAM/MGB-NFQ) kit. Heterozygous ES cells showed almost half the amount of *Suclg2* mRNA compared with parent cells see results in **Chapter 5.9**.

Neither *Sucla2* –/– nor *Suclg2* –/– mice were ever born from mating heterozygous mice, suggesting that complete absence of either gene is incompatible with life in mice, and as also reported in [21]. By mating *Sucla2* heterozygous mice with *Suclg2* heterozygous mice, double transgenic (*Sucla2+/–/Suclg2+/–*) mice were born and viable.
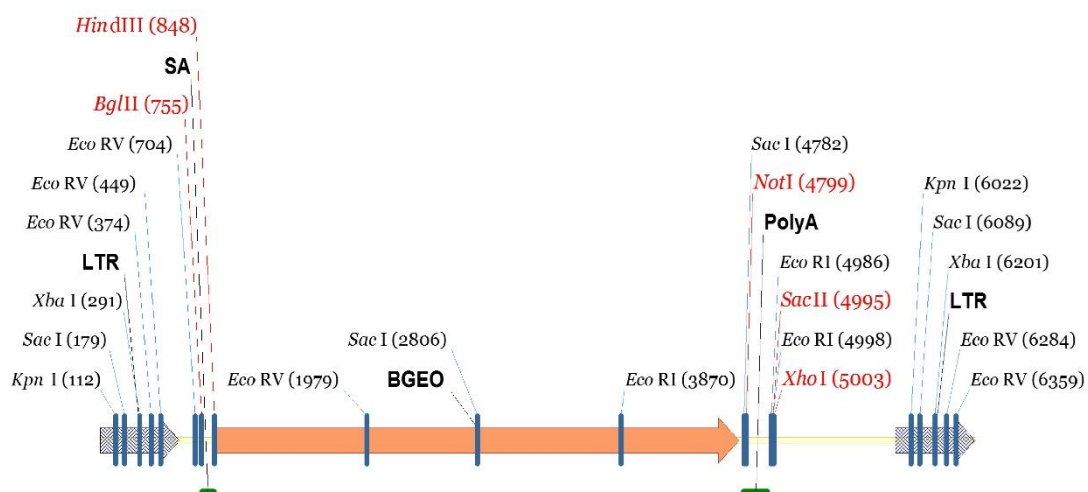
Figure 7 Generation of *Sucla2* mutant mice
Gene trap vector for generating *Sucla2* mutant mice.
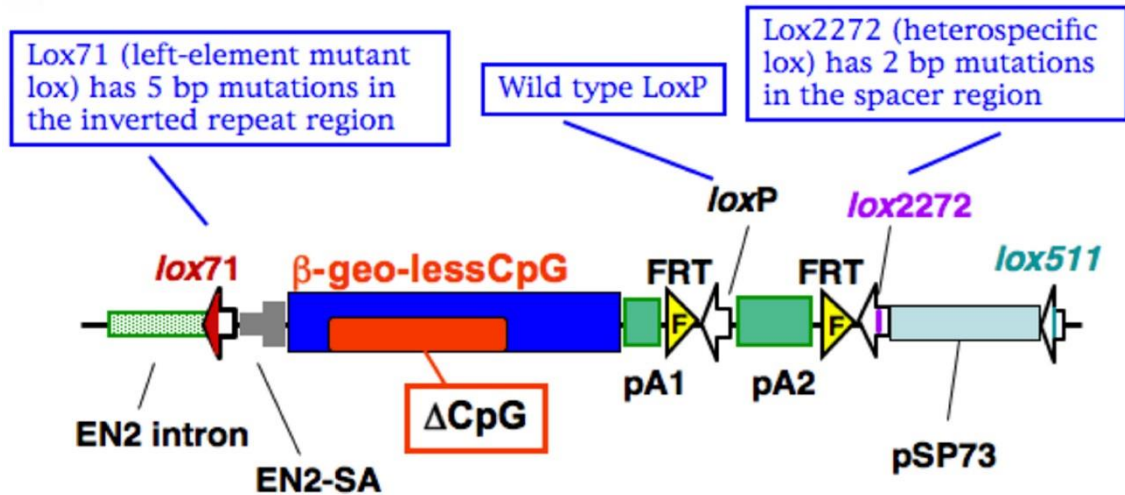
Figure 8 Generation of *Suclg2* mutant mice
Gene trap vector for generating *Suclg2* mutant mice
(adapted from http://egtc.jp/action/access/vector_detail?vector=pU-21W)

4.2 Isolation of mitochondria

Isolation of mitochondria from mouse liver, heart, and brain: liver and heart mitochondria from all animals were isolated as described in ref. [143], with the modifications described in refs [36] and [35]. Nonsynaptic brain mitochondria were isolated on a Percoll gradient as described previously [144], with minor modifications detailed in ref. [145]. Protein concentration was determined using the bicinchoninic acid assay as described below in **Chapter 4.3**.

Yields were typically 0.2 ml of ~20 mg/ml per two brains; for liver, yields were typically 0.7 ml of ~70 mg/ml per two livers, and for heart mitochondria, yields were typically 0.1 ml of ~15 mg/ml per two hearts.

4.3 Determination of protein concentration

Protein concentration was determined using the bicinchoninic acid assay [146] (ThermoFisher SCIENTIFIC – Pierce™ BCA Protein Assay Kit) , and calibrated using bovine serum standards using a Tecan Infinite® 200 PRO series plate reader (Tecan Deutschland GmbH, Crailsheim, Germany).

4.4 Mitochondrial substrates and substrate combinations

In our experiments and protocols, it is critical to use adequate substrate combinations to maintain mitochondrial respiration. While some substrates would rather support, others

would rather not support substrate-level phosphorylation. Glutamate (glut) and α-ketoglutarate (α-KG) are two substrates that support substrate-level phosphorylation to the greatest extent, however, these should be combined with malate (mal) because it assists in the entry into mitochondria of other substrates including glutamate and α-ketoglutarate. Malate alone has no effect on mitochondrial substrate-level phosphorylation. β-hydroxybutyrate (βOH) is a ketone body, that can be converted to acetoacetate (AcAc) by β-hydroxybutyrate dehydrogenase in the following reaction [147]:

$$(R) - 3 - hydroxybutyrate + NAD^+ \leftrightarrow acetoacetate + NADH + H^+$$

It also has no direct effect on substrate-level phosphorylation; however, βOH decrease matrix NAD^+/NADH ratio, and therefore reduce mitochondrial substrate-level phosphorylation through blocking succinyl-CoA production by alpha-ketoglutarate dehydrogenase complex, the enzyme that needs oxidized NAD^+ [56, 57].

4.5 Determination of membrane potential (ΔΨm) in isolated liver mitochondria

ΔΨm of isolated mitochondria (0.5-1 mg -depending on the tissue of origin- per two ml of medium containing, in mM: KCl 8, K-gluconate 110, NaCl 10, Hepes 10, KH_2PO_4 10, EGTA 0.005, mannitol 10, $MgCl_2$ 1, substrates as indicated in the figure legends, 0.5 mg/ml bovine serum albumin [fatty acid-free], pH 7.25, and 5 mM safranine O) was estimated fluorometrically with safranine O [148]. Traces obtained from mitochondria were calibrated to millivolts as described in [36]. Fluorescence was recorded in a Hitachi F-7000 spectrofluorometer (Hitachi High Technologies, Maidenhead, UK) at a 5-Hz acquisition rate, using 495- and 585-nm excitation and emission wavelengths, respectively, or at a 1-Hz rate using the O2k-Fluorescence LED2-Module of the Oxygraph-2k (Oroboros Instruments, Innsbruck, Austria) equipped with an LED exhibiting a wavelength maximum of 465 +/– 25 nm (current for light intensity adjusted to 2 mA, i.e., level '4') and an <505 nm shortpass excitation filter (dye-based, filter set "Safranin"). Emitted light was detected by a photodiode (range of sensitivity: 350-700 nm), through an >560 nm longpass emission filter (dye-based). Experiments were performed at 37 °C. Safranine O is known to exert adverse effects on mitochondria if used at sufficiently high concentrations (i.e. above 5 μM, discussed in [57]). However, for

optimal conversion of the fluorescence signal to $\Delta\Psi m$, a concentration of 5 μM safranine O is required, even if it leads to a diminishment of the respiratory control ratio by approximately one unit (not shown). Furthermore, the non-specific binding component of safranine O to mitochondria (dictated by the mitochondria/safranine O ratio) was within 10% of the total safranine O fluorescence signal, estimated by the increase in fluorescence caused by the addition of a detergent to completely depolarized mitochondria (not shown). As such, it was accounted for, during the calibration of the fluorescence signal to $\Delta\Psi m$.

4.6 Mitochondrial respiration

Oxygen consumption was estimated polarographically using an Oxygraph-2k. 0.5-1 mg -depending on the tissue of origin- mitochondria was suspended in 2 ml incubation medium, the composition of which was identical to that for $\Delta\Psi m$ determination. Experiments were performed at 37 ^{o}C. Oxygen concentration and oxygen flux ($pmol \cdot s^{-1} \cdot mg^{-1}$; negative time derivative of oxygen concentration, divided by mitochondrial mass per volume and corrected for instrumental background oxygen flux arising from oxygen consumption of the oxygen sensor and back-diffusion into the chamber) were recorded using DatLab software (Oroboros Instruments).

4.7 Cell cultures

Fibroblast cultures from skin biopsies from the patient with no SUCLA2 expression and a control subject were prepared. Cells were grown on poly-L-ornithine coated flasks for 5-7 days in RPMI1640 medium (GIBCO, Life Technologies, Carlsbad, CA, USA) supplemented with 10% fetal bovine serum and 2 mM glutamine and kept at 37 ^{o}C in 5% CO_2. The medium was also supplemented with penicillin, streptomycin, and amphotericin (Sigma-Aldrich St. Louis, MO, USA).

4.8 Mitochondrial membrane potential ($\Delta\Psi m$) determination in *in situ* mitochondria of permeabilized fibroblast cells

$\Delta\Psi m$ was estimated using fluorescence quenching of the cationic dye safranine O due to its accumulation inside energized mitochondria [148]. Fibroblasts were harvested by trypsinization, permeabilized as detailed in [61] and suspended in a medium identical to that as for $\Delta\Psi m$ measurements in isolated mitochondria. Substrates were 5 mM glutamate

and 5 mM malate. Fluorescence was recorded in a Tecan Infinite® 200 PRO series plate reader using 495 and 585 nm excitation and emission wavelengths, respectively. Experiments were performed at 37 °C.

4.9 Western blot analysis

Isolated mitochondria were solubilized in RIPA buffer containing a cocktail of protease inhibitors (Protease Inhibitor Cocktail Set I, Merck Millipore, Billerica, MA, USA) and frozen at -80 °C for further analysis. Frozen pellets were thawed on ice, their protein concentration was determined using the bicinchoninic acid assay as detailed above, loaded at a concentration of 3.75 µg per well on the gels and separated by sodium dodecyl sulfate − polyacrylamide gel electrophoresis (SDS-PAGE). Separated proteins were transferred to a methanol-activated polyvinylidene difluoride membrane. Immunoblotting was performed as recommended by the manufacturers of the antibodies. Rabbit polyclonal anti-SUCLG1, anti-SUCLG2, anti-VDAC1 (Abcam, Cambridge, UK), and anti-SUCLA2 (Proteintech Europe Ltd, Manchester, UK) primary antibodies were used at titers of 1:5000. Immunoreactivity was detected using the appropriate peroxidase-linked secondary antibody (1:5000, donkey anti-rabbit Jackson Immunochemicals Europe Ltd, Cambridgeshire, UK) and enhanced chemiluminescence detection reagent (ECL system; Amersham Biosciences GE Healthcare Europe GmbH, Vienna, Austria). Densitometric analysis of the bands was performed in Fiji [149].

4.10 mtDNA content

Total DNA was isolated from 4 pooled tissues from each mouse group using QIAamp DNA Mini Kit (QIAGEN) following the manufacturer's instructions. Relative mtDNA content was quantified in triplicate by real-time PCR using primers for cox1 (forward primer 5'-TGCTAGCCGCAGGCATTA C-3' reverse primer 5'-GGGTGCCCAAAGAATCAGAAC-3' and normalized against the nuclear encoded actinB gene (forward primer 5′GGAAAAGAGCCTCAGGGCAT-3′, reverse primer-5′-GAAGAGCTATGAGCTGCCTGA-3′), as previously described [150]. DNA was amplified in an ABI 7900 system as follows: 95°C for 10 min followed by 45 cycles of a two-stage temperature profile of 95°C for 15 sec and 60°C for 1 min.

4.11 Protein purification

The gene sequences for mature human SUCLG1 (residues 29-333, ~33.2 kDa, GenBank: CAG33420.1) and mature human SUCLG2 (residues 39-432, ~43.6 kDa, GenBank: AAH68602.1) were sequence optimized for expression in E. coli, synthesized, incorporated in pJ411 plasmids bearing kanamycin resistance, and sequence verified (DNA2.0, Cambridge, UK). The native protein sequence in each case was supplemented with a C-terminal hexahistidine tag (GSHHHHHH). Each pJ411-SUCLG1/2 plasmid was transfected into inducible E. coli BL21 (DE3) strain, and the bacteria were grown in Luria-Bertani medium at 37°C. Protein expression was induced with 1 mM isopropyl β-D-1-thiogalactopyranoside for 3 hours. The collected bacteria were sonicated in 10 ml lysis buffer (25 mM Tris (pH 8.5), 150 mM NaCl, 0.5 mg/ml lysozyme, 0.2% Triton X-100) per gram of wet pellet. Both proteins formed inclusion bodies when overexpressed, with minimal or no presence in the soluble fraction of the lysate. The proteins were purified in their unfolded state (7M urea, 200 mM NaCl) with affinity chromatography, after binding to Ni-Sepharose™ 6 Fast Flow resin (GE Healthcare). The eluates were diluted 15-fold in 20 mM Tris (pH 8.5), 100 mM NaCl, the precipitated protein was removed, and the supernatants were dialyzed against the same buffer. The purity of the two proteins was assessed with SDS PAGE, and the final protein concentrations were estimated using the bicinchoninic acid assay as detailed above. The protein stocks were aliquoted, flash-frozen in liquid nitrogen and stored at −80 °C.

4.12 Electron transport chain complex and citrate synthase activity assays

Enzymatic activities of rotenone-sensitive NADH CoQ reductase (complex I), succinate cytochrome c reductase (complex II/III), succinate dehydrogenase (complex II, SDH), cytochrome c oxidase (COX, complex IV) and citrate synthase (CS), a mitochondrial marker enzyme, were determined in isolated mitochondria as we have previously described [91], [90]. The samples were once freeze-thaw isolated mitochondria stored in a buffer used for mitochondrial isolation (225 mM mannitol, 75 mM sucrose, 5 mM HEPES, 1 mg/ml Bowine Serum Albumin (fatty acid-free). The summarization of the enzyme kinetic tests is found in the following table:

Table 2 Electron transport chain complex and citrate synthase activity assays method summarization

Enzyme	Reaction condition	Measured reactant	Detection wavelength	Extinction coefficient	Reaction initiator
complex I	25 mM potassium phosphate buffer, 5 mM $MgCl_2$, pH 7.2 2 mM KCN 2.5 mg/ml BSA 0.13 mM NADH 2 µg/ml antimycin A 65 µM ubiquinone$_1$, 2mg/ml rotenone in ethanol	NADH	340 nm	6.81 $mM^{-1}cm^{-1}$	sample
complex II	25 mM potassium phosphate buffer, 5 mM $MgCl_2$, pH 7.2 20 mM sodium succinate 50 µM DCPIP 2 mM KCN 2 µg/ml antimycin A 2 µg/ml rotenone in ethanol 65 µM ubiquinone$_1$	DCPIP	600 nm	19.1 $mM^{-1}cm^{-1}$	ubiquinone1
complex II/III	25 mM potassium phosphate buffer, 5 mM $MgCl_2$, pH 7.2 20 mM sodium succinate 2 mM KCN 2 µg/ml rotenone 37.5 µM cytochrome c (oxidized)	cytochrome c (oxidized)	550 nm	18.7 $mM^{-1}cm^{-1}$	cytochrome c
complex IV	20 mM potassium phosphate, pH 7.0 0.45 mM n-dodecyl-b-D-maltoside 15 µM cytochrome c (reduced)	cytochrome c (reduced)	550 nm	18.7 $mM^{-1}cm^{-1}$	sample
citrate synthase	100 mM Tris–HCl, pH 8.0 100 µM DTNB 50 µM acetyl coenzyme A 0.1% (w/v) Triton X-100 250 µM oxaloacetate	DTNB	412 nm	13.6 $mM^{-1}cm^{-1}$	oxaloacetate

4.13 Determination of succinyl-CoA ligase activity

ATP- and GTP-forming succinyl-CoA ligase activity in isolated mitochondria was determined at 30 °C, as described in [151], with the modifications detailed in [152]. Mitochondria (0.25 mg) were added in an assay mixture (2 ml) containing: 20 mM potassium phosphate, pH 7.2, 10 mM $MgCl_2$, and 2 mM ADP or GDP. The reactions were initiated by adding 0.2 mM succinyl-CoA and 0.2 mM DTNB (5,5′-dithiobis (2-nitrobenzoic acid)) in quick succession. The molar extinction coefficient value at 412 nm for the 2-nitro-5-thiobenzoate anion formed upon reaction of DTNB with CoASH was considered as 13,600 M^{-1} cm^{-1}. Rates of 2-nitro-5-thiobenzoate formation were followed spectrophotometrically during constant stirring. The sample free thiol concentration was measured in parallel in the same conditions (without the addition of succinyl-CoA) and was taken into account for calculation of the succinyl-CoA ligase activity.

4.14 Determination of acylcarnitines

Multiple reaction monitoring transitions of butyl ester derivatives of acylcarnitines from dry blood spots and stable isotope internal standards were analyzed by electrospray ionization-tandem mass spectrometry (MS-MS) using a Waters Alliance 2795 separations module coupled to a Waters Micromass quarto micro API mass spectrometer monitoring for acylcarnitines (Milford MA USA), as described in [121].

4.15 Determination of *Sucla2* mRNA by qRT-PCR

mRNA coding for *Sucla2* was quantified by qPCR in two different laboratories using two different 'housekeeping' mRNAs for normalization, ß-actin or proteasome 26S subunit, ATPase 4 (Psmc4). In both cases, total RNA was isolated from the organs (livers, hearts, brains) of at least four mice per age group and genotype (WT or *Sucla2+/–*) with RNeasy Micro Kit (Qiagen, Hilden, Germany) according to the manufacturer's instructions. 1 µg RNA was reverse transcribed with QuantiTect Reverse Transcription Kit (Qiagen). Subsequently, quantitative Real-Time PCR (qRT-PCR) was carried out using predesigned TaqMan Gene Expression Assays (Thermo Fisher Scientific, Waltham, Massachusetts, USA): *Sucla2* (Mm01310541_m1) and Actb (Mm00607939_s1). The real-time reaction was performed on a QuantStudio 7 Flex Real-Time PCR system (Applied Biosystem, Life Technologies, Carlsbad, California, USA) according to the

manufacturer's protocol. Gene expression level was normalized to ß-actin. Fold change (FC) was calculated using the 2-ΔΔCt method [111]. Alternatively, the expression level of *Sucla2* mRNA was determined by real-time PCR using TaqMan Gene Expression assay kit and 7500 Real-Time PCR System (Applied Biosystems), using the TaqMan Gene Expression Assays, XS, *Sucla2* (AB, 4331182, FAM/MGB-NFQ) kit. Measured values were normalized by using the TaqMan Gene Expression Controls, Psmc4 mouse (AB, 4448489, VIC-MGB) kit, as recommended by Applied Biosystems for standard gene expression experiments because of their design criteria.

4.16 Statistics

Data are presented as averages ± standard error of the mean (SEM) or standard deviation (SD) where indicated. Significant differences between two groups were evaluated by Student's t-test; significant differences between three or more groups were evaluated by one-way analysis of variance followed by Tukey's or Dunnett's posthoc analysis. $p \leq 0.05$ was considered statistically significant. If normality test failed, ANOVA on Ranks was performed. Wherever single graphs are presented, they are representative of at least 3 independent experiments.

4.17 Reagents

Standard laboratory chemicals, enzyme substrates, and itaconic acid were from Sigma-Aldrich. SF 6847 was from Enzo Life Sciences (ELS AG, Lausen, Switzerland). Carboxyatractyloside (cATR) was from Merck (Merck KGaA, Darmstadt, Germany). KM4549SC (LY266500) was from Molport (SIA Molport, Riga, Latvia). Mitochondrial substrate stock solutions were dissolved in bi-distilled water and titrated to pH 7.0 with KOH. ADP was purchased as a K^+ salt of the highest purity available (Merck) and titrated to pH 6.9. TaqMan Gene Expression Assays, XS, *Suclg2* (AB, 4448892, FAM/MGB-NFQ) kit and Actb (AB, 4448489, VIC-MGB) kit were from Thermo Fisher Scientific. qPCR reaction mix was qPCRBIO SyGreen Mix Hi-Rox (PCR Biosystems).

5. RESULTS

5.1 The effect of deleting one *Sucla2* allele on *Sucla2* mRNA level

Total RNA was isolated from the livers, hearts, and brains of 3-, 6- and 12-month-old WT and *Sucla2+/−* mice (four animals per group), and *Sucla2* mRNA was quantified by qPCR, ratioed to β-actin (**Figure 9A**) or Psmc4 expression (**Figure 9B**). As shown in **Figures 9A** and **B**, mRNA coding for Sucla2 was significantly decreased (26–71%) in the tissues obtained from *Sucla2+/−* mice, compared with those obtained from WT littermates.
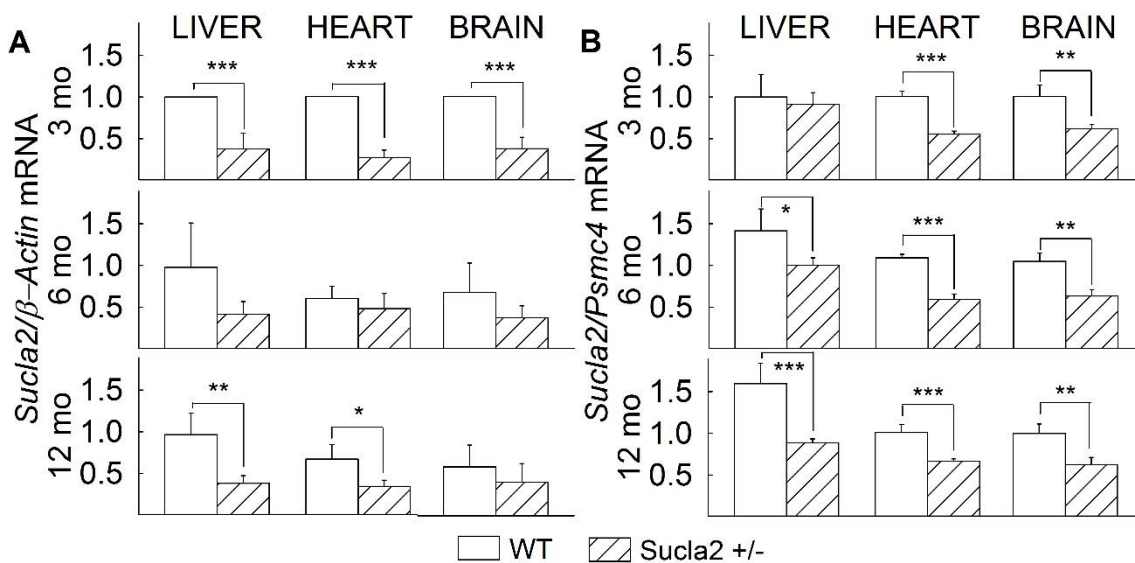
Figure 9 Sucla2 mRNA quantification.
(**A**) Bar graphs of qPCR of Sucla2 mRNA ratioed to β-actin mRNA of 3-, 6- and 12-month-old WT and *Sucla2+/−* mice from liver, heart and brain. (**B**) Bar graphs of qPCR of *Sucla2* mRNA ratioed to Psmc4 mRNA of 3-, 6- and 12-month-old WT and *Sucla2+/−* mice from liver, heart and brain. *p ≤ 0.05, **p < 0.01 and ***p ≤ 0.001. Data are SEM from four different organs per animal group.

## 5.2 Characterization of succinyl-CoA ligase subunit expressions of WT and *Sucla2+/–* mice

Our data found in **Chapter 5.1** are in accordance with those obtained from immunodetection of Sucla2 subunit by Western blotting. These data are depicted in **Figure 10**. Mitochondria were prepared from the livers, hearts, and brains of 3-, 6-, and 12-month-old WT and *Sucla2+/−* mice and SUCLG1, SUCLA2, SUCLG2, and VDAC1 were immunodetected by Western blotting. Only 3.75 mg of purified mitochondria (pooled from mitochondria obtained from eight organs per group) were loaded on each gel lane so as not to saturate the final enhanced chemiluminescence signals (see the 'Experimental Procedures' section). Scanned images of representative Western blots are shown in **Figure 10 A–C**. As shown in the first two lanes of the left topmost panel in **Figure 10**, purified recombinant SUCLG1 or SUCLG2 protein has been immunodetected. Purified protein has been loaded in the leftmost lane (30 ng) and the adjacent right one (3 ng). In the remaining subpanels of **Figure 10 A–C**, 30 ng of either SUCLG1 or SUCLG2 was loaded. From the bands obtained from the purified proteins in relation to those obtained from the purified mitochondria, we deduce that (i) the bands detected from the mitochondrial samples corresponding to slightly lower though nearly identical molecular weight (MW) presumably due to the hexahistidine tags of the recombinant proteins genuinely represent the sought proteins and (ii) the amount of either SUCLG1 or SUCLG2 in 3.75 mg of purified mitochondria corresponds to between 3 and 30 ng. The antibody directed against SUCLA2 protein has been validated in ref. [66] using fibroblasts from a patient with *SUCLA2* deletion. Anti-VDAC1 was used as a loading control. As shown in **Figure 10 A–C** and from the quantification of the band densities in relation to that of VDAC1 illustrated in **Figure 10 D–F**, respectively, *Sucla2+/−* mice exhibited up to 76% decrease in Sucla2 expression, depending on the tissue and the age of the mice. Concomitantly, *Sucla2+/−* mice exhibited up to 66% reduction in Suclg1 protein, but also up to 177% increase in Suclg2 protein. We also can conclude from representative Western blot pictures the succinyl-CoA ligase expression pattern among the three examined organs are in accordance with previously reported findings (described in **Chapter 2.4**).
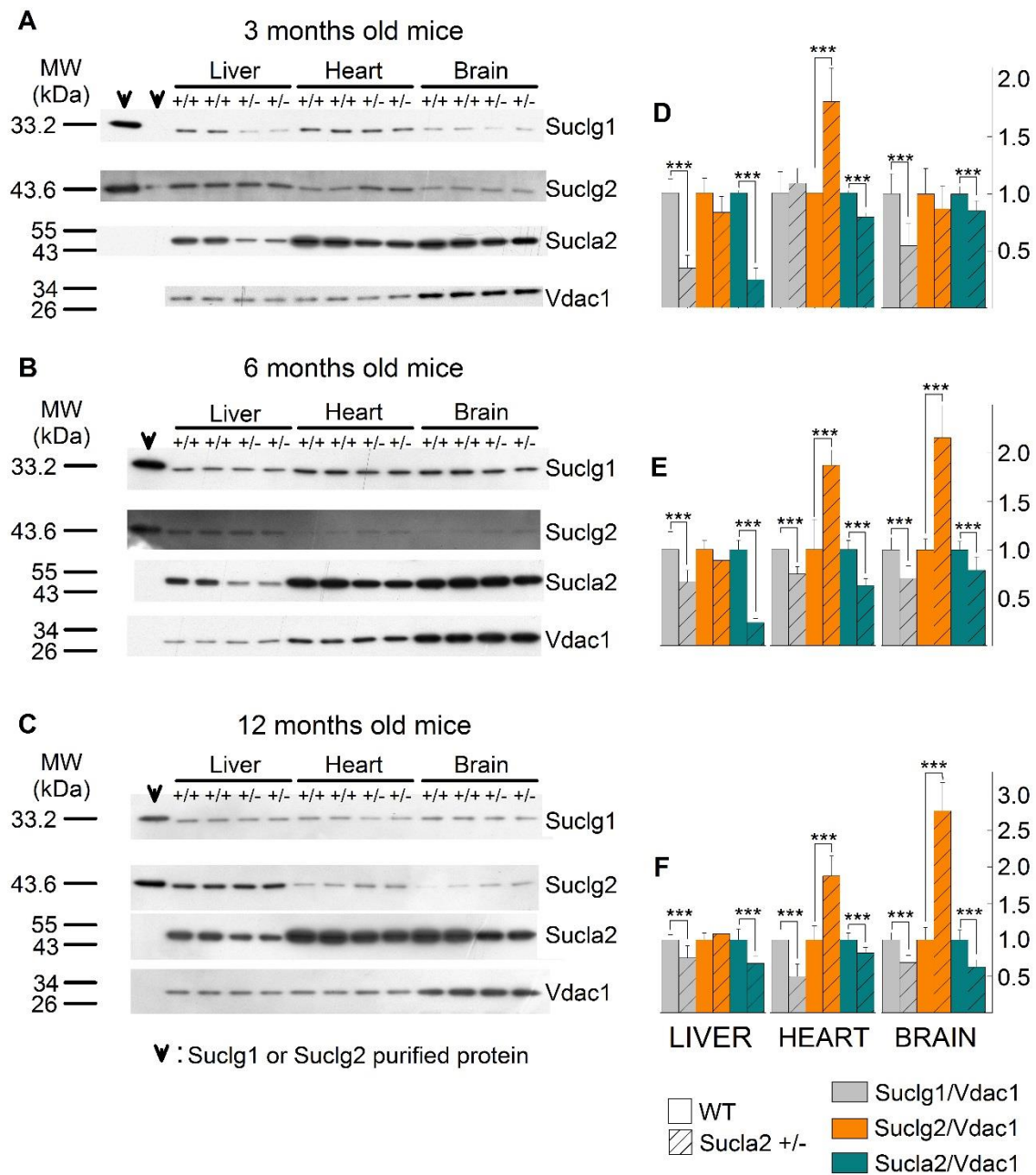
10. Figure Succinyl-CoA ligase **subunit expression in WT vs. *Sucla2*+/− mice.**
(**A–C**) Scanned images of Western blotting of purified SUCLG1 and SUCLG2 and mitochondria of 3-, 6- and 12-month-old WT and *Sucla2*+/− mice from liver, heart and brain. (**D–F**) Band density quantification of the scanned images shown in A–C, respectively. Data were arbitrarily normalized to the average density of the first two bands of WT mice per organ. ***p ≤ 0.001. Each Western blot lane contains mitochondria (except those containing the purified SUCLG1 or SUCLG2 proteins) pooled from two or four organs per animal group. Data shown in the bar graphs are SEM.

5.3 ATP- and GTP-forming succinyl-CoA ligase activities of WT and *Sucla2+/−* mice

ATP-forming activity of *Sucla2+/−* mice decreased, while GTP-forming activity increased, though only in heart mitochondria, for all ages (**Figure 11**). From the experiments in **Chapter 5.2**, we obtained the information that deletion of one *Sucla2* allele is associated with a decrease in Suclg1 expression and a rebound increase in Suclg2 expression, and this is reflected in reciprocal decrease vs. increase in ATP-forming vs. GTP-forming succinyl-CoA ligase activity (see **Figure 11 A** and **B**).
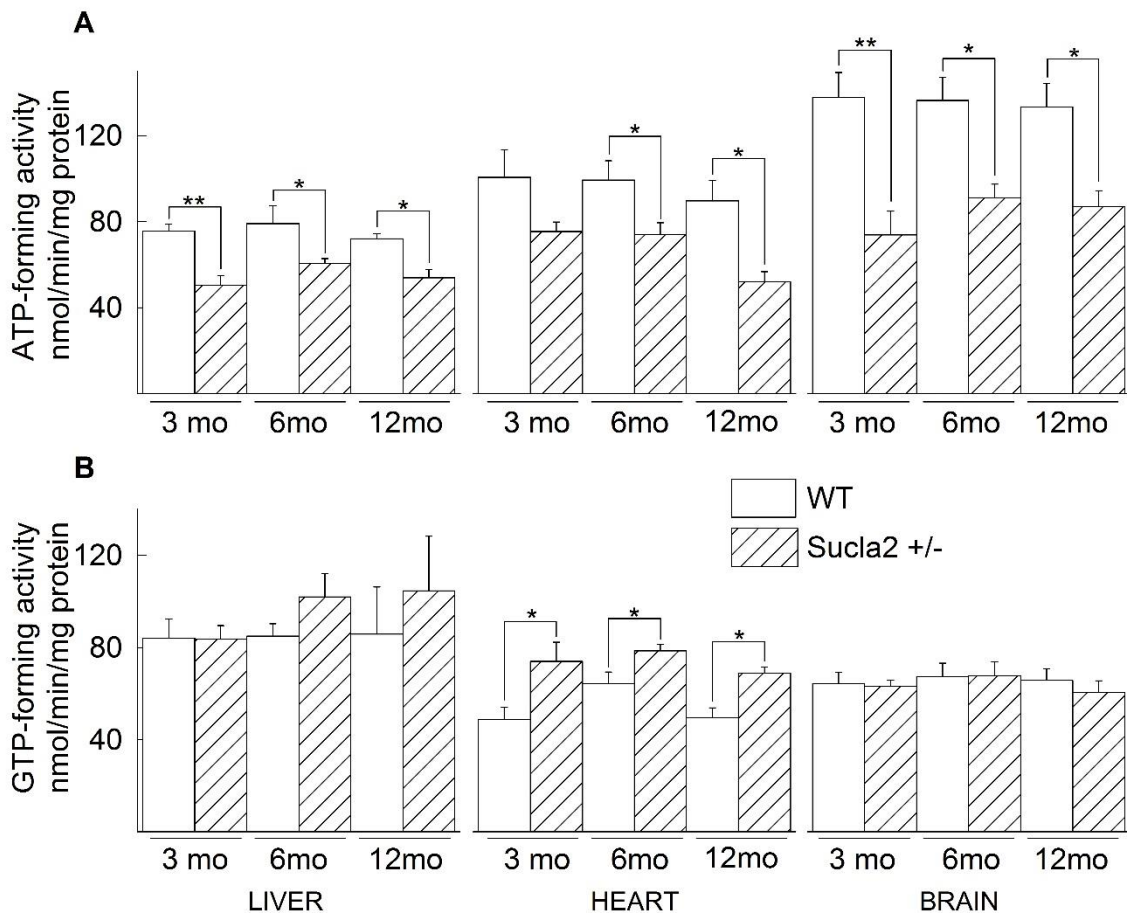
Figure 11 ATP- and GTP- forming SUCL activity in WT vs Sucla2+/− mice.
(A) Bar graphs of ATP-forming SUCL activity from mitochondria of 3-, 6- and 12-month-old WT (solid) and *Sucla2+/−* (striped) mice from liver, heart and brain**. (B)** Bar graphs of GTP-forming SUCL activity from mitochondria of 3-, 6- and 12-month-old WT and *Sucla2+/−* mice from liver, heart and brain. *p ≤ 0.05, **p < 0.01.
Data shown are SEM from two or four pooled organs per animal group from four independent experiments.

5.4 The effect of deleting one *Sucla2* allele on mtDNA content

Because of the involvement of succinyl-CoA ligase in the maintenance of mtDNA, we compared the amount of mtDNA in the tissues of WT vs. *Sucla2+/−* mice. As shown in **Figure 12**, relative mtDNA content from the livers, hearts, and brains of 3-, 6- and 12-month-old mice was quantitated by real-time PCR. It is evident that there is a moderate but statistically significant decrease in mtDNA in all tissues of 3-month-old mice and the brains of 3-month-old and 12-month-old mice.
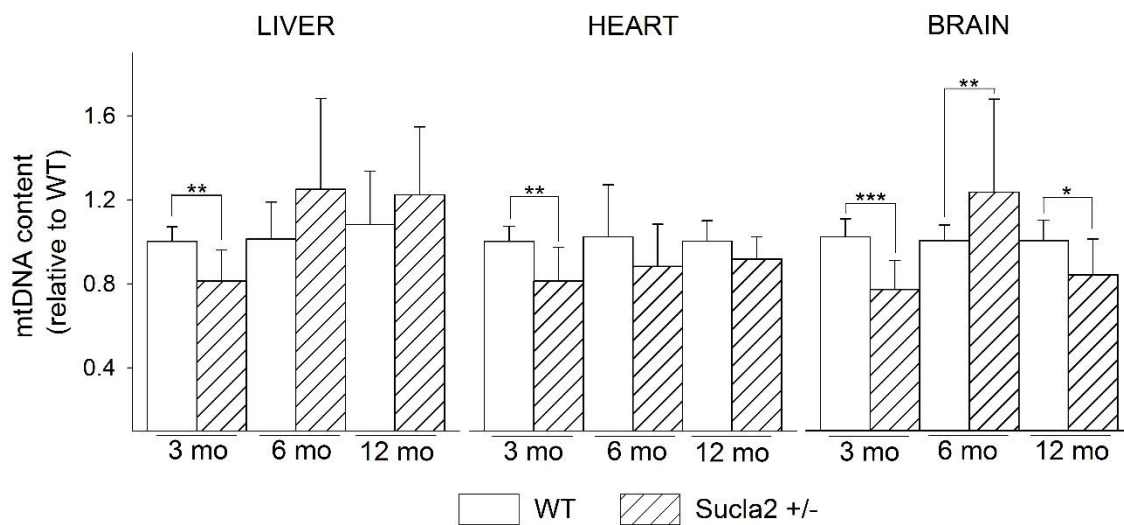
Figure 12 Bar graphs of relative measurements of mtDNA content of livers, hearts and brains from 3-, 6- and 12-month-old WT (solid) compared with that from *Sucla2+/−* (striped) mice *$p \leq 0.05$ **$p < 0.01$ and ***$p \leq 0.001$. Data shown are SD from four pooled organs per animal group from four independent experiments.
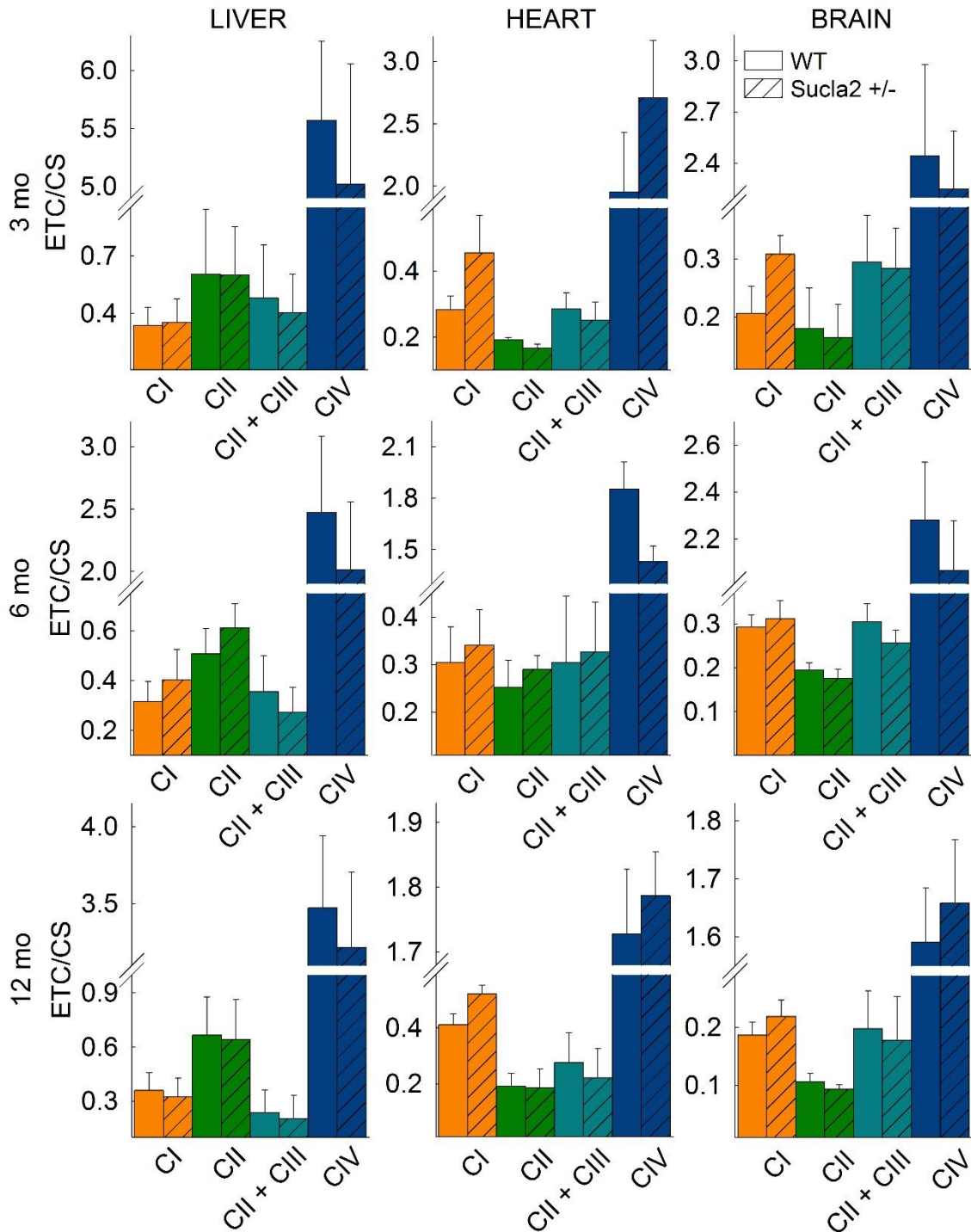
5.5 The effect of deleting one *Sucla2* allele on respiratory complex activities

Figure 13 Bar graphs of measurements of complex I, II, II + III and IV activities (ETC) ratioed to CS activity in isolated mitochondria of 3-, 6- and 12-month-old WT (solid), *Sucla2+/−* (striped) mice from liver, heart and brain. Data shown are SEM from two or four pooled organs per animal group from four independent experiments.

Mindful that some patients suffering from SUCLA2 deficiency exhibited decreases in the activities of electron transport chain complexes, we investigated the effect of deleting one

Sucla2 allele in mice on complex I, II, II/III and IV activities, ratioed to citrate synthase activity. As shown in **Figure 13**, mitochondria from all tissues and all ages revealed no statistically significant differences between WT and *Sucla2+/–* mice.

5.6 The effect of deleting one *Sucla2* allele on blood acylcarnitine ester levels

In view of the association of succinyl-CoA ligase activity with the catabolism of a particular group of biomolecules converging to succinyl-CoA through propionyl-CoA and methylmalonyl-CoA which are in equilibrium with their carnitine esters, we measured the levels of carnitine and 20 carnitine esters in the blood of mice. As shown in **Figure 14**, there are statistically significant increases in 28 out of 63 comparisons of carnitine esters in the blood of *Sucla2+/−* mice from all age groups compared with that from WT mice, but also 7 occasions in which carnitine esters of *Sucla2+/−* mice is decreased compared with those of WT mice. What is also noteworthy is that although SUCLA2 deficiency in humans is associated with elevations of C3 and C4-DC levels, in the *Sucla2+/−* mice there was an elevation of several additional esters including those encompassing long-chain fatty acid chains (C16-OH, C18:1, C:18 and C18-OH).
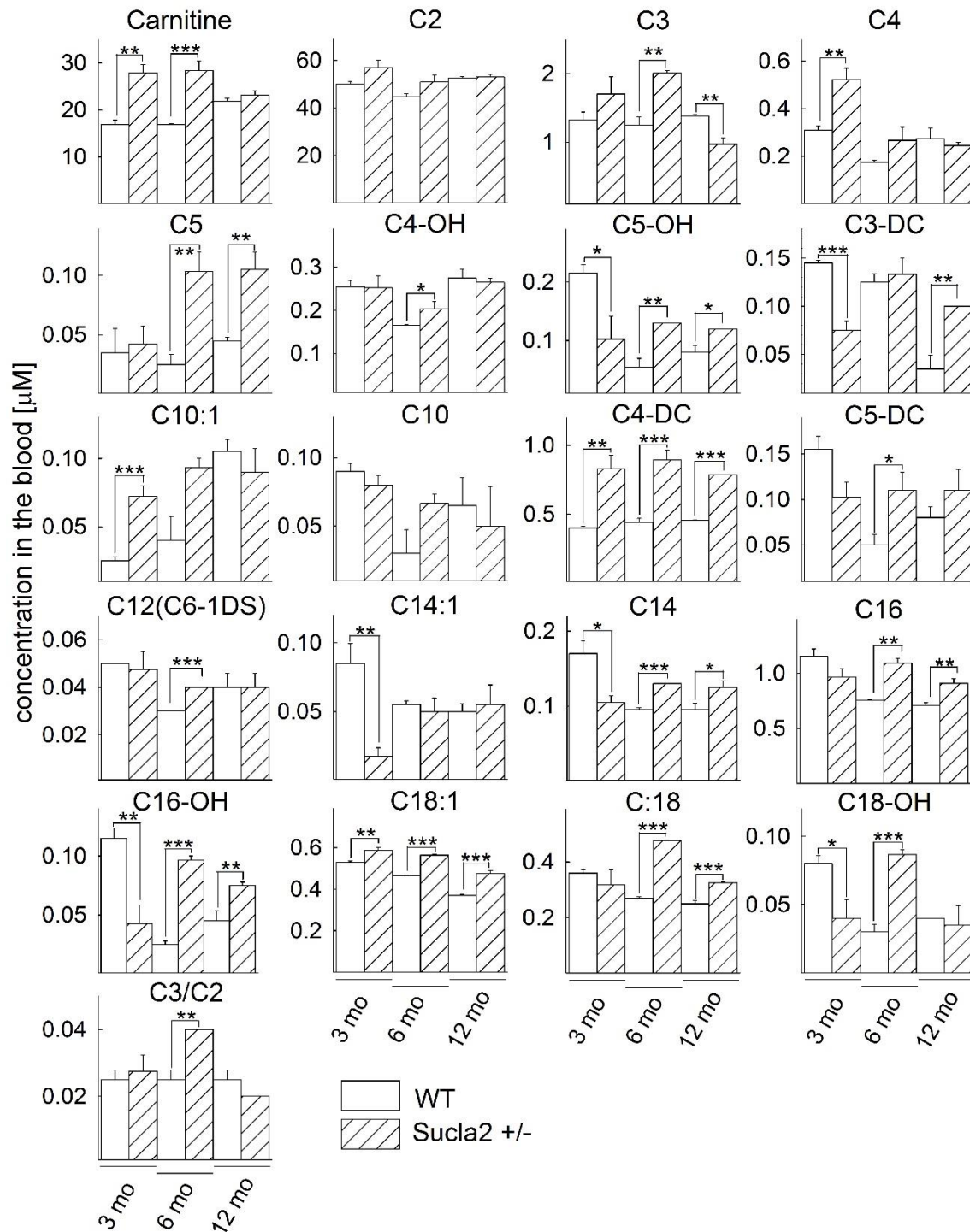
Figure 14 Bar graphs of measurements of carnitine and its esters in the blood of 3-, 6- and 12-month-old WT (solid) and *Sucla2+/−* (striped)

*p ≤ 0.05, **p < 0.01 and ***p ≤ 0.001. Data shown are SEM from four blood draws per animal group from four mice each. Carnitine (free); C2 (acetyl); C3 (propionyl); C4 (butyryl/isobutyryl); C5 (isovaleryl/2-methylbutyryl/pivaloyl); C4-OH(3-hydroxybutyryl); C5-OH (3-hydroxy isovaleryl/2-methyl 3-hydroxybutyryl); C3-DC (malonyl); C10:1 (decenoyl); C10 (decanoyl); C4-DC (methylmalonyl/succinyl); C5-DC (glutaryl); C12 (C6-1DS, dodecanoyl); C14:1 (tetradecenoyl); C14 (myristoyl); C16 (palmitoyl; C16-OH (3-hydroxyhexadecenoyl); C18:1 (oleyl); C18 (stearoyl); C18-OH (3-hydroxystearoyl).

5.7 The effect of deleting one *Sucla2* allele on substrate-level phosphorylation and bioenergetic parameters

5.7.1 The effect of deleting one Sucla2 allele on ΔΨm and substrate-level phosphorylation during inhibition of complex I by rotenone or true anoxia

Mitochondrial substrate-level phosphorylation can be assessed by recording the directionality of the ANT during respiratory inhibition as it was described in materials and methods previously in **Chapter 4.5**. Respiratory inhibition can be reached with either pharmacologically (i.e. by inhibiting complex I with rotenone) or with true anoxia. The assessment of the directionality of the ANT can be performed by a 'biosensor test' developed in our laboratory earlier [36]. This test is based on the concept that one molecule of ATP^{4-} is exchanged for one molecule of ADP^{3-} (both nucleotides being Mg^{2+}-free and deprotonated) by the ANT. Therefore, the abolition of its operation during forward mode of the ANT (one ATP moving outward from mitochondria while one molecule of ADP moving inward to mitochondrial matrix) by a specific inhibitor such as cATR leads to an increase in ΔΨm, whereas with the opposite directionality -the reverse mode of ANT-, cATR leads to a loss of ΔΨm. In this chapter, I evaluated matrix substrate-level phosphorylation during either inhibition of complex I by rotenone or during anoxia. Mitochondria were prepared from the livers, hearts, and brains of 3-, 6-, and 12-month-old WT (black traces) and *Sucla2+/−* (red traces) mice (see **Chapter 4.2**), and ΔΨm was evaluated using different mitochondrial substrates combinations. (see **Chapter 4.4**)

Time-lapse recordings of safranin O fluorescence reflecting ΔΨm were achieved by using a Hitachi F-7000 spectrofluorometer (Hitachi High Technologies, Maidenhead, UK) (see **Chapter 4.5**) for experiments where we measured only the membrane potential and inhibited the mitochondrial respiration pharmacologically with a complex I inhibitor, Rotenone. Another method was used measuring membrane potential and oxygen consumption parallel. For these experiments, an Oxygraph-2k (Oroboros Instruments, Innsbruck, Austria) were used (more details in **Chapter 4.5** and **4.6**). In Hitachi measurements after recording 50 seconds of baseline, mitochondria were added to 2 ml preheated experimental buffer (see **Chapter 4.5**) and allowed to repolarize to 100 seconds. As such the sequence of further additions were ADP (2mM, 150s) causing depolarization; rotenone (1µM, 300s) which is coincided either of a depolarization; cATR (1µM, 450s) caused either a re- or depolarization, implying that the ANT was operating
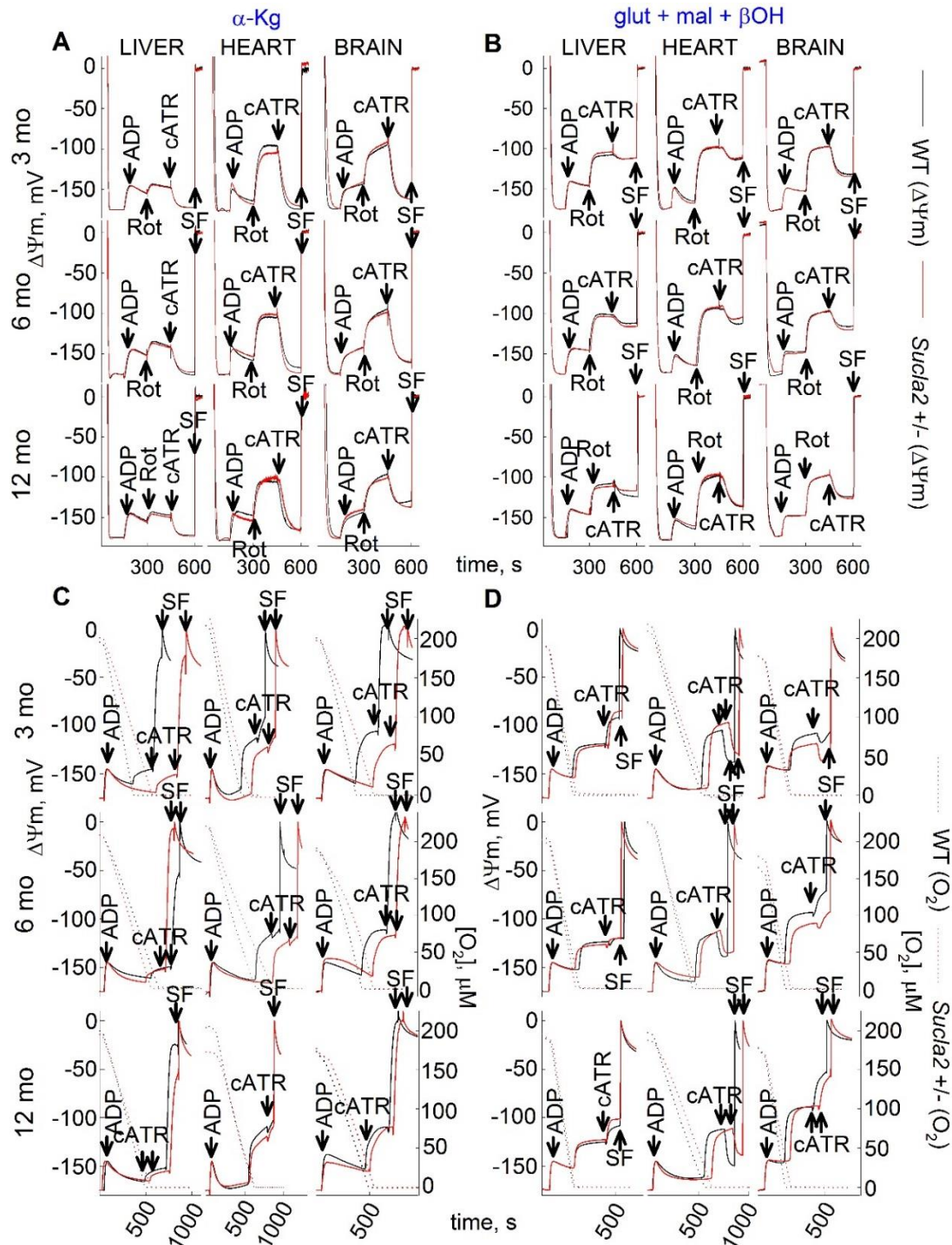
in the forward or reverse mode; SF6847 an uncoupler (1μM, 600s) caused a complete depolarization assisting in calibrating of the fluorescence signal.

In the more complex Oroboros experiments mitochondria were allowed to deplete the oxygen dissolved in the air-sealed chamber and additions of chemicals through a tiny bore hole did not allow re-oxygenation of the buffer from the ambient atmosphere. The sequences of additions were as follows: mitochondria were added in 2 ml of buffer (see 'Experimental Procedures') containing substrates as indicated in the panels and allowed to polarize fully (solid traces). State 3 respiration was initiated by ADP (2 mM) depolarizing mitochondria; within a few minutes (depending on the substrates), mitochondria became anoxic as verified by recording 'zero' levels of dissolved oxygen in the chamber (dotted traces). Anoxia also coincided with the onset of an additional depolarization leading to a clamp of $\Delta\Psi$m (t_a). The subsequent addition of cATR (1 μM, t_a + 200s) caused either a moderate re- or depolarization, implying that the ANT was operating in the forward or reverse mode, respectively. Further addition of the uncoupler SF 6847 (1 μM, t_a + 300s) was subsequently used to cause a complete collapse of $\Delta\Psi$m and assist in the calibration of the fluorescence signal.

As shown in **Figure 15-16 A** and **B** panel; **Figure 17 A** panel, there were no differences between mitochondria from WT and *Sucla2+/−* mice. Likewise, when substrate-level phosphorylation was examined during inhibition of the respiratory chain by real anoxia instead of complex I inhibitor (rotenone), no differences between WT and *Sucla2+/−* mice mitochondria were observed. See **Figure 15-16 C** and **D** panel**; Figure 17 B** panel.
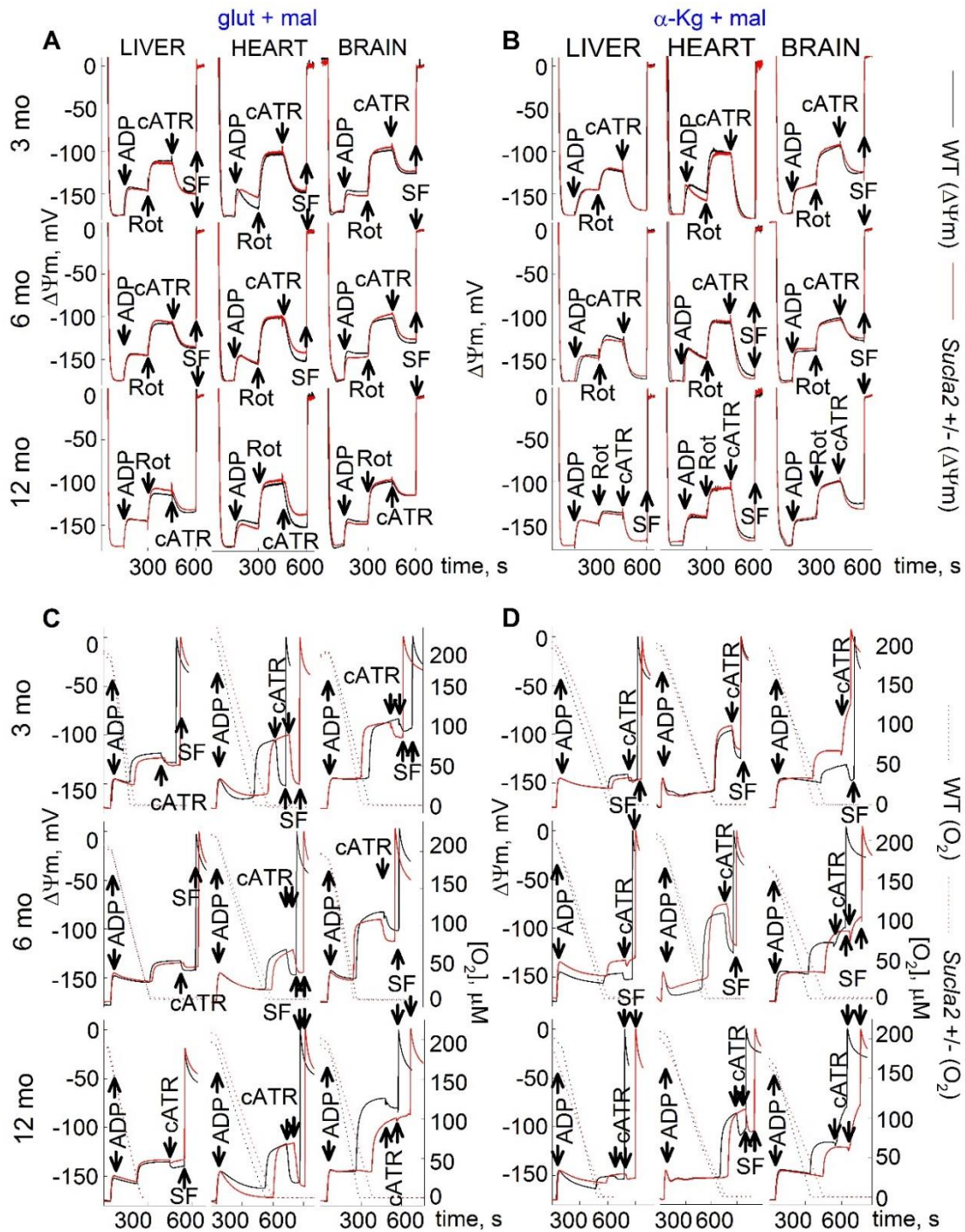
15. Figure Reconstructed time courses of safranine O signal calibrated to ΔΨm (solid traces), and parallel measurements of oxygen concentration in the medium (dotted traces) in mitochondria of 3-, 6- and 12 months old WT (black) and *Sucla2+/−* (red) mice isolated from liver, heart, and brain. ADP: 2 mM; carboxyatractyloside (cATR), 1 μM. Substrates are indicated in the panels; their concentrations were: glutamate (5 mM), malate (5 mM), α-ketoglutarate (α-Kg, 5 mM). At the end of each experiment 1 μM SF6847 was added to achieve complete depolarization. Data shown are representative of at least four independent experiments.

16. Figure Reconstructed time courses of safranine O signal calibrated to ΔΨm (solid traces), and parallel measurements of oxygen concentration in the medium (dotted traces) in mitochondria of 3-, 6- and 12 months old WT (black) and *Sucla2+/−* (red) mice isolated from liver, heart, and brain. ADP: 2 mM; carboxyatractyloside (cATR): 1 µM. Substrates are indicated in the panels; their concentrations were: glutamate (5 mM), malate (5 mM), β-hydroxybutyrate (βOH, 4 mM), α-ketoglutarate (α-Kg, 5 mM). Rot: rotenone, 1 µM. At the end of each experiment 1 µM SF6847 was added to achieve complete depolarization. Data shown are representative of at least four independent experiments.

17. Figure Reconstructed time courses of safranine O signal calibrated to ΔΨm (solid traces), and parallel measurements of oxygen concentration in the medium (dotted traces) in mitochondria of 3-, 6- and 12 months old WT (black) and *Sucla2+/–* (red) mice isolated from liver, heart, and brain. ADP: 2 mM; carboxyatractyloside (cATR): 1 µM. Substrates are indicated in the panels; their concentrations were: pyruvate (5 mM), malate (5 mM). Rot: rotenone, 1 µM. At the end of each experiment 1 µM SF6847 was added to achieve complete depolarization. Data shown are representative of at least four independent experiments.

5.7.2 The effect of itaconate on Sucla2 heterozygous mice

Since there was no difference in substrate-level phosphorylation between WT or *Sucla2+/–* mice, we applied a submaximal amount of itaconate [104] (also see in **Chapter 2.5-i**) to reveal any slight difference in mitochondrial substrate-level phosphorylation between WT and heterozygous mitochondria. As it is depicted in **Figure 18**, in the case of 3- and 12-month-old liver and brain in *Sucla2+/–* mice ANT were reversed, which further means that these mitochondria are less able to perform substrate-level phosphorylation, whereas heart 3-, 6-, and 12-month-old mitochondria did not show any
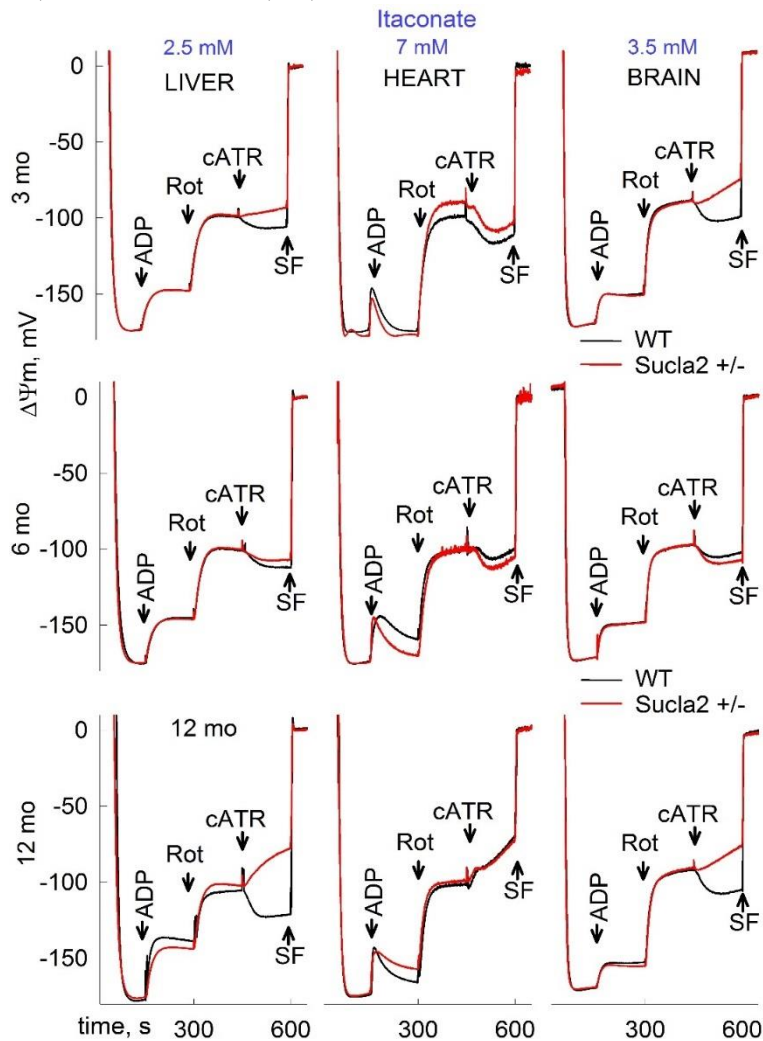
Figure 18 Reconstructed time courses of safranine O signal calibrated to ΔΨm (solid traces) of mitochondria from 3-, 6- and 12 months old WT (black) and Sucla2+/– (red) mice isolated from liver, heart and brain in the presence of itaconate (concentrations indicated in the panels). The concentration of itaconate was titrated so that the differences between WT and Sucla2 +/– on substrate-level phosphorylation were the greatest. ADP: 2 mM; carboxyatractyloside (cATR), 1 µM. Rot: rotenone, 1 µM. At the end of each experiment 1 µM SF 6847 was added to achieve complete depolarization. Data shown are representative of at least four independent experiments.

difference. Furthermore, as we see in **Figure 19**, there was no difference between WT and *Sucla2+/–* in mitochondrial substrate-level phosphorylation when the respiratory chain was inhibited by true anoxia.
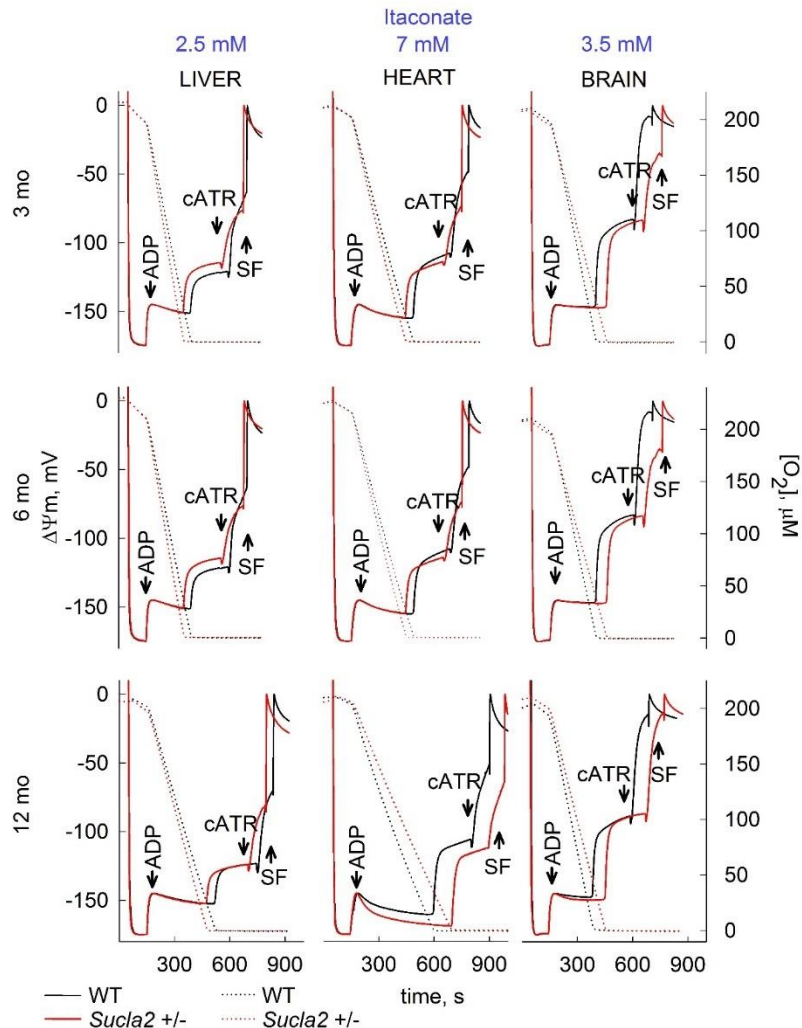
Figure 19 Reconstructed time courses of safranine O signal calibrated to ΔΨm (solid traces), and parallel measurements of oxygen concentration in the medium (dotted traces) in mitochondria of 3-, 6- and 12 months old WT (black) and Sucla2+/– (red) mice isolated from liver, heart and brain in the presence of itaconate (concentrations indicated in the panels).
The concentration of itaconate was titrated so that the differences on substrate-level phosphorylation among WT and *Sucla2 +/–* mouse mitochondria were the greatest. ADP: 2 mM; carboxyatractyloside (cATR), 1 µM. At the end of each experiment 1 µM SF 6847 was added to achieve complete depolarization. Data shown are representative of at least four independent experiments.

5.7.3 The effect of KM4549SC on sucla2 heterozygous mice

KM4549SC (LY266500), an inhibitor of succinyl-CoA ligase [104, 153]. The purpose of using this compound was the same as it was described regarding itaconate in **Chapter 5.7.2**. We would have liked to reveal any slight difference between WT and *Sucla2+/–* mitochondria. As it is seen in **Figure 20** there was no difference in liver and brain, however, in 3-, and 6-month old heart, according to these representative figures WT mitochondria performed less substrate-level phosphorylation than mitochondria isolated from *Sucla2+/–* mice.
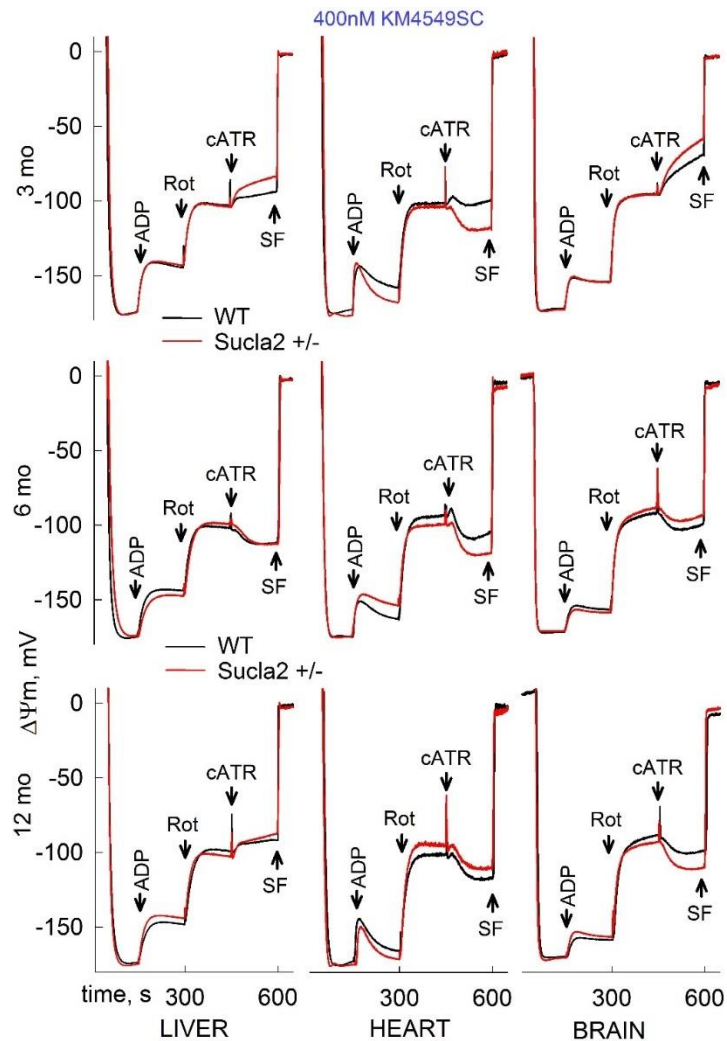
Figure 20 Reconstructed time courses of safranine O signal calibrated to ΔΨm (solid traces) of mitochondria from 3-, 6- and 12 months old WT (black) and *Sucla2+/–* (red) mice isolated from liver, heart and brain in the presence of 400 nM KM4549SC. ADP: 2 mM; carboxyatractyloside (cATR), 1 µM. Rot: rotenone, 1 µM. At the end of each experiment 1 µM SF 6847 was added to achieve complete depolarization. Data shown are representative of at least four independent experiments.

5.7.4 The effect of deleting one Sucla2 allele on oxygen consumption
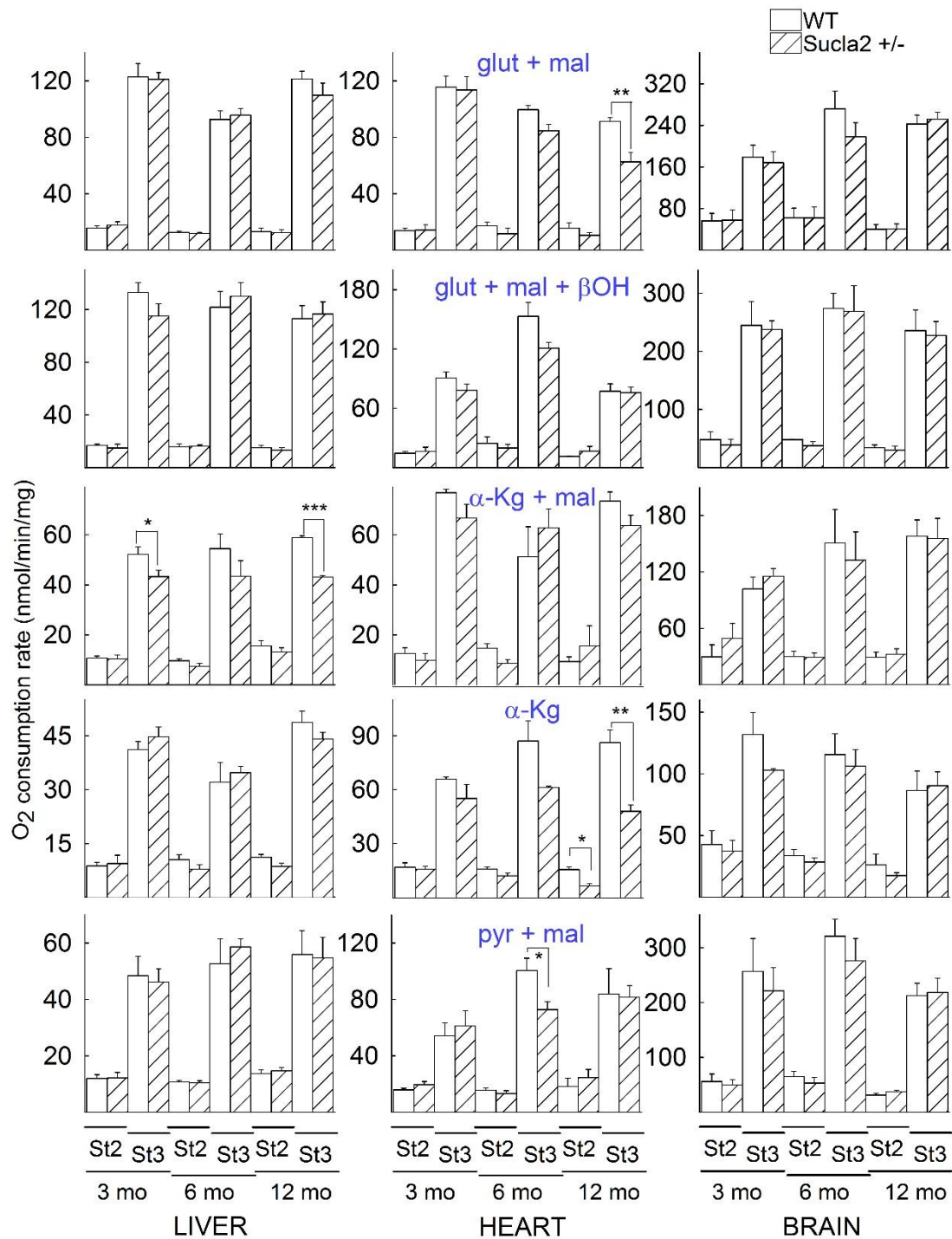
Figure 21 Bar graphs of measurements of oxygen consumption in the medium containing isolated mitochondria of 3-, 6- and 12-month-old WT (solid) and *Sucla2+/−* (striped) mice from liver, heart and brain.
Substrate combinations used as indicated in the panels, all at concentration of 5 mM, except β-hydroxybutyrate (βOH) that was 4 mM. St2: state 2 respiration; St3: state 3 respiration. *p ≤ 0.05, **p < 0.01 and ***p ≤ 0.001. Data shown are SEM from two or four pooled organs per animal group from four independent experiments.

Mitochondria were prepared from the livers, hearts, and brains of 3-, 6- and 12-month-old WT and *Sucla2+/−* mice. States 2 respiration (oxygen consumption in the presence of substrates, but in the absence of ADP) and state 3 respiration (oxygen consumption in the presence of substrates induced by 2 mM ADP) were evaluated using an array of substrates, as indicated in **Figure 21**.

As shown in **Figure 21**, except one combination for state 2 respiration and five combinations for state 3 respiration, the remaining 84 combinations of substrates per tissue of origin per age of mice did not reveal statistically significant differences between WT and *Sucla2+/−* mice.

5.8 The lack of substrate-level phosphorylation in fibroblasts from patient suffering from complete *SUCLA2* deletion

Another evidence to support the notion that succinyl-CoA ligase is critical for substrate-level phosphorylation, is the findings where, by applying the 'biosensor test' in permeabilized fibroblasts from a control subject vs. a patient suffering from complete deletion of *SUCLA2* [154]. The *in situ* mitochondria from the patient were unable to perform substrate-level phosphorylation during respiratory inhibition by rotenone. See results in **Figure 22**.
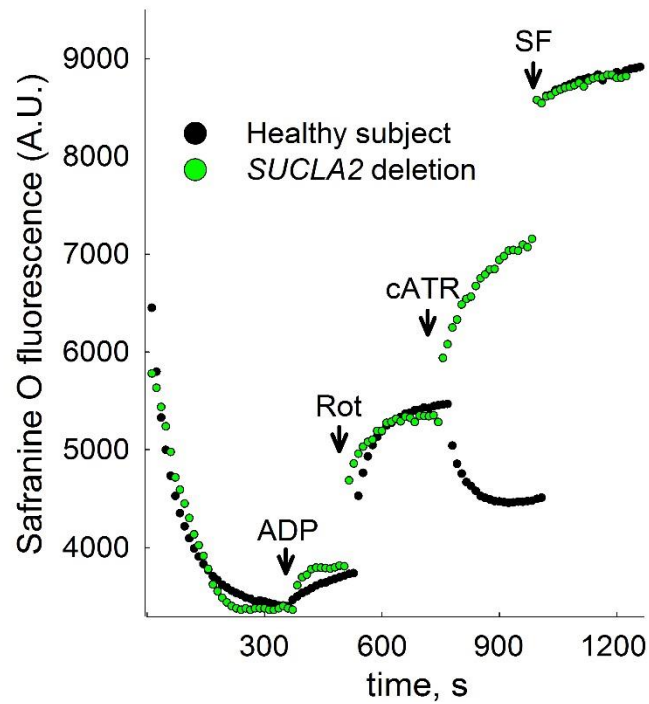
Figure 22 Reconstructed time course of safranin O signal from permeabilized fibroblasts of a control subject (black dots) and a patient suffering from complete *SUCLA2* deletion (green dots).
Rot: ADP: 2 mM; cATR, 1 mM rotenone, 1 mM. At the end of each experiment, 1 mM SF6847 was added to achieve complete depolarization. Data shown are representative of at least four independent experiments. Substrates were glutamate (5 mM) and malate (5 mM).

5.9 The effect of deleting one *Suclg2* allele on *Suclg*2 mRNA level

Mutant *Suclg2* mice were generated using a gene-trapping technique as detailed in **Chapter 4.1** and ref. [142]. To investigate the expression level of *Suclg2* mRNA of *Suclg2* heterozygote, the original ES cell line (Ayu21-KBW131: +/−) was compared with the parental strain (KAB6: +/+). mRNA was purified from parental ES cells (+/+) and 21-KBW131 (+/−). Suclg2 expression levels of these cells were analyzed by real-time PCR using the TaqMan Gene Expression Assays, XS, Suclg2 (AB, 4448892, FAM/MGB-NFQ) kit and normalized by a TaqMan probe for β-actin (AB, 4448489, VIC-MGB). Heterozygous ES cells showed almost half the amount of Suclg2 mRNA compared with parent cells. See mRNA quantification result in **Figure 23**.
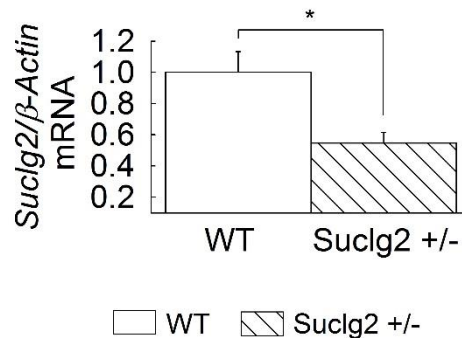
Figure 23 *Suclg2* mRNA quantification
Suclg2+/− heterozygote ES cell line (Ayu21-KBW131: +/−) was compared with parental strain (KAB6: WT). mRNA was purified from parental ES cells (+/+) and *Suclg2* heterozygote (+/−). *Suclg2* mRNA expression level was analyzed by real-time PCR using a TaqMan probe for *Suclg2* (AB, 4448892, FAM/MGB-NFQ) and normalized by a TaqMan probe for β-actin (AB, 4448489, VIC-MGB). Data shown are SEM from four independent experiments. *p ≤ 0.05

5.10 Characterization of succinyl-CoA ligase subunit expressions of WT and *Suclg2* +/− mice
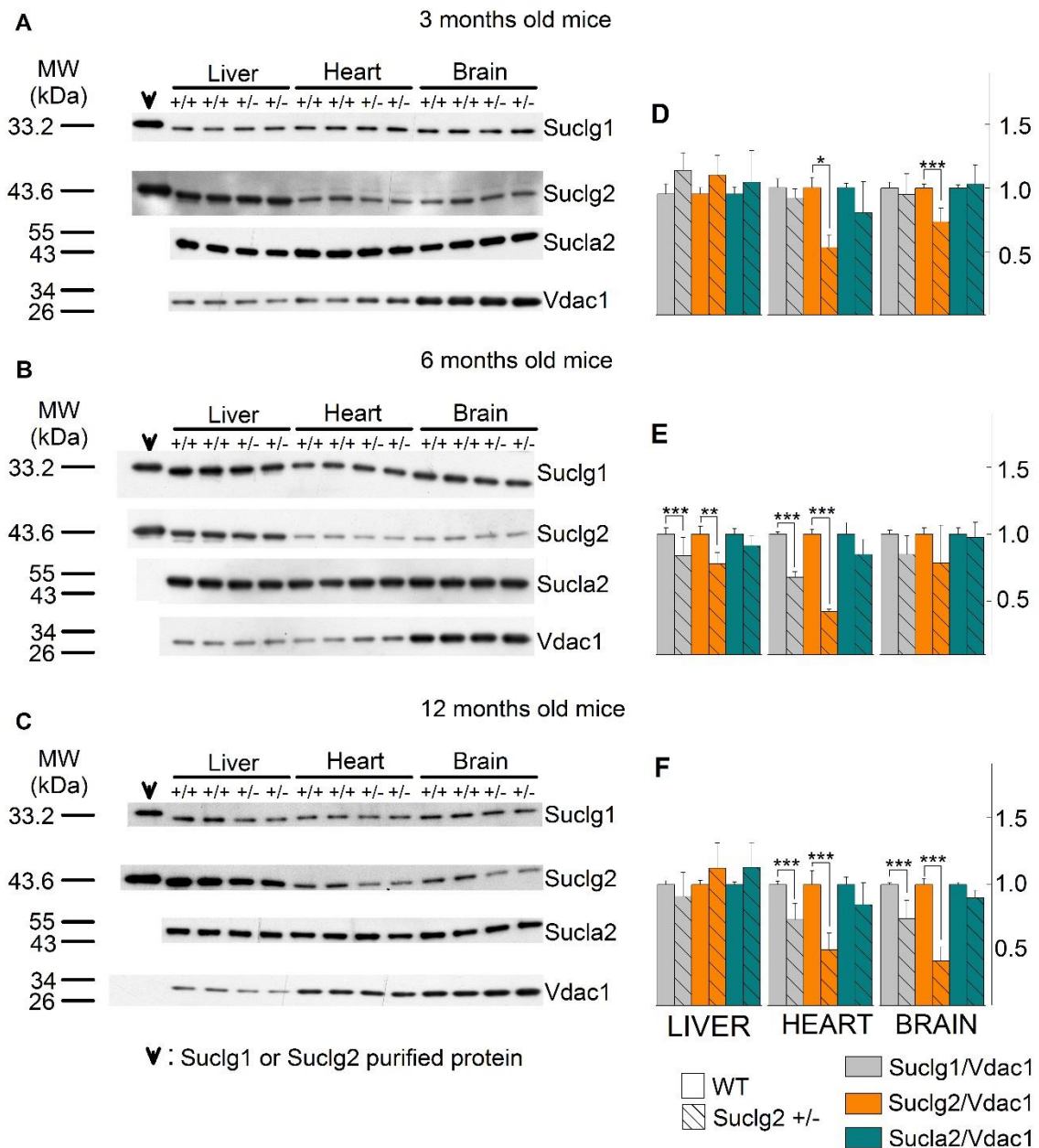
Figure 24 SUCL subunit expression in WT vs. *Suclg2*+/− mice.
(A–C) Scanned images of Western blotting of purified SUCLG1 and SUCLG2 and mitochondria of 3-, 6- and 12-month-old WT and *Suclg2*+/− mice from liver, heart and brain. **(D–F)** Band density quantification of the scanned images shown in A–C, respectively. Data were arbitrarily normalized to the average density of the first two bands of WT mice per organ. *p ≤ 0.05, **p < 0.01 and ***p ≤ 0.001. Each Western blot lane contains mitochondria (except those containing the purified SUCLG1 or SUCLG2 proteins) pooled from two or four organs per animal group. Data shown in the bar graphs are SEM.

Mitochondria were prepared from the livers, hearts, and brains of 3-, 6- and 12-month-old WT and *Suclg2* +/− mice, and SUCLG1, SUCLA2, SUCLG2, and VDAC1 were immunodetected by Western blotting, exactly as described in **Chapter 5.2** and **Figure 10**. Scanned images of representative Western blots are shown in **Figure 24 A–C**. As shown in the first lane of the left topmost panel in **Figure 24 A**, purified recombinant SUCLG1 or SUCLG2 protein has been immunodetected. Purified protein has been loaded in the leftmost lane (30 ng). From the bands obtained from the purified proteins in relation to those obtained from the purified mitochondria, we deduce that (i) the bands detected from the mitochondrial samples corresponding to slightly lower though nearly identical MW presumably due to the hexahistidine tags of the recombinant proteins genuinely represent the sought proteins and (ii) the amount of either SUCLG1 or SUCLG2 in 3.75 mg of purified mitochondria corresponds to slightly <30 ng. Anti-VDAC1 was used as a loading control. As shown in **Figure 24 A–C** and from the quantification of the band densities in relation to that of VDAC1 shown in **Figure 24 D–F**, respectively, *Suclg2+/−* mice exhibited up to 56% decrease in Suclg2 expression, a mostly insignificant decrease in Suclg1 expression, and no rebound increase in Sucla2 expression. The variability in the decrease in Suclg2 (and Sucla2) expression in these transgenic mouse lines probably reflects the 'leakiness' of the mutant allele that could produce WT mRNAs by alternative splicing around the gene trap cassette, as has been shown in several similar situations [150, 155-157]. From the above experiments, we obtained the information that deletion of one *Suclg2* allele was not associated with the rebound effects as seen in the *Sucla2+/−* mice. Because of the lack of a rebound effect on Sucla2 expression in *Suclg2+/−* mice, in conjunction with the fact that SUCLG2 deficiency has only been reported twice in humans, this transgenic strain was further investigated only regarding respiration and substrate-level phosphorylation during chemical or true anoxia.

5.11 The effect of deleting one *Suclg2* allele on substrate-level phosphorylation and bioenergetic parameters

5.11.1 The effect of deleting one Suclg2 allele on ΔΨm and substrate-level phosphorylation during inhibition of complex I by rotenone or true anoxia
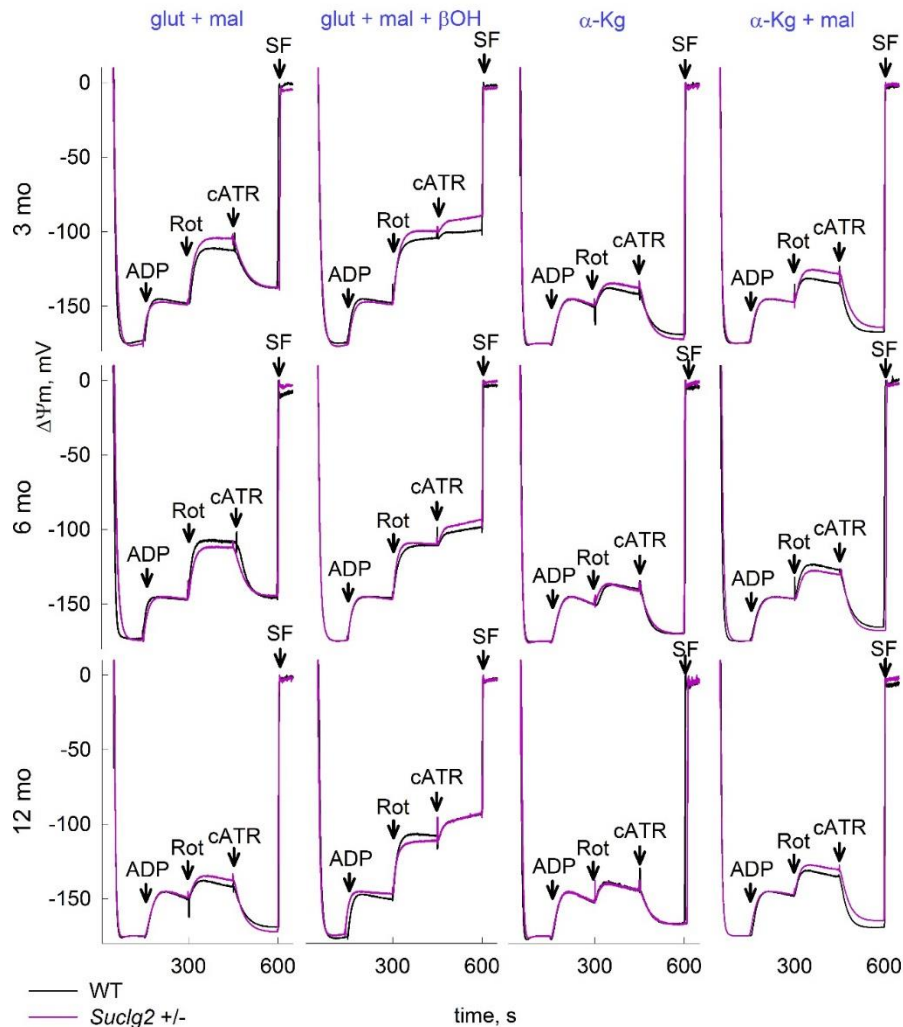
Figure 25 Reconstructed time courses of safranine O signal calibrated to ΔΨm in mitochondria of 3-, 6- and 12 months old WT (black) and *Suclg2+/−* (magenta) mice isolated from liver.
ADP: 2 mM; carboxyatractyloside (cATR), 1 µM. Substrates are indicated in the panels; their concentrations were: glutamate (5 mM), malate (5 mM), α-ketoglutarate (α-Kg, 5 mM), β-hydroxybutyrate (βOH, 4 mM). Rot: rotenone, 1 µM. At the end of each experiment 1 µM SF 6847 was added to achieve complete depolarization. Data shown are representative of at least four independent experiments.

As we have seen in **Chapter 5.10** the deletion of one *Suclg2* allele showed a milder decrease in Suclg2 level than in the case of *Sucla2* deletion. Accordance with these findings it is not surprising that as we saw in *Sucla2+/−* heterozygous mice, there is also

no difference between WT and *Suclg2+/–* mitochondrial substrate-level phosphorylation either used rotenone or true anoxia. See results in **Figure 25** and **26**.
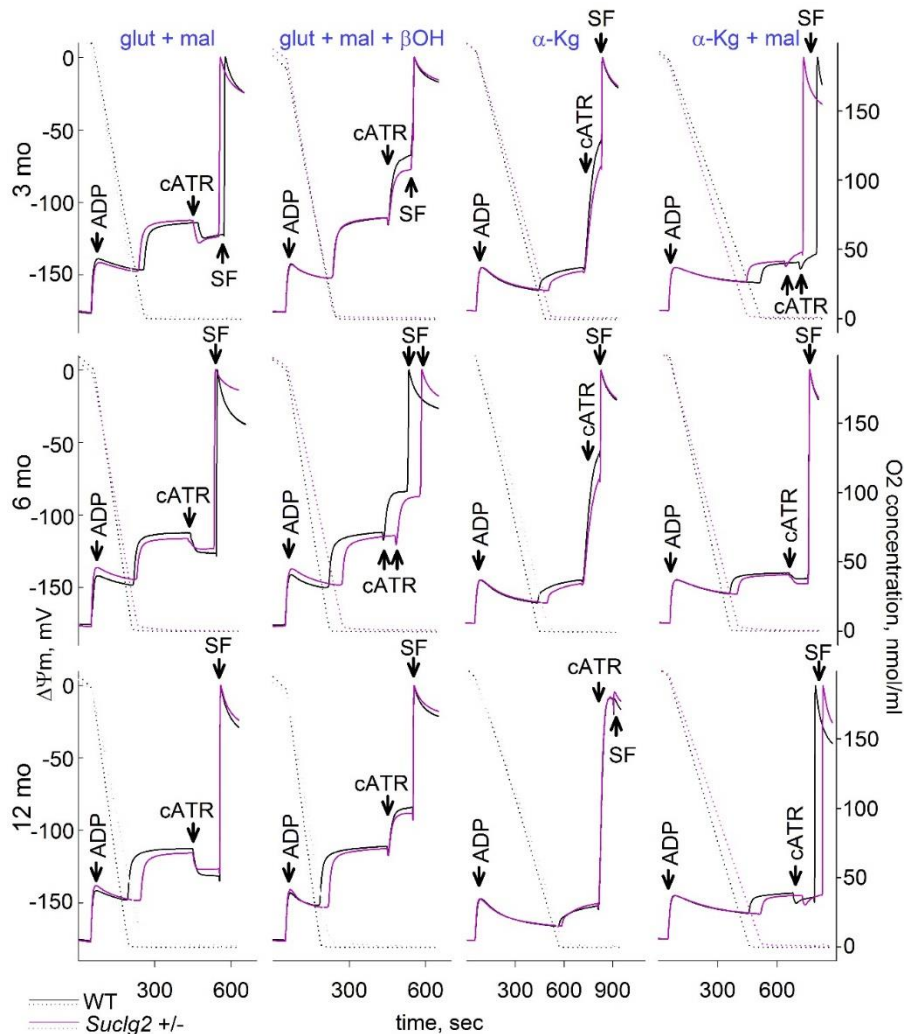
Figure 26 Reconstructed time courses of safranine O signal calibrated to ΔΨm (solid traces), and parallel measurements of oxygen concentration in the medium (dotted traces) in mitochondria of 3-, 6- and 12 months old WT (black) and *Suclg2+/–* (magenta) mice isolated from liver.

ADP: 2 mM; carboxyatractyloside (cATR), 1 μM. Substrates are indicated in the panels; their concentrations were: glutamate (5 mM), malate (5 mM), α-ketoglutarate (α-Kg, 5 mM), β-hydroxybutyrate (βOH, 4 mM). At the end of each experiment 1 μM SF 6847 was added to achieve complete depolarization. Data shown are representative of at least four independent experiments.

5.11.2 The effect of deleting one Sucla2 allele on oxygen consumption

Mitochondria were prepared from livers of 3-, 6- and 12-month-old WT and *Suclg2+/−* mice. States 2 respiration (oxygen consumption in the presence of substrates, but in the absence of ADP) and state 3 respiration (oxygen consumption in the presence of substrates induced by 2 mM ADP) were evaluated using an array of substrates, as indicated in **Figure 27**.

As shown in **Figure 27**, except one combination for state 2 respiration and four combinations for state 3 respiration, the remaining 25 combinations of substrates per tissue of origin per age of mice did not reveal statistically significant differences between WT and *Suclg2+/−* mice.
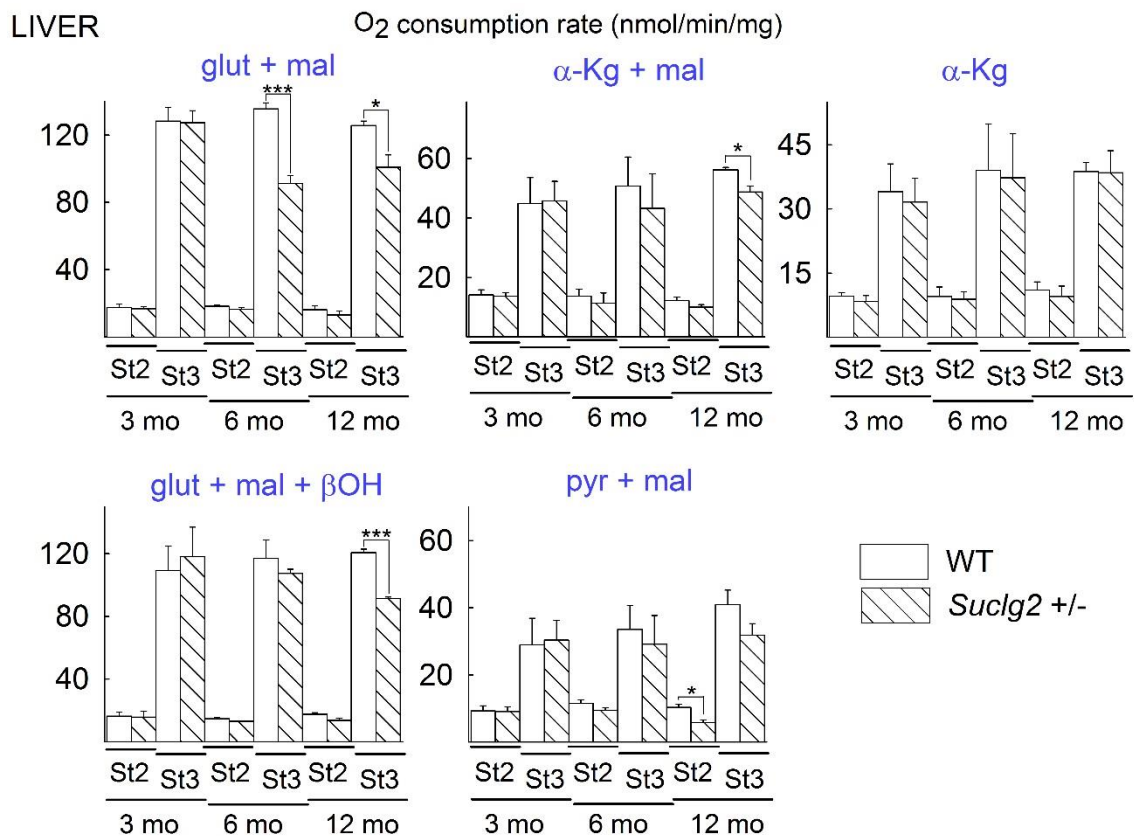
Figure 27 Bar graphs of measurements of oxygen consumption in the medium containing isolated mitochondria of 3-, 6- and 12 months old WT (solid) and *Suclg2+/– (striped) mice from liver.*
Substrate combinations used as indicated in the panels, all at concentration of 5 mM, except β-hydroxybutyrate (βOH) that was 4 mM. St2: state 2 respiration; St3: state 3 respiration. . *p ≤ 0.05, **p < 0.01 and ***p ≤ 0.001. Data shown are SEM from two or four pooled organs per animal group from four independent experiments.

5.12 The effect of deleting both one Sucla2 and one *Suclg2* allele on succinyl-CoA ligase subunit expressions

Since the deletion of one *Sucla2* allele led to a rebound increase in Suclg2 expression, we investigated the effect of combined loss of one allele from each *Sucla2* and *Suclg2* gene. Thus, we cross-bred *Sucla2+/−* mice with *Suclg2+/−* mice, which yielded viable *Sucla2+/−/Suclg2+/−* offspring. The results of Western blotting of mitochondria isolated from the brains, livers, and hearts of 12-month-old WT vs. *Sucla2+/−/Suclg2+/−* mice probing for SUCLG1, SUCLG2 and SUCLA2 (and VDAC1 as a loading control) are shown in **Figure 28 A** (performed exactly as described in **Figure 10** and **Chapter 5.2**). The quantification of the band densities in relation to that of VDAC1 is shown in **Figure 28 B**. As shown in **Figure 28 B**, deletion of one *Sucla2* allele still yields a rebound increase in Sucgl2 expression in liver, albeit protracted because these mice also lack one *Suclg2* allele. By the same token, the anticipated decrease (due to deletion of one *Suclg2* allele) in Suclg2 expression is lost, presumably because of the effect(s) of deletion of the *Sucla2* allele, antagonizing the diminution in the expression of Suclg2.
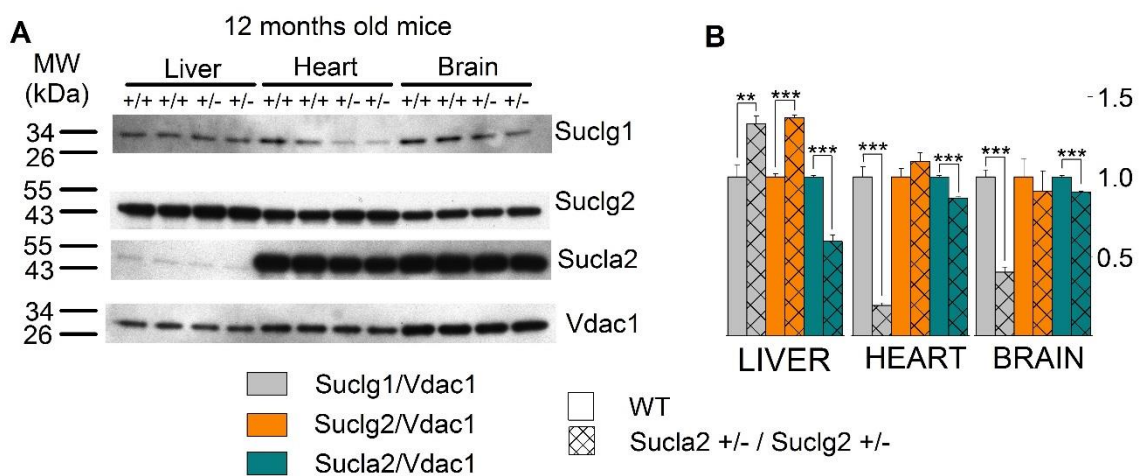
Figure 28 Characterization of succinyl-CoA ligase subunit expression of *Sucla2+/−/Suclg2+/−* mice (dhz: double heterozygote)
(A) Scanned images of Western blotting of 12-month-old WT and *Sucla2+/−/Suclg2+/−* mice from liver, heart and brain. **(B)** Band density quantification of the scanned images shown in A. Data were arbitrarily normalized to the average density of the first two bands of WT mice per organ. *$p \leq 0.05$, **$p < 0.01$ and ***$p \leq 0.001$. Each Western blot lane contains mitochondria pooled from two or four organs per animal group. Data shown in the bar graph are SEM.

5.13 ATP- and GTP-forming succinyl-CoA ligase activities of WT and *Sucla2+/–/Suclg2+/–* mice

After performing Western blot, we also measured ATP- and GTP-forming activities of WT vs. *Sucla2+/−/Suclg2+/−* mice, shown in **Figure 29 A** and **B** respectively. ATP-forming activity is diminished in the double heterozygote mice, compared with WT littermates due to loss of one *Sucla2* allele; however, GTP-forming activity remains unaffected, despite the loss of one *Suclg2* allele.
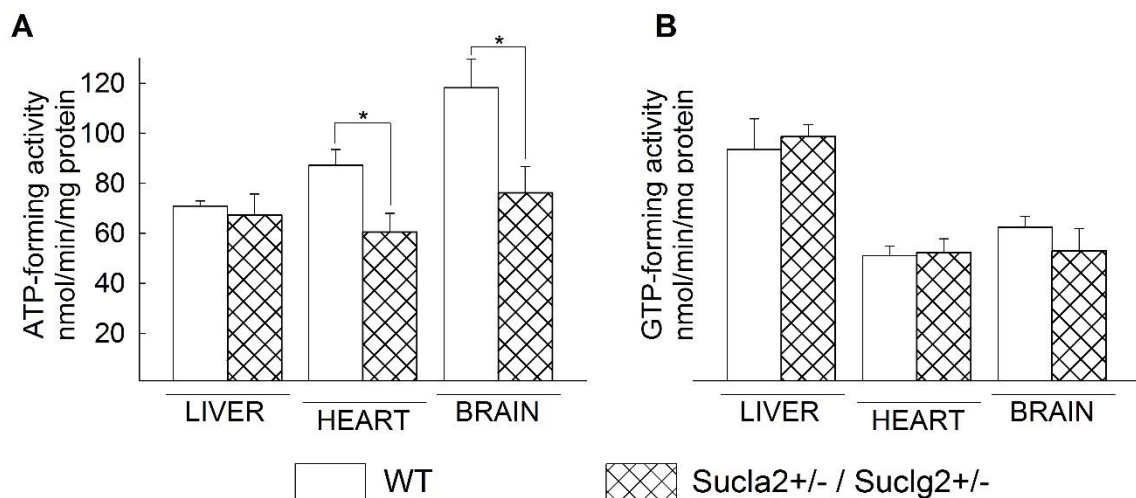
Figure 29 ATP- and GTP- forming succinyl-CoA ligase activity in WT vs *Sucla2+/−/Suclg2+/−* mice (dhz: double heterozygote)
(A) Bar graphs of ATP-forming succinyl-CoA ligase activity from mitochondria of 12-month-old WT (solid) and *Sucla2+/−/Suclg2+/−* (double-striped) mice from liver. **(B)** Bar graphs of GTP-forming succinyl-CoA ligase activity from mitochondria of 12-month-old WT (solid) and *Sucla2+/−/Suclg2+/−* (double-striped) mice from liver. ***p ≤ 0.05** Data shown in A and B are SEM from two or four pooled organs per group from four independent experiments.

5.14 The effect of deleting both one Sucla2 and one *Suclg2* allele on mtDNA content

As shown in **Figure 30**, by comparing WT vs. *Sucla2+/−/Suclg2+/−* double heterozygote mice, there was a much greater statistically significant decrease in mtDNA in the livers and brains of double heterozygote mice, compared with WT littermates than in *Sucla2+/−* mice.
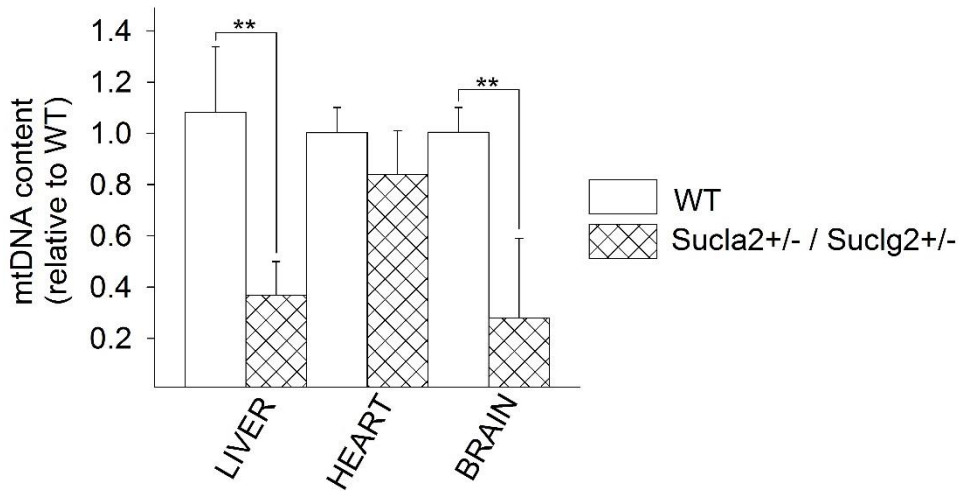
Figure 30 Bar graphs of relative measurements of mtDNA content of livers, hearts and brains from 12-month-old WT (solid) compared with that from *Sucla2+/−/Suclg2+/−* (double-striped) mice
**p < 0.01 Data shown are SD from four pooled organs per animal group from four independent experiments.

5.15 The effect of deleting both one Sucla2 and one *Suclg2* allele on respiratory complex activities

As shown in **Figure 31**, by comparing WT vs. *Sucla2+/−/Suclg2+/−* double heterozygote mice, there was a statistically significant increase in succinate dehydrogenase activity in heart mitochondria, echoing the results of Donti et al. [21] in *Sucla2−/−* mouse embryonic fibroblasts.
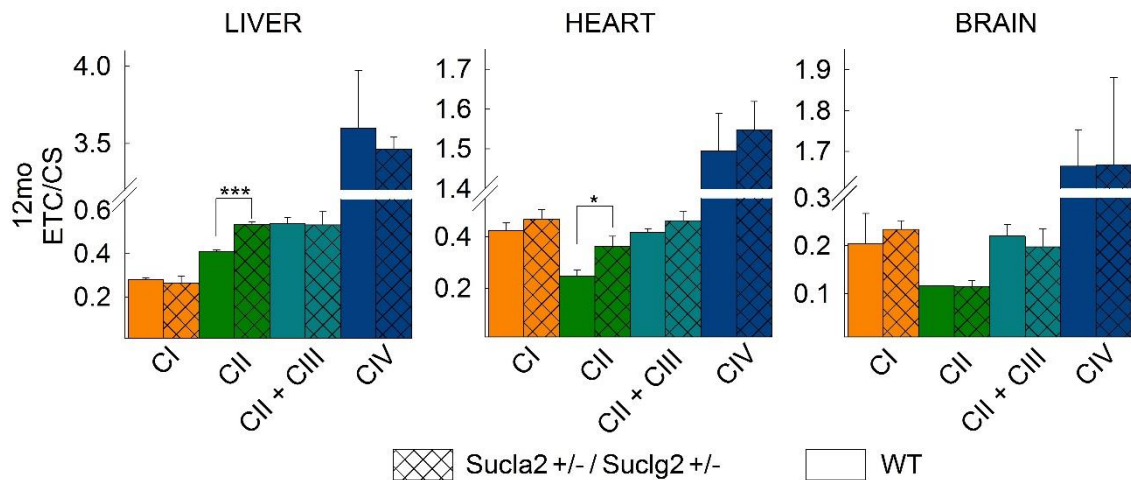
Figure 31 Bar graphs of measurements of complex I, II, II + III and IV activities (ETC) ratioed to CS activity in isolated mitochondria of 12-month-old WT (solid), and *Sucla2+/−/Suclg2+/−* (double-striped) mice from liver, heart and brain.
*p ≤ 0.05; ***p ≤ 0.001 Data shown are SEM from two or four pooled organs per animal group from four independent experiments.

5.16 The effect of deleting both one Sucla2 and one *Suclg2* allele on blood acylcarnitine ester levels

By comparing WT vs. *Sucla2+/−/Suclg2+/−* double heterozygote mice, there was a greater statistically significant increase in 12 out of 21 comparisons of carnitine esters in the blood of *Sucla2+/−/Suclg2+/−* double heterozygote mice from all age groups compared with that from WT mice. See results in **Figure 32**.
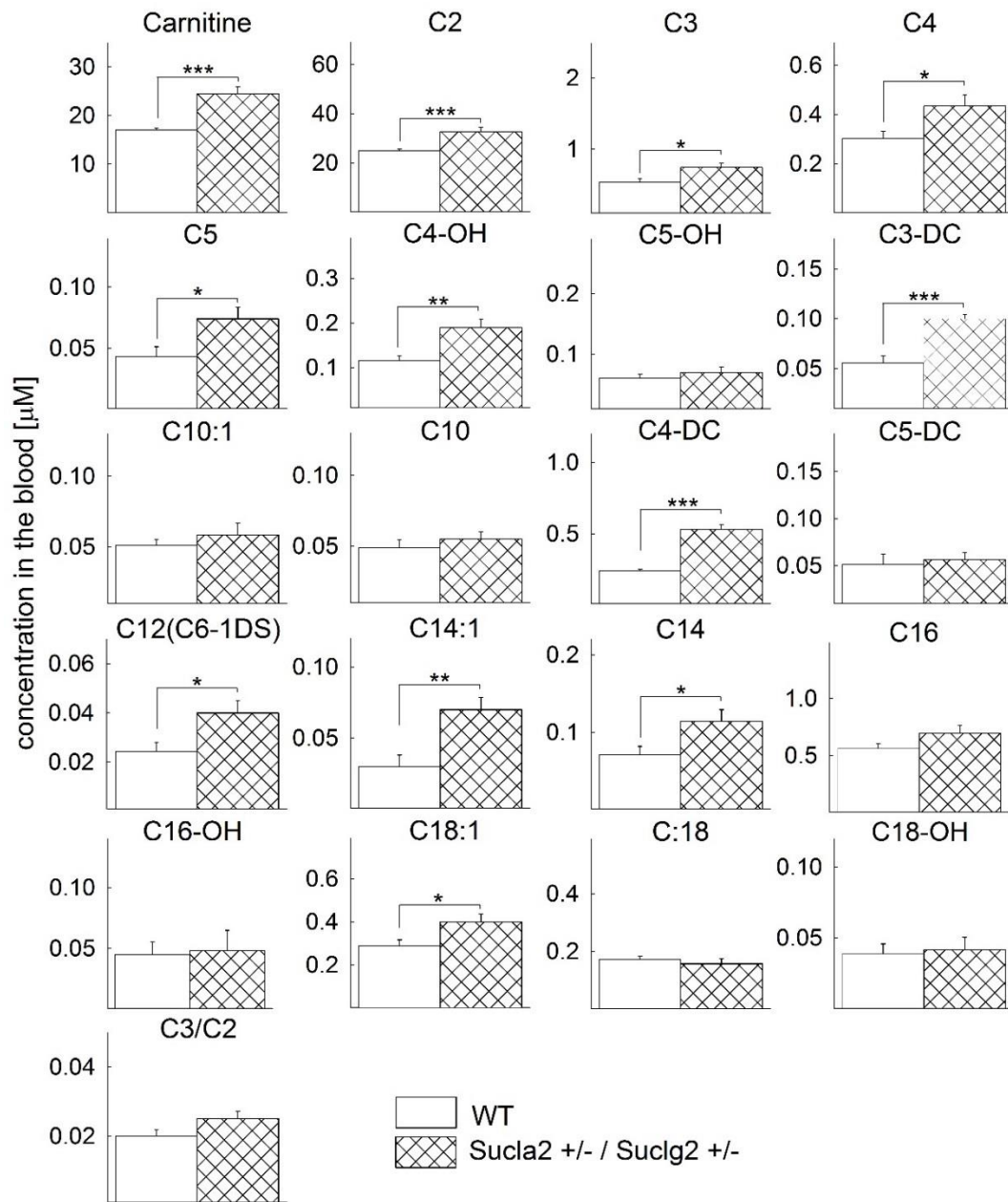
Figure 32 Bar graphs of measurements of carnitine and its esters in the blood of 12-month-old WT (solid) and *Sucla2+/−/Suclg2+/−* (double-striped) mice.
*p ≤ 0.05, **p < 0.01 and ***p ≤ 0.001. Data shown are SEM from four blood draws per animal group from four mice each. Carnitine (free); C2 (acetyl); C3 (propionyl); C4 (butyryl/isobutyryl); C5 (isovaleryl/2-methylbutyryl/pivaloyl); C4-OH (3-hydroxybutyryl); C5-OH (3-hydroxy isovaleryl/2-methyl 3-hydroxybutyryl); C3-DC (malonyl); C10:1 (decenoyl); C10(decanoyl); C4-DC (methylmalonyl/succinyl); C5-DC (glutaryl); C12 (C6-1DS, dodecanoyl); C14:1 (tetradecenoyl); C14 (myristoyl); C16 (palmitoyl; C16-OH (3-hydroxyhexadecenoyl); C18:1 (oleyl); C18 (stearoyl); C18-OH (3-hydroxystearoyl).

5.17 The effect of deleting both one Sucla2 and one *Suclg2* allele on ΔΨm and substrate-level phosphorylation during inhibition of complex I by rotenone

By comparing WT vs. *Sucla2+/−/Suclg2+/−* double heterozygote mice, we also observed no difference in the ability of substrate-level phosphorylation to maintain ANT in the forward mode, with the exception of using glutamate + malate + β-hydroxybutyrate (βOH does not favor substrate-level phosphorylation, see **Chapter 4.4**) as substrates in liver mitochondria, where we obtained the full spectrum of results, ranging from maintenance of substrate-level phosphorylation to its abolition, see **Figure 33**.
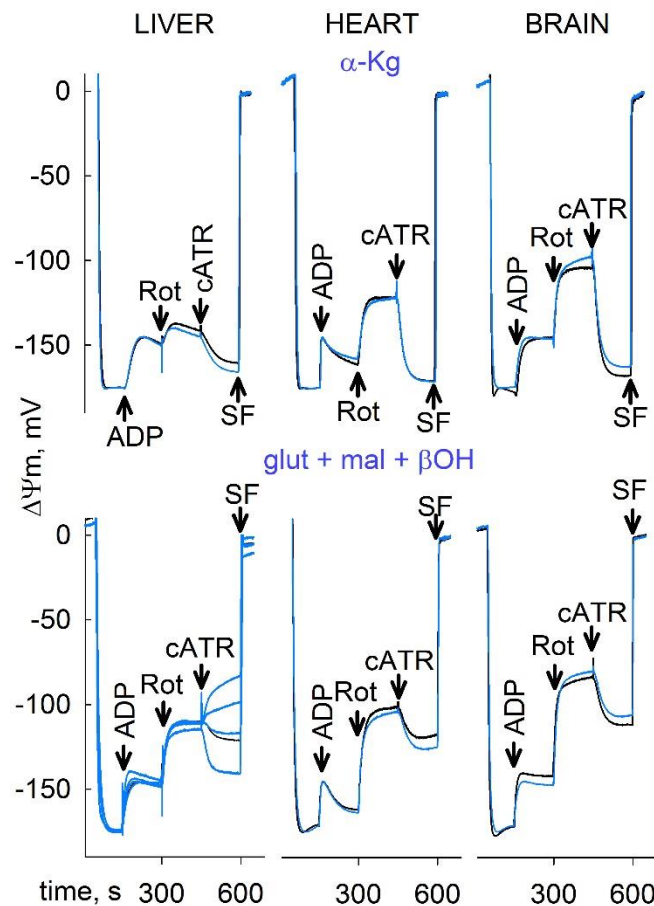
Figure 33 Reconstructed time courses of safranine O signal calibrated to ΔΨm in mitochondria of 12 months old WT (black) and *Sucla2+/–/Suclg2+/–* (blue) mice isolated from liver. ADP: 2 mM; carboxyatractyloside (cATR), 1 μM. Substrates are indicated in the panels; their concentrations were: glutamate (5 mM), malate (5 mM), α-ketoglutarate (α-Kg, 5 mM), β-hydroxybutyrate (βOH, 4 mM). Rot: rotenone, 1 μM. At the end of each experiment 1 μM SF 6847 was added to achieve complete depolarization. Data shown are representative of at least four independent experiments.

6. DISCUSSION

As it has been discussed above, succinyl-CoA ligase deficiencies cause severe phenotypic alterations (see **Chapter 2.6**); however, heterozygous patients are asymptomatic. In our study, we generated transgenic mice lacking either one *Sucla2* or one *Suclg2* allele or both one *Sucla2* and one *Suclg2* (double heterozygote). Homozygous knockout mice for both gene were never born, as also observed in Donti et al. [21] suggesting that complete absence of both gene is incompatible with life in mice. Therefore, we used these heterozygous mice for our experimental work. At the time this work was commenced, the *Suclg2* mutation in humans had not been published. Since the most common succinyl-CoA ligase affected mutation in humans is on *SUCLA2* allele our primary focus was on *Sucla2+/−* mice. The most significant results of the present work are those which were obtained by the comparisons of these *Sucla2+/−* animals with wild type littermates. To reveal all differences at all functional levels thoroughly, we examined the *Sucla2* mRNA content, protein expressions, and direct and indirect effects of the mutation.

With mRNA evaluation, both *Sucla2+/−* and *Suclg2+/−* mice could be validated. The lack of one *Sucla2* or one *Suclg2* allele led to significant decrease, (26–71%) and (~50%) in *Sucla2* and *Suclg2* mRNA content respectively (see **Chapter 5.1** and **Chapter 5.9**).

At protein level, the differences were not remarkable in all cases, however, we could conclude that *Sucla2+/−* mice exhibited up to 76% decrease in Sucla2 expression, depending on the tissue and the age of the mice. Furthermore, one of our most striking results is the rebound increase in Suclg2 expression (**Chapter 5.2**) and associated also increased GTP-forming activity (see **Chapter 5.3** and below).

One *Sucla2* allele deletion had no effect on bioenergetic parameters including substrate-level phosphorylation and oxygen consumption, whereas the deficiency of alpha-ketoglutarate dehydrogenase complex -exhibiting 21-48% decrease in alpha-ketoglutarate dehydrogenase complex activity- led the abolition of mitochondrial substrate-level phosphorylation. To explain this phenomenon, an important fact should be understood. In the citric acid cycle alpha-ketoglutarate dehydrogenase complex has the highest flux control coefficient [158-163]. It means that this enzyme has the largest impact on the citric acid cycle pathway's flux [164]. The succinyl-CoA ligase presence may be redundant compared to alpha-ketoglutarate dehydrogenase complex or other

enzymes, thus it could explain that the decrease of Sucla2 (or Suclg2) had no significant effect on bioenergetic parameters. Furthermore, from experiments where oxygen consumption rates were examined, we concluded that a partial decrease in Sucla2 expression did not impact the mitochondrial respiration negatively to an appreciable extent. In addition to this, it is possible that the flux control coefficient of succinyl-CoA ligase regarding mitochondrial respiration is small enough, so that inhibition of this enzyme to the extent observed hereby in the *Sucla2+/−* transgenic mice was insufficient to warrant a measurable effect on mitochondrial respiration. When we aimed to highlight any slight difference between the two examined groups, we used succinyl-CoA ligase inhibitors. A submaximal inhibition of succinyl-CoA ligase by KM4549SC or itaconate [104] revealed that mitochondria obtained from *Sucla2+/−* mice are less able to perform substrate-level phosphorylation in some cases (see **Chapter 5.7.2** and **Chapter 5.7.3** in **Figure 18**, **Figure 19** and **Figure 20**).

Another possible mechanism which could compensate for the effect of one *Sucla2* allele deletion is mediated by the other GTP-forming subunit's compensatory upregulation and associated increases in GTP-forming succinyl-CoA ligase activity that in turn could impact on mitochondrial ATP output through the concerted action of the nucleotide diphosphate kinase. To visualize the efficacy of the compensation of the GTP-forming subunit, the total succinyl-CoA ligase activity is depicted in **Figure 34**. As shown in
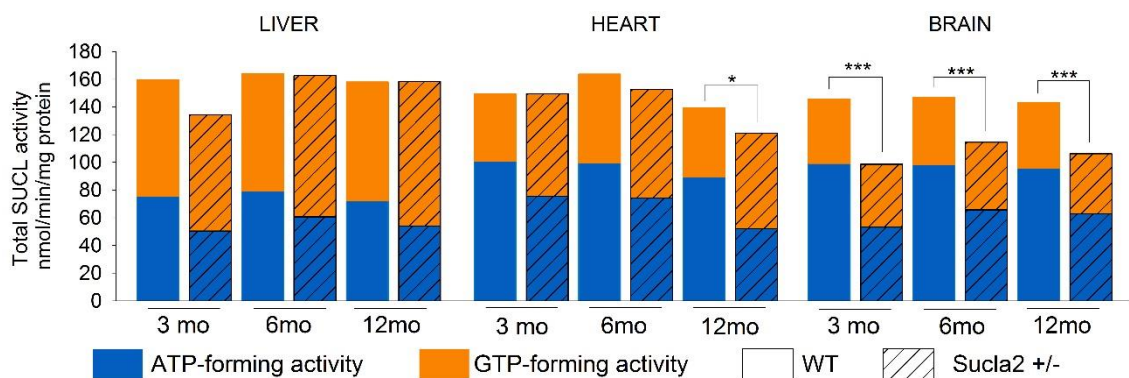
Figure 34 Total high-energy phosphates (ATP, GTP) forming activity of SUCL.
Bar graphs of total SUCL activity from mitochondria of 3-, 6- and 12-month-old WT and Sucla2+/− mice from liver, heart and brain. *$p \leq 0.05$, ***$p \leq 0.001$. Data were adapted from **Chapter 5.3**, **Figure 11**.

Figure 34, except brain and 12-month-old heart the significance differences -between WT and Sucla2 +/− mitochondria- vanished with the addition of GTP-forming activity to

ATP-forming activity. As for the brain, if we consider that this tissue contains much less Suclg2 than the heart and the liver (see **Figure 10** panel **A**, **B,** and **C** in **Chapter 5.2**); it is not surprising that the efficacy of the compensatory mechanism -*Suclg2* upregulation- is insufficient. As seen in **Chapter 2.4** on **Figure 3** and also in **Chapter 5.2** on **Figure 10**, both Sucla2 and Suclg2 are expressed in heart tissue. Therefore, in SUCLA2 deficient patient *SUCLG2* compensatory upregulation can be the reason for the fact that the ATP-forming subunit deficiency is not accompanied by heart failure (see also in **Chapter 2.6**). According to Western blot analyzes the rebound increase in Suclg2 expression in *Sucla2+/−* mice seemed to occur mostly in heart mitochondria, also in brain mitochondria but only from the older (6–12-month-old) mice and not in liver mitochondria. Furthermore, the increase in GTP-forming activity also seemed heart-specific, as well as the changes in complex II activity observed in *Sucla2+/−/Suclg2+/−* mice.

Obviously, the molecular mechanisms responsible for these rebound effects are tissue-specific and appear to be operational in the heart and at least some brain-specific cells, but not in the liver. Furthermore, it can also be explained by the fact that in liver (according to the literature and our Western blot findings) the dominant subunit is Suclg2 and the loss of one *Sucla2* allele is not affecting the level of Suclg2 to a notable extent. However, we did not find alteration or rebound Sucla2 expression in *Suclg2+/–* mice (see **Chapter 5.10 Figure 24**). A possible explanation for this is that Suclg2 is responsible for compensatory mechanisms unlike Sucla2, and the loss of one *Suclg2* allele upregulate the residuary *Suclg2* allele causing only a mild decrease in the total Suclg2 level.

The elucidation of such molecular mechanisms may be of great value in setting an example of gene–gene interactions of similar nature.

In addition to the finding regarding compensatory upregulation, in heart mitochondria, KM4549SC was more efficient in inhibition of substrate-level phosphorylation on samples obtained from WT compared to *Sucla2 +/–* (see **Chapter 5.7.3**, **Figure 20**). Despite the fact that total succinyl-CoA ligase activity did not appear to be higher in *Sucla2+/–* mice than in WT mice in **Figure 34,** a question arose: What if the compensative upregulation of GTP-forming subunit had an 'overbound' effect resulting in higher substrate-level phosphorylation capacity? Only in heart mitochondria did the *Sucla2* deletion result in a significant increase in GTP-forming activity.

Not a study related observation; however, it should be mentioned that according to our results found in **Chapter 5.7.2 Figure 18-19**, itaconate has a tissue-specific inhibitory potency suggested by the fact that we had to use different itaconate concentrations to reach the same submaximal inhibitory effect in tissues (liver, heart, brain).

As it was shown, when itaconate forms itaconyl-CoA through succinyl-CoA ligase [104, 165], succinyl-CoA can act as a 'CoASH trap'. Despite the fact that Coenzyme A can be transported into mitochondria, the local concentration in the mitochondrial matrix may be limited [166]. Free CoASH in the matrix is crucial for -among other things- alpha-ketoglutarate dehydrogenase complex [160-162, 167] and acylcarnitine metabolism. As we discussed in **Chapter 2.3,** alpha-ketoglutarate dehydrogenase complex is critical to maintaining substrate-level phosphorylation. The oxygen consumption experiment results, found in **Chapter 5.7.4,** also support this notion. In **Chapter 5.7.4 Figure 21,** when using α-ketoglutarate (α-Kg) as a substrate, heart mitochondria (which are dependent on CoASH for optimal catabolism of fatty acids) of *Sucla2+/−* mice exhibited smaller state 2 and state 3 respiration rates than WT mice, implying that alpha-ketoglutarate dehydrogenase complex activity may be impaired, possibly due to insufficient amounts of CoASH. Furthermore, the fact that SUCLA2 deficiency in humans is associated with elevations of C3 and C4-DC carnitine levels [65, 111, 133], and in the *Sucla2+/−* mice, we found an elevation of several additional esters including those encompassing long-chain fatty acid chains (C16-OH, C18:1, C:18 and C18-OH), further confirmed our hypothesis. But it also must be taken into account that increased acyl-CoA levels by the accumulation of succinyl-CoA can act as a 'CoASH trap' itself.

Regarding acyl-carnitines, another incident should be highlighted. As it was discussed in **Chapter 2.6.2,** human SUCLA2 deficiency affects L-leucine catabolism leading to elevation of L-leucine catabolic intermediers such as 3-hydroxyisovaleric acid and 3-methylglutaconic acid, likewise isovaleric acid and isovaleryl-CoA which are the direct precursors of 3-hydroxyisocvaleric acid. In view of the fact that i) the level of C5 (isovaleryl/2-methylbutyryl/pivaloyl) carnitine and C5-OH (3-hydroxy isovaleryl/2-methyl 3-hydroxybutyryl) carnitine levels were elevated in bloodspot analyses (see **Chapter 5.6**, **Figure 14**) in *Sucla2+/−* mice compared with WT mice except for the 3-month-old group; and ii) isovaleric acid has a succinyl-CoA ligase inhibitory effect [139],

it may be possible that worsening ('negative feedback') effect does not only exist in *SUCLA2* deficient patient, but also in heterozygous mice.

Finally, as we discussed in the introduction (**Chapter 2.5**), succinyl-CoA ligase is associated with mitochondrial nucleoside diphosphate kinase. Nucleoside-diphosphate kinase was originally considered as housekeeping enzyme for maintaining the constant level of nucleoside triphosphates; in addition to that, nucleoside-diphosphate kinase implicated the direct activation of some GTP-binding proteins [168, 169]. Since it is involved in compartment-specific mitochondrial GTP synthesis, it is not surprising that it could also contribute to the activation of β-cell and other mitochondrial GTP-binding protein involving processes, such as mitochondrial protein synthesis, steroidogenesis, protein transport, membrane fusion, and permeability transition [70, 170]. Unlike ATP, GTP is not transported through the inner mitochondrial membrane by nucleotide translocase [71, 171], therefore there should be a GTP forming enzyme, which is nucleoside-diphosphate kinase. [81]

mtDNA depletion was not present in all patients with SUCLA2 deficiency. As it was published, *SUCLG2* upregulation could compensate mtDNA depletion in the SUCLA2 deficient patient [154]; nevertheless, the knockdown of SUCLG2 in cells with complete SUCLA2 deficiency led to serious mtDNA depletion suggesting the existence of the compensatory effect. From another aspect, we can conclude that nucleoside-diphosphate kinase binds the GTP-forming subunit rather. According to our results, the effect of deletion of one *Sucla2* allele in mice caused a moderate mtDNA decrease only in the 3-month-old group and in brain in case of the 12-month-old group (see **Chapter 5.4**, **Figure 12**). Whereas when one *Suclg2* allele was also deleted in double heterozygote mice, we found a more considerable decrease in relative mtDNA content (see **Chapter 5.14**, **Figure 30**) (only 12-month-old group was examined). Hereby it should be emphasized that the succinyl-CoA ligase has tissue-specific expression pattern, so the interaction between succinyl-CoA ligase and nucleoside-diphosphate kinase also possibly varies from tissue to tissue. C. Miller et al. in [154] examined mtDNA depletion only in fibroblast cells not in all tissue types, therefore it cannot be excluded that in other cells, mtDNA level was affected. Also important is to take into account the fact that the decrease in Sucla2 level was accompanied by reducing Suclg1 expression.

The alterations in mtDNA should be attributed to changes in the activity of succinyl-CoA ligase with caution; it has been recently reported that GABA transaminase is essential for mitochondrial nucleoside metabolism and thus is necessary for mtDNA maintenance, and it co-immunoprecipitates with SUCLG1, SUCLG2 and SUCLA2 [172].

7. CONCLUSIONS

The most important finding of this thesis is, that the upregulation of *Suclg2* in *Sucla2+/–* mice can compensate the severity of the phenotype of this genetic modification. However, as we could see in **Chapter 5.10** and also in the **Discussion** *Suclg2* one-allele deletion was not accompanied by *Sucla2* upregulation. From the experiments with *Sucla2+/–* mice we obtained the information that deletion of one *Sucla2* allele is associated with a decrease in Suclg1 expression and a rebound increase in Suclg2 expression. Furthermore, this is reflected in reciprocal decrease vs. increase in ATP-forming vs. GTP-forming succinyl-CoA ligase activity. However, from the experiments with *Suclg2+/–* mice, we concluded that deletion of one *Suclg2* allele was not associated with the rebound effects as seen in the *Sucla2+/–* mice. A plausible explanation of this finding is that the Suclg2 is responsible for compensatory mechanisms and the upregulation of the one residual *Suclg2* allele is so strong that it can compensate the loss of the knocked-out allele. We also could see in the experiments with *Sucla2+/–/Suclg2+/–* mice that the anticipated decrease (due to deletion of one *Suclg2* allele) in Suclg2 expression is lost, presumably because of the effect(s) of deletion of the *Sucla2* allele, antagonizing the diminution in the expression of Suclg2. We concluded that the effect of deleting one *Sucla2* allele up-regulating *Suclg2* expression is so dominant that it adequately antagonizes or even supersedes the effect(s) of a concomitant loss of one *Suclg2* allele.

Regarding the fact that succinyl-CoA ligase is at the intersection of several metabolic pathways it is surprising that *SUCLA2* heterozygous patients are asymptomatic. According to our data regarding bloodspot analyses, we found a phenotypic alteration in heterozygous mice, namely in acyl-carnitine levels. These results are suggesting, that heterozygous patient with only one *SUCLA2* mutant allele may also show changes in blood acyl-carnitines.

With our study we could profile the metabolism of two transgenic mouse models for β-subunit components of succinyl-CoA ligase and highlight a compensatory mechanism. The fact that in those patients where *SUCLA2* or *SUCLG2* mutations were found showed milder severity compared to those where the invariant α subunit was affected, also supports the notion that α subunit is responsible for maintaining both ATP- and GTP-forming activities. We further concluded from these results that the loss of the alpha subunit cannot be compensated by the upregulation of any other subunit.

8. BIBLIOGRAPHY

1. Scheffler IE, *Mitochondria (Chapter 6 - Metabolic Pathways Inside Mitochondria)*. Wiley, New Jersey, USA 2008: 246-273.

2. Rego ACOliveira CR, *Mitochondrial dysfunction and reactive oxygen species in excitotoxicity and apoptosis: implications for the pathogenesis of neurodegenerative diseases.* Neurochem Res, 2003: **28**(10): p. 1563-1574.

3. Fiskum G, Murphy ANBeal MF, *Mitochondria in neurodegeneration: acute ischemia and chronic neurodegenerative diseases.* J Cereb Blood Flow Metab, 1999: **19**(4): p. 351-369.

4. Brookes PS, Yoon Y, Robotham JL, Anders MWSheu SS, *Calcium, ATP, and ROS: a mitochondrial love-hate triangle.* Am J Physiol Cell Physiol, 2004: **287**(4): p. C817-833.

5. Chinopoulos CAdam-Vizi V, *Mitochondria as ATP consumers in cellular pathology.* Biochim Biophys Acta, 2010: **1802**(1): p. 221-227.

6. Chinopoulos C, *Mitochondrial consumption of cytosolic ATP: not so fast.* FEBS Lett, 2011: **585**(9): p. 1255-1259.

7. Grover GJ, Atwal KS, Sleph PG, Wang FL, Monshizadegan H, Monticello TGreen DW, *Excessive ATP hydrolysis in ischemic myocardium by mitochondrial F1F0-ATPase: effect of selective pharmacological inhibition of mitochondrial ATPase hydrolase activity.* Am J Physiol Heart Circ Physiol, 2004: **287**(4): p. H1747-1755.

8. McKenzie M, Liolitsa D, Akinshina N, Campanella M, Sisodiya S, Hargreaves I, Nirmalananthan N, Sweeney MG, Abou-Sleiman PM, Wood NW, Hanna MGDuchen MR, *Mitochondrial ND5 gene variation associated with encephalomyopathy and mitochondrial ATP consumption.* J Biol Chem, 2007: **282**(51): p. 36845-36852.

9. Elliott HR, Samuels DC, Eden JA, Relton CLChinnery PF, *Pathogenic mitochondrial DNA mutations are common in the general population.* Am J Hum Genet, 2008: **83**(2): p. 254-260.

10. Schaefer AM, Taylor RW, Turnbull DMChinnery PF, *The epidemiology of mitochondrial disorders--past, present and future.* Biochim Biophys Acta, 2004: **1659**(2-3): p. 115-120.

11. Schaefer AM, McFarland R, Blakely EL, He L, Whittaker RG, Taylor RW, Chinnery PFTurnbull DM, *Prevalence of mitochondrial DNA disease in adults.* Ann Neurol, 2008: **63**(1): p. 35-39.

12. Graham BH, *Diagnostic challenges of mitochondrial disorders: complexities of two genomes.* Methods Mol Biol, 2012: **837**: p. 35-46.

13. Akman HO, Dorado B, Lopez LC, Garcia-Cazorla A, Vila MR, Tanabe LM, Dauer WT, Bonilla E, Tanji KHirano M, *Thymidine kinase 2 (H126N) knockin mice show the essential role of balanced deoxynucleotide pools for mitochondrial DNA maintenance.* Hum Mol Genet, 2008: **17**(16): p. 2433-2440.

14. Hance N, Ekstrand MITrifunovic A, *Mitochondrial DNA polymerase gamma is essential for mammalian embryogenesis.* Hum Mol Genet, 2005: **14**(13): p. 1775-1783.

15. Haraguchi M, Tsujimoto H, Fukushima M, Higuchi I, Kuribayashi H, Utsumi H, Nakayama A, Hashizume Y, Hirato J, Yoshida H, Hara H, Hamano S, Kawaguchi H, Furukawa T, Miyazono K, Ishikawa F, Toyoshima H, Kaname T, Komatsu M, Chen ZS, Gotanda T, Tachiwada T, Sumizawa T, Miyadera K, Osame M, Yoshida H, Noda T, Yamada YAkiyama S, *Targeted deletion of both thymidine phosphorylase and uridine phosphorylase and consequent disorders in mice.* Mol Cell Biol, 2002: **22**(14): p. 5212-5221.

16. Kimura T, Takeda S, Sagiya Y, Gotoh M, Nakamura YArakawa H, *Impaired function of p53R2 in Rrm2b-null mice causes severe renal failure through attenuation of dNTP pools.* Nat Genet, 2003: **34**(4): p. 440-445.

17. Lopez LC, Akman HO, Garcia-Cazorla A, Dorado B, Marti R, Nishino I, Tadesse S, Pizzorno G, Shungu D, Bonilla E, Tanji KHirano M, *Unbalanced deoxynucleotide pools cause mitochondrial DNA instability in thymidine phosphorylase-deficient mice.* Hum Mol Genet, 2009: **18**(4): p. 714-722.

18. Martinez-Azorin F, Calleja M, Hernandez-Sierra R, Farr CL, Kaguni LSGaresse R, *Over-expression of the catalytic core of mitochondrial DNA (mtDNA) polymerase in the nervous system of Drosophila melanogaster reduces median life span by inducing mtDNA depletion.* J Neurochem, 2008: **105**(1): p. 165-176.

19. Tyynismaa H, Mjosund KP, Wanrooij S, Lappalainen I, Ylikallio E, Jalanko A, Spelbrink JN, Paetau ASuomalainen A, *Mutant mitochondrial helicase Twinkle causes multiple mtDNA deletions and a late-onset mitochondrial disease in mice.* Proc Natl Acad Sci U S A, 2005: **102**(49): p. 17687-17692.

20. Viscomi C, Spinazzola A, Maggioni M, Fernandez-Vizarra E, Massa V, Pagano C, Vettor R, Mora MZeviani M, *Early-onset liver mtDNA depletion and late-onset proteinuric nephropathy in Mpv17 knockout mice.* Hum Mol Genet, 2009: **18**(1): p. 12-26.

21. Donti TR, Stromberger C, Ge M, Eldin KW, Craigen WJGraham BH, *Screen for abnormal mitochondrial phenotypes in mouse embryonic stem cells identifies a model for succinyl-CoA ligase deficiency and mtDNA depletion.* Dis Model Mech, 2014: **7**(2): p. 271-280.

22.   Rodwell V, Weil PA, Botham KM, Bender DKennelly PJ, Bioenergetics (Section III) *Harpers Illustrated Biochemistry 30th Edition*. McGraw-Hill Education, New York. 2015: 112-139

23.   Brand MDNicholls DG, *Assessing mitochondrial dysfunction in cells*. Biochem J, 2011: **435**(2): p. 297-312.

24.   Gerencser AA, Chinopoulos C, Birket MJ, Jastroch M, Vitelli C, Nicholls DGBrand MD, *Quantitative measurement of mitochondrial membrane potential in cultured cells: calcium-induced de- and hyperpolarization of neuronal mitochondria*. J Physiol, 2012: **590**(12): p. 2845-2871.

25.   Rouslin W, Erickson JLSolaro RJ, *Effects of oligomycin and acidosis on rates of ATP depletion in ischemic heart muscle*. Am J Physiol, 1986: **250**(3 Pt 2): p. H503-508.

26.   Rouslin W, Broge CWGrupp IL, *ATP depletion and mitochondrial functional loss during ischemia in slow and fast heart-rate hearts*. Am J Physiol, 1990: **259**(6 Pt 2): p. H1759-1766.

27.   McMillin JBPauly DF, *Control of mitochondrial respiration in muscle*. Mol Cell Biochem, 1988: **81**(2): p. 121-129.

28.   Petronilli V, Azzone GFPietrobon D, *Analysis of mechanisms of free-energy coupling and uncoupling by inhibitor titrations: theory, computer modeling and experiments*. Biochim Biophys Acta, 1988: **932**(3): p. 306-324.

29.   Wisniewski E, Kunz WSGellerich FN, *Phosphate affects the distribution of flux control among the enzymes of oxidative phosphorylation in rat skeletal muscle mitochondria*. J Biol Chem, 1993: **268**(13): p. 9343-9346.

30.   Walker JE, *The regulation of catalysis in ATP synthase*. Curr Opin Struct Biol, 1994: **4**(6): p. 912-918.

31.   Boyer PD, *A research journey with ATP synthase*. J Biol Chem, 2002: **277**(42): p. 39045-39061.

32.   Feniouk BAYoshida M, *Regulatory mechanisms of proton-translocating F(O)F (1)-ATP synthase*. Results Probl Cell Differ, 2008: **45**: p. 279-308.

33.   Klingenberg MRottenberg H, *Relation between the gradient of the ATP/ADP ratio and the membrane potential across the mitochondrial membrane*. Eur J Biochem, 1977: **73**(1): p. 125-130.

34.   Vajda S, Mandi M, Konrad C, Kiss G, Ambrus A, Adam-Vizi VChinopoulos C, *A re-evaluation of the role of matrix acidification in uncoupler-induced Ca2+ release from mitochondria*. FEBS J, 2009: **276**(10): p. 2713-2724.

35. Chinopoulos C, Vajda S, Csanady L, Mandi M, Mathe KAdam-Vizi V, *A novel kinetic assay of mitochondrial ATP-ADP exchange rate mediated by the ANT.* Biophys J, 2009: **96**(6): p. 2490-2504.

36. Chinopoulos C, Gerencser AA, Mandi M, Mathe K, Torocsik B, Doczi J, Turiak L, Kiss G, Konrad C, Vajda S, Vereczki V, Oh RJAdam-Vizi V, *Forward operation of adenine nucleotide translocase during F0F1-ATPase reversal: critical role of matrix substrate-level phosphorylation.* FASEB J, 2010: **24**(7): p. 2405-2416.

37. Ferguson SJ, *ATP synthase: from sequence to ring size to the P/O ratio.* Proc Natl Acad Sci U S A, 2010: **107**(39): p. 16755-16756.

38. Watt IN, Montgomery MG, Runswick MJ, Leslie AGWalker JE, *Bioenergetic cost of making an adenosine triphosphate molecule in animal mitochondria.* Proc Natl Acad Sci U S A, 2010: **107**(39): p. 16823-16827.

39. Aprille JR, *Mechanism and regulation of the mitochondrial ATP-Mg/P(i) carrier.* J Bioenerg Biomembr, 1993: **25**(5): p. 473-481.

40. Yaniv Y, Juhaszova M, Nuss HB, Wang S, Zorov DB, Lakatta EGSollott SJ, *Matching ATP supply and demand in mammalian heart: in vivo, in vitro, and in silico perspectives.* Ann N Y Acad Sci, 2010: **1188**: p. 133-142.

41. Cross RLMuller V, *The evolution of A-, F-, and V-type ATP synthases and ATPases: reversals in function and changes in the H+/ATP coupling ratio.* FEBS Lett, 2004: **576**(1-2): p. 1-4.

42. Tomashek JJBrusilow WS, *Stoichiometry of energy coupling by proton-translocating ATPases: a history of variability.* J Bioenerg Biomembr, 2000: **32**(5): p. 493-500.

43. Wu F, Zhang EY, Zhang J, Bache RJBeard DA, *Phosphate metabolite concentrations and ATP hydrolysis potential in normal and ischaemic hearts.* J Physiol, 2008: **586**(17): p. 4193-4208.

44. Gerencser AAAdam-Vizi V, *Mitochondrial Ca2+ dynamics reveals limited intramitochondrial Ca2+ diffusion.* Biophys J, 2005: **88**(1): p. 698-714.

45. Duchen MR, Leyssens ACrompton M, *Transient mitochondrial depolarizations reflect focal sarcoplasmic reticular calcium release in single rat cardiomyocytes.* J Cell Biol, 1998: **142**(4): p. 975-988.

46. O'Reilly CM, Fogarty KE, Drummond RM, Tuft RAWalsh JV, Jr., *Quantitative analysis of spontaneous mitochondrial depolarizations.* Biophys J, 2003: **85**(5): p. 3350-3357.

47.   Warburg O, *On the origin of cancer cells.* Science, 1956: **123**(3191): p. 309-14.

48.   Chinopoulos C, *Which way does the citric acid cycle turn during hypoxia? The critical role of alpha-ketoglutarate dehydrogenase complex.* J Neurosci Res, 2013: **91**(8): p. 1030-1043.

49.   Wilson DF, Erecinska MSchramm VL, *Evaluation of the relationship between the intra- and extramitochondrial [ATP]/[ADP] ratios using phosphoenolpyruvate carboxykinase.* J Biol Chem, 1983: **258**(17): p. 10464-10473.

50.   Lambeth DO, *What is the function of GTP produced in the Krebs citric acid cycle?* IUBMB Life, 2002: **54**(3): p. 143-144.

51.   Stark R, Pasquel F, Turcu A, Pongratz RL, Roden M, Cline GW, Shulman GIKibbey RG, *Phosphoenolpyruvate cycling via mitochondrial phosphoenolpyruvate carboxykinase links anaplerosis and mitochondrial GTP with insulin secretion.* J Biol Chem, 2009: **284**(39): p. 26578-26590.

52.   Ottaway JH, McClellan JASaunderson CL, *Succinic thiokinase and metabolic control.* Int J Biochem, 1981: **13**(4): p. 401-410.

53.   Jacobson JDuchen MR, *'What nourishes me, destroys me': towards a new mitochondrial biology.* Cell Death Differ, 2001: **8**(10): p. 963-966.

54.   Chinopoulos C, *The "B space" of mitochondrial phosphorylation.* J Neurosci Res, 2011: **89**(12): p. 1897-1904.

55.   Phillips D, Aponte AM, French SA, Chess DJBalaban RS, *Succinyl-CoA synthetase is a phosphate target for the activation of mitochondrial metabolism.* Biochemistry, 2009: **48**(30): p. 7140-7149.

56.   Kiss G, Konrad C, Doczi J, Starkov AA, Kawamata H, Manfredi G, Zhang SF, Gibson GE, Beal MF, Adam-Vizi VChinopoulos C, *The negative impact of alpha-ketoglutarate dehydrogenase complex deficiency on matrix substrate-level phosphorylation.* FASEB J, 2013: **27**(6): p. 2392-2406.

57.   Kiss G, Konrad C, Pour-Ghaz I, Mansour JJ, Nemeth B, Starkov AA, Adam-Vizi VChinopoulos C, *Mitochondrial diaphorases as NAD(+) donors to segments of the citric acid cycle that support substrate-level phosphorylation yielding ATP during respiratory inhibition.* FASEB J, 2014: **28**(4): p. 1682-1697.

58.   Giorgio M, Migliaccio E, Orsini F, Paolucci D, Moroni M, Contursi C, Pelliccia G, Luzi L, Minucci S, Marcaccio M, Pinton P, Rizzuto R, Bernardi P, Paolucci FPelicci PG, *Electron transfer between cytochrome c and p66Shc generates reactive oxygen species that trigger mitochondrial apoptosis.* Cell, 2005: **122**(2): p. 221-233.

59. Akbar H, Kim J, Funk K, Cancelas JA, Shang X, Chen L, Johnson JF, Williams DAZheng Y, *Genetic and pharmacologic evidence that Rac1 GTPase is involved in regulation of platelet secretion and aggregation.* J Thromb Haemost, 2007: **5**(8): p. 1747-1755.

60. Li X, Dash RK, Pradhan RK, Qi F, Thompson M, Vinnakota KC, Wu F, Yang FBeard DA, *A database of thermodynamic quantities for the reactions of glycolysis and the tricarboxylic acid cycle.* J Phys Chem B, 2010: **114**(49): p. 16068-16082.

61. Johnson JD, Mehus JG, Tews K, Milavetz BILambeth DO, *Genetic evidence for the expression of ATP- and GTP-specific succinyl-CoA synthetases in multicellular eucaryotes.* J Biol Chem, 1998: **273**(42): p. 27580-27586.

62. Li X, Wu FBeard DA, *Identification of the kinetic mechanism of succinyl-CoA synthetase.* Biosci Rep, 2013: **33**(1): p. 145-163.

63. Lambeth DO, Tews KN, Adkins S, Frohlich DMilavetz BI, *Expression of two succinyl-CoA synthetases with different nucleotide specificities in mammalian tissues.* J Biol Chem, 2004: **279**(35): p. 36621-36624.

64. Lambeth DO, *Reconsideration of the significance of substrate-level phosphorylation in the citric acid cycle.* Biochem Mol Biol Educ, 2006: **34**(1): p. 21-29.

65. Morava E, Steuerwald U, Carrozzo R, Kluijtmans LA, Joensen F, Santer R, Dionisi-Vici CWevers RA, *Dystonia and deafness due to SUCLA2 defect; Clinical course and biochemical markers in 16 children.* Mitochondrion, 2009: **9**(6): p. 438-442.

66. Dobolyi A, Ostergaard E, Bago AG, Doczi T, Palkovits M, Gal A, Molnar MJ, Adam-Vizi VChinopoulos C, *Exclusive neuronal expression of SUCLA2 in the human brain.* Brain Struct Funct, 2015: **220**(1): p. 135-151.

67. Dobolyi A, Bago AG, Gal A, Molnar MJ, Palkovits M, Adam-Vizi VChinopoulos C, *Localization of SUCLA2 and SUCLG2 subunits of succinyl CoA ligase within the cerebral cortex suggests the absence of matrix substrate-level phosphorylation in glial cells of the human brain.* J Bioenerg Biomembr, 2015: **47**(1-2): p. 33-41.

68. Aldwell FE, Cross ML, Fitzpatrick CE, Lambeth MR, de Lisle GWBuddle BM, *Oral delivery of lipid-encapsulated Mycobacterium bovis BCG extends survival of the bacillus in vivo and induces a long-term protective immune response against tuberculosis.* Vaccine, 2006: **24**(12): p. 2071-2078.

69. Pall ML, *GTP: a central regulator of cellular anabolism.* Curr Top Cell Regul, 1985: **25**: p. 1-20.

70.   Thomson M, *What are guanosine triphosphate-binding proteins doing in mitochondria?* Biochim Biophys Acta, 1998: **1403**(3): p. 211-218.

71.   Pfaff E, Klingenberg MHeldt HW, *Unspecific permeation and specific exchange of adenine nucleotides in liver mitochondria.* Biochim Biophys Acta, 1965: **104**(1): p. 312-315.

72.   McKee EE, Bentley AT, Smith RM, Jr.Ciaccio CE, *Origin of guanine nucleotides in isolated heart mitochondria.* Biochem Biophys Res Commun, 1999: **257**(2): p. 466-472.

73.   McKee EE, Bentley AT, Smith RM, Jr., Kraas JRCiaccio CE, *Guanine nucleotide transport by atractyloside-sensitive and -insensitive carriers in isolated heart mitochondria.* Am J Physiol Cell Physiol, 2000: **279**(6): p. C1870-1879.

74.   Kleineke J, Sauer HSoling HD, *On the specificity of the tricarboxylate carrier system in rat liver mitochondria.* FEBS Lett, 1973: **29**(2): p. 82-86.

75.   Tretter L, Patocs AChinopoulos C, *Succinate, an intermediate in metabolism, signal transduction, ROS, hypoxia, and tumorigenesis.* Biochim Biophys Acta, 2016: **1857**(8): p. 1086-1101.

76.   Krebs HA, *The citric acid cycle and the Szent-Gyorgyi cycle in pigeon breast muscle.* Biochem J, 1940: **34**(5): p. 775-779.

77.   Labbe RF, Kurumada TOnisawa J, *The role of succinyl-CoA synthetase in the control of heme biosynthesis.* Biochim Biophys Acta, 1965: **111**(2): p. 403-415.

78.   Fukao T, Mitchell G, Sass JO, Hori T, Orii KAoyama Y, *Ketone body metabolism and its defects.* J Inherit Metab Dis, 2014: **37**(4): p. 541-551.

79.   Kadrmas EF, Ray PDLambeth DO, *Apparent ATP-linked succinate thiokinase activity and its relation to nucleoside diphosphate kinase in mitochondrial matrix preparations from rabbit.* Biochim Biophys Acta, 1991: **1074**(3): p. 339-346.

80.   Kavanaugh-Black A, Connolly DM, Chugani SAChakrabarty AM, *Characterization of nucleoside-diphosphate kinase from Pseudomonas aeruginosa: complex formation with succinyl-CoA synthetase.* Proc Natl Acad Sci U S A, 1994: **91**(13): p. 5883-5887.

81.   Kowluru A, Tannous MChen HQ, *Localization and characterization of the mitochondrial isoform of the nucleoside diphosphate kinase in the pancreatic beta cell: evidence for its complexation with mitochondrial succinyl-CoA synthetase.* Arch Biochem Biophys, 2002: **398**(2): p. 160-169.

82.   Suomalainen AIsohanni P, *Mitochondrial DNA depletion syndromes--many genes, common mechanisms.* Neuromuscul Disord, 2010: **20**(7): p. 429-437.

83. Ostergaard E, *Disorders caused by deficiency of succinate-CoA ligase.* J Inherit Metab Dis, 2008: **31**(2): p. 226-229.

84. Coude FX, Sweetman LNyhan WL, *Inhibition by propionyl-coenzyme A of N-acetylglutamate synthetase in rat liver mitochondria. A possible explanation for hyperammonemia in propionic and methylmalonic acidemia.* J Clin Invest, 1979: **64**(6): p. 1544-1551.

85. Glasgow AMChase HP, *Effect of propionic acid on fatty acid oxidation and ureagenesis.* Pediatr Res, 1976: **10**(7): p. 683-686.

86. Stewart PMWalser M, *Failure of the normal ureagenic response to amino acids in organic acid-loaded rats. Proposed mechanism for the hyperammonemia of propionic and methylmalonic acidemia.* J Clin Invest, 1980: **66**(3): p. 484-492.

87. Scriver C, Beaudet, A., Sly, W., Valle, D., Childs, B., Kinzler, K., *The Metabolic and Molecular Bases of Inherited Disease - 94: Disorders of Propionate and Methylmalonate Metabolism.* McGraw-Hill Companies (Incorporated) 2000:

88. Hillman RE, Sowers LHCohen JL, *Inhibition of glycine oxidation in cultured fibroblasts by isoleucine.* Pediatr Res, 1973: **7**(12): p. 945-947.

89. Hoffman PL, Wermuth Bvon Wartburg JP, *Human brain aldehyde reductases: relationship to succinic semialdehyde reductase and aldose reductase.* J Neurochem, 1980: **35**(2): p. 354-366.

90. Picklo MJ, Sr., Olson SJ, Hayes JD, Markesbery WRMontine TJ, *Elevation of AKR7A2 (succinic semialdehyde reductase) in neurodegenerative disease.* Brain Res, 2001: **916**(1-2): p. 229-238.

91. Ris MMvon Wartburg JP, *Heterogeneity of NADPH-dependent aldehyde reductase from human and rat brain.* Eur J Biochem, 1973: **37**(1): p. 69-77.

92. Minuk GY, *Gamma-aminobutyric acid and the liver.* Dig Dis, 1993: **11**(1): p. 45-54.

93. Shin JH, Yang JY, Jeon BY, Yoon YJ, Cho SN, Kang YH, Ryu DHHwang GS, *(1)H NMR-based metabolomic profiling in mice infected with Mycobacterium tuberculosis.* J Proteome Res, 2011: **10**(5): p. 2238-2247.

94. Wibom C, Surowiec I, Moren L, Bergstrom P, Johansson M, Antti HBergenheim AT, *Metabolomic patterns in glioblastoma and changes during radiotherapy: a clinical microdialysis study.* J Proteome Res, 2010: **9**(6): p. 2909-2919.

95. Kvitvang HF, Andreassen T, Adam T, Villas-Boas SGBruheim P, *Highly sensitive GC/MS/MS method for quantitation of amino and nonamino organic acids.* Anal Chem, 2011: **83**(7): p. 2705-2711.

96.   Strelko CL, Lu W, Dufort FJ, Seyfried TN, Chiles TC, Rabinowitz JDRoberts MF, *Itaconic acid is a mammalian metabolite induced during macrophage activation.* J Am Chem Soc, 2011: **133**(41): p. 16386-16389.

97.   McFadden BAPurohit S, *Itaconate, an isocitrate lyase-directed inhibitor in Pseudomonas indigofera.* J Bacteriol, 1977: **131**(1): p. 136-144.

98.   Patel TRMcFadden BA, *Caenorhabditis elegans and Ascaris suum: inhibition of isocitrate lyase by itaconate.* Exp Parasitol, 1978: **44**(2): p. 262-268.

99.   Williams JO, Roche TEMcFadden BA, *Mechanism of action of isocitrate lyase from Pseudomonas indigofera.* Biochemistry, 1971: **10**(8): p. 1384-1390.

100.   Adler J, Wang SFLardy HA, *The metabolism of itaconic acid by liver mitochondria.* J Biol Chem, 1957: **229**(2): p. 865-879.

101.   Booth AN, Taylor J, Wilson RHDeeds F, *The inhibitory effects of itaconic acid in vitro and in vivo.* J Biol Chem, 1952: **195**(2): p. 697-702.

102.   Wang SF, Adler JLardy HA, *The pathway of itaconate metabolism by liver mitochondria.* J Biol Chem, 1961: **236**: p. 26-30.

103.   Dervartanian DVVeeger C, *Studies on Succinate Dehydrogenase. I. Spectral Properties of the Purified Enzyme and Formation of Enzyme-Competitive Inhibitor Complexes.* Biochim Biophys Acta, 1964: **92**: p. 233-247.

104.   Nemeth B, Doczi J, Csete D, Kacso G, Ravasz D, Adams D, Kiss G, Nagy AM, Horvath G, Tretter L, Mocsai A, Csepanyi-Komi R, Iordanov I, Adam-Vizi VChinopoulos C, *Abolition of mitochondrial substrate-level phosphorylation by itaconic acid produced by LPS-induced Irg1 expression in cells of murine macrophage lineage.* FASEB J, 2016: **30**(1): p. 286-300.

105.   Zhang Z, Tan M, Xie Z, Dai L, Chen YZhao Y, *Identification of lysine succinylation as a new post-translational modification.* Nat Chem Biol, 2011: **7**(1): p. 58-63.

106.   Mills EO'Neill LA, *Succinate: a metabolic signal in inflammation.* Trends Cell Biol, 2014: **24**(5): p. 313-320.

107.   Tannahill GM, Curtis AM, Adamik J, Palsson-McDermott EM, McGettrick AF, Goel G, Frezza C, Bernard NJ, Kelly B, Foley NH, Zheng L, Gardet A, Tong Z, Jany SS, Corr SC, Haneklaus M, Caffrey BE, Pierce K, Walmsley S, Beasley FC, Cummins E, Nizet V, Whyte M, Taylor CT, Lin H, Masters SL, Gottlieb E, Kelly VP, Clish C, Auron PE, Xavier RJO'Neill LA, *Succinate is an inflammatory signal that induces IL-1beta through HIF-1alpha.* Nature, 2013: **496**(7444): p. 238-242.

108. Selak MA, Armour SM, MacKenzie ED, Boulahbel H, Watson DG, Mansfield KD, Pan Y, Simon MC, Thompson CBGottlieb E, *Succinate links TCA cycle dysfunction to oncogenesis by inhibiting HIF-alpha prolyl hydroxylase.* Cancer Cell, 2005: **7**(1): p. 77-85.

109. Semenza GL, *HIF-1 mediates metabolic responses to intratumoral hypoxia and oncogenic mutations.* J Clin Invest, 2013: **123**(9): p. 3664-3671.

110. Latif F, Tory K, Gnarra J, Yao M, Duh FM, Orcutt ML, Stackhouse T, Kuzmin I, Modi W, Geil Let al., *Identification of the von Hippel-Lindau disease tumor suppressor gene.* Science, 1993: **260**(5112): p. 1317-1320.

111. Carrozzo R, Dionisi-Vici C, Steuerwald U, Lucioli S, Deodato F, Di Giandomenico S, Bertini E, Franke B, Kluijtmans LA, Meschini MC, Rizzo C, Piemonte F, Rodenburg R, Santer R, Santorelli FM, van Rooij A, Vermunt-de Koning D, Morava EWevers RA, *SUCLA2 mutations are associated with mild methylmalonic aciduria, Leigh-like encephalomyopathy, dystonia and deafness.* Brain, 2007: **130**(Pt 3): p. 862-784.

112. Carrozzo R, Verrigni D, Rasmussen M, de Coo R, Amartino H, Bianchi M, Buhas D, Mesli S, Naess K, Born AP, Woldseth B, Prontera P, Batbayli M, Ravn K, Joensen F, Cordelli DM, Santorelli FM, Tulinius M, Darin N, Duno M, Jouvencel P, Burlina A, Stangoni G, Bertini E, Redonnet-Vernhet I, Wibrand F, Dionisi-Vici C, Uusimaa J, Vieira P, Osorio AN, McFarland R, Taylor RW, Holme EOstergaard E, *Succinate-CoA ligase deficiency due to mutations in SUCLA2 and SUCLG1: phenotype and genotype correlations in 71 patients.* J Inherit Metab Dis, 2016: **39**(2): p. 243-252.

113. Elpeleg O, Miller C, Hershkovitz E, Bitner-Glindzicz M, Bondi-Rubinstein G, Rahman S, Pagnamenta A, Eshhar SSaada A, *Deficiency of the ADP-forming succinyl-CoA synthase activity is associated with encephalomyopathy and mitochondrial DNA depletion.* Am J Hum Genet, 2005: **76**(6): p. 1081-1086.

114. Gungor O, Ozkaya AK, Gungor G, Karaer K, Dilber CAydin K, *Novel mutation in SUCLA2 identified on sequencing analysis.* Pediatr Int, 2016: **58**(7): p. 659-661.

115. Jaberi E, Chitsazian F, Ali Shahidi G, Rohani M, Sina F, Safari I, Malakouti Nejad M, Houshmand M, Klotzle BElahi E, *The novel mutation p.Asp251Asn in the beta-subunit of succinate-CoA ligase causes encephalomyopathy and elevated succinylcarnitine.* J Hum Genet, 2013: **58**(8): p. 526-530.

116. Lamperti C, Fang M, Invernizzi F, Liu X, Wang H, Zhang Q, Carrara F, Moroni I, Zeviani M, Zhang JGhezzi D, *A novel homozygous mutation in SUCLA2 gene identified by exome sequencing.* Mol Genet Metab, 2012: **107**(3): p. 403-408.

117.   Maas RR, Marina AD, de Brouwer AP, Wevers RA, Rodenburg RJWortmann SB, *SUCLA2 Deficiency: A Deafness-Dystonia Syndrome with Distinctive Metabolic Findings (Report of a New Patient and Review of the Literature).* JIMD Rep, 2016: **27**: p. 27-32.

118.   Matilainen S, Isohanni P, Euro L, Lonnqvist T, Pihko H, Kivela T, Knuutila SSuomalainen A, *Mitochondrial encephalomyopathy and retinoblastoma explained by compound heterozygosity of SUCLA2 point mutation and 13q14 deletion.* Eur J Hum Genet, 2015: **23**(3): p. 325-330.

119.   Navarro-Sastre A, Tort F, Garcia-Villoria J, Pons MR, Nascimento A, Colomer J, Campistol J, Yoldi ME, Lopez-Gallardo E, Montoya J, Unceta M, Martinez MJ, Briones PRibes A, *Mitochondrial DNA depletion syndrome: new descriptions and the use of citrate synthase as a helpful tool to better characterise the patients.* Mol Genet Metab, 2012: **107**(3): p. 409-415.

120.   Nogueira C, Meschini MC, Nesti C, Garcia P, Diogo L, Valongo C, Costa R, Videira A, Vilarinho LSantorelli FM, *A novel SUCLA2 mutation in a Portuguese child associated with "mild" methylmalonic aciduria.* J Child Neurol, 2015: **30**(2): p. 228-232.

121.   Ostergaard E, Hansen FJ, Sorensen N, Duno M, Vissing J, Larsen PL, Faeroe O, Thorgrimsson S, Wibrand F, Christensen ESchwartz M, *Mitochondrial encephalomyopathy with elevated methylmalonic acid is caused by SUCLA2 mutations.* Brain, 2007: **130**(Pt 3): p. 853-861.

122.   Pupavac M, Tian X, Chu J, Wang G, Feng Y, Chen S, Fenter R, Zhang VW, Wang J, Watkins D, Wong LJRosenblatt DS, *Added value of next generation gene panel analysis for patients with elevated methylmalonic acid and no clinical diagnosis following functional studies of vitamin B12 metabolism.* Mol Genet Metab, 2016: **117**(3): p. 363-368.

123.   Chu J, Pupavac M, Watkins D, Tian X, Feng Y, Chen S, Fenter R, Zhang VW, Wang J, Wong LJRosenblatt DS, *Next generation sequencing of patients with mut methylmalonic aciduria: Validation of somatic cell studies and identification of 16 novel mutations.* Mol Genet Metab, 2016: **118**(4): p. 264-271.

124.   Honzik T, Tesarova M, Magner M, Mayr J, Jesina P, Vesela K, Wenchich L, Szentivanyi K, Hansikova H, Sperl WZeman J, *Neonatal onset of mitochondrial disorders in 129 patients: clinical and laboratory characteristics and a new approach to diagnosis.* J Inherit Metab Dis, 2012: **35**(5): p. 749-759.

125.   Landsverk ML, Zhang VW, Wong LCAndersson HC, *A SUCLG1 mutation in a patient with mitochondrial DNA depletion and congenital anomalies.* Mol Genet Metab Rep, 2014: **1**: p. 451-454.

126. Ostergaard E, Christensen E, Kristensen E, Mogensen B, Duno M, Shoubridge EAWibrand F, *Deficiency of the alpha subunit of succinate-coenzyme A ligase causes fatal infantile lactic acidosis with mitochondrial DNA depletion.* Am J Hum Genet, 2007: **81**(2): p. 383-387.

127. Randolph LM, Jackson HA, Wang J, Shimada H, Sanchez-Lara PA, Wong DA, Wong LJBoles RG, *Fatal infantile lactic acidosis and a novel homozygous mutation in the SUCLG1 gene: a mitochondrial DNA depletion disorder.* Mol Genet Metab, 2011: **102**(2): p. 149-152.

128. Rivera H, Merinero B, Martinez-Pardo M, Arroyo I, Ruiz-Sala P, Bornstein B, Serra-Suhe C, Gallardo E, Marti R, Moran MJ, Ugalde C, Perez-Jurado LA, Andreu AL, Garesse R, Ugarte M, Arenas JMartin MA, *Marked mitochondrial DNA depletion associated with a novel SUCLG1 gene mutation resulting in lethal neonatal acidosis, multi-organ failure, and interrupted aortic arch.* Mitochondrion, 2010: **10**(4): p. 362-368.

129. Rouzier C, Le Guedard-Mereuze S, Fragaki K, Serre V, Miro J, Tuffery-Giraud S, Chaussenot A, Bannwarth S, Caruba C, Ostergaard E, Pellissier JF, Richelme C, Espil C, Chabrol BPaquis-Flucklinger V, *The severity of phenotype linked to SUCLG1 mutations could be correlated with residual amount of SUCLG1 protein.* J Med Genet, 2010: **47**(10): p. 670-676.

130. Sakamoto O, Ohura T, Murayama K, Ohtake A, Harashima H, Abukawa D, Takeyama J, Haginoya K, Miyabayashi SKure S, *Neonatal lactic acidosis with methylmalonic aciduria due to novel mutations in the SUCLG1 gene.* Pediatr Int, 2011: **53**(6): p. 921-925.

131. Valayannopoulos V, Haudry C, Serre V, Barth M, Boddaert N, Arnoux JB, Cormier-Daire V, Rio M, Rabier D, Vassault A, Munnich A, Bonnefont JP, de Lonlay P, Rotig ALebre AS, *New SUCLG1 patients expanding the phenotypic spectrum of this rare cause of mild methylmalonic aciduria.* Mitochondrion, 2010: **10**(4): p. 335-341.

132. Van Hove JL, Saenz MS, Thomas JA, Gallagher RC, Lovell MA, Fenton LZ, Shanske S, Myers SM, Wanders RJ, Ruiter J, Turkenburg MWaterham HR, *Succinyl-CoA ligase deficiency: a mitochondrial hepatoencephalomyopathy.* Pediatr Res, 2010: **68**(2): p. 159-164.

133. Liu Y, Li X, Wang Q, Ding Y, Song JYang Y, *Five novel SUCLG1 mutations in three Chinese patients with succinate-CoA ligase deficiency noticed by mild methylmalonic aciduria.* Brain Dev, 2016: **38**(1): p. 61-67.

134. Ostergaard E, Schwartz M, Batbayli M, Christensen E, Hjalmarson O, Kollberg GHolme E, *A novel missense mutation in SUCLG1 associated with mitochondrial DNA depletion, encephalomyopathic form, with methylmalonic aciduria.* Eur J Pediatr, 2010: **169**(2): p. 201-205.

135.   Wakil S, *Lipid Metabolism*. 2012: Elsevier Science.

136.   Huang X, Bedoyan JK, Demirbas D, Harris DJ, Miron A, Edelheit S, Grahame G, DeBrosse SD, Wong LJ, Hoppel CL, Kerr DS, Anselm IBerry GT, *Succinyl-CoA synthetase (SUCLA2) deficiency in two siblings with impaired activity of other mitochondrial oxidative enzymes in skeletal muscle without mitochondrial DNA depletion.* Mol Genet Metab, 2016.

137.   Smith CMWilliamson JR, *Inhibition of citrate synthase by succinyl-CoA and other metabolites.* FEBS Lett, 1971: **18**(1): p. 35-38.

138.   Patel MS, Nemeria NS, Furey WJordan F, *The pyruvate dehydrogenase complexes: structure-based function and regulation.* J Biol Chem, 2014: **289**(24): p. 16615-16623.

139.   Bergen BJ, Stumpf DA, Haas R, Parks JKEguren LA, *A mechanism of toxicity of isovaleric acid in rat liver mitochondria.* Biochem Med, 1982: **27**(2): p. 154-160.

140.   Morava E, Rodenburg R, van Essen HZ, De Vries MSmeitink J, *Dietary intervention and oxidative phosphorylation capacity.* J Inherit Metab Dis, 2006: **29**(4): p. 589.

141.   Hansen GM, Markesich DC, Burnett MB, Zhu Q, Dionne KM, Richter LJ, Finnell RH, Sands AT, Zambrowicz BPAbuin A, *Large-scale gene trapping in C57BL/6N mouse embryonic stem cells.* Genome Res, 2008: **18**(10): p. 1670-1679.

142.   Araki M, Nakahara M, Muta M, Itou M, Yanai C, Yamazoe F, Miyake M, Morita A, Araki M, Okamoto Y, Nakagata N, Yoshinobu K, Yamamura KAraki K, *Database for exchangeable gene trap clones: pathway and gene ontology analysis of exchangeable gene trap clone mouse lines.* Dev Growth Differ, 2014: **56**(2): p. 161-174.

143.   Tyler DDGonze J, *[11] The preparation of heart mitochondria from laboratory animals*, in *Methods in Enzymology*. 1967, Academic Press. p. 75-77.

144.   Sims NR, *Rapid isolation of metabolically active mitochondria from rat brain and subregions using Percoll density gradient centrifugation.* J Neurochem, 1990: **55**(2): p. 698-707.

145.   Chinopoulos C, Starkov AAFiskum G, *Cyclosporin A-insensitive permeability transition in brain mitochondria: inhibition by 2-aminoethoxydiphenyl borate.* J Biol Chem, 2003: **278**(30): p. 27382-27389.

146.   Smith PK, Krohn RI, Hermanson GT, Mallia AK, Gartner FH, Provenzano MD, Fujimoto EK, Goeke NM, Olson BJKlenk DC, *Measurement of protein using bicinchoninic acid.* Anal Biochem, 1985: **150**(1): p. 76-85.

147. Sekuzu I, Jurtshuk P, Jr.Green DE, *On the isolation and properties of the D(-)beta-hydroxybutyric dehydrogenase of beef heart mitochondria.* Biochem Biophys Res Commun, 1961: **6**: p. 71-75.

148. Åkerman KEOWikström MKF, *Safranine as a probe of the mitochondrial membrane potential.* FEBS Letters, 1976: **68**(2): p. 191-197.

149. Saada A, Bar-Meir M, Belaiche C, Miller CElpeleg O, *Evaluation of enzymatic assays and compounds affecting ATP production in mitochondrial respiratory chain complex I deficiency.* Anal Biochem, 2004: **335**(1): p. 66-72.

150. Voss AK, Thomas TGruss P, *Compensation for a gene trap mutation in the murine microtubule-associated protein 4 locus by alternative polyadenylation and alternative splicing.* Dev Dyn, 1998: **212**(2): p. 258-266.

151. Alarcon C, Wicksteed B, Prentki M, Corkey BERhodes CJ, *Succinate Is a Preferential Metabolic Stimulus-Coupling Signal for Glucose-Induced Proinsulin Biosynthesis Translation.* Diabetes, 2002: **51**(8): p. 2496-2504.

152. Klingenberg M, *The ADP and ATP transport in mitochondria and its carrier.* Biochim Biophys Acta, 2008: **1778**(10): p. 1978-2021.

153. Hunger-Glaser I, Brun R, Linder MSeebeck T, *Inhibition of succinyl CoA synthetase histidine-phosphorylation in Trypanosoma brucei by an inhibitor of bacterial two-component systems.* Mol Biochem Parasitol, 1999: **100**(1): p. 53-59.

154. Miller C, Wang L, Ostergaard E, Dan PSaada A, *The interplay between SUCLA2, SUCLG2, and mitochondrial DNA depletion.* Biochim Biophys Acta, 2011: **1812**(5): p. 625-629.

155. Gonzalez-Billault C, Demandt E, Wandosell F, Torres M, Bonaldo P, Stoykova A, Chowdhury K, Gruss P, Avila JSanchez MP, *Perinatal lethality of microtubule-associated protein 1B-deficient mice expressing alternative isoforms of the protein at low levels.* Mol Cell Neurosci, 2000: **16**(4): p. 408-421.

156. Pires-daSilva A, Nayernia K, Engel W, Torres M, Stoykova A, Chowdhury KGruss P, *Mice deficient for spermatid perinuclear RNA-binding protein show neurologic, spermatogenic, and sperm morphological abnormalities.* Dev Biol, 2001: **233**(2): p. 319-328.

157. Salminen M, Meyer BI, Bober EGruss P, *Netrin 1 is required for semicircular canal formation in the mouse inner ear.* Development, 2000: **127**(1): p. 13-22.

158. Patel MS, *Inhibition by the branched-chain 2-oxo acids of the 2-oxoglutarate dehydrogenase complex in developing rat and human brain.* Biochem J, 1974: **144**(1): p. 91-97.

159. Cooney GJ, Taegtmeyer HNewsholme EA, *Tricarboxylic acid cycle flux and enzyme activities in the isolated working rat heart.* Biochem J, 1981: **200**(3): p. 701-703.

160. Taegtmeyer H, *On the inability of ketone bodies to serve as the only energy providing substrate for rat heart at physiological work load.* Basic Res Cardiol, 1983: **78**(4): p. 435-450.

161. Russell RR, 3rdTaegtmeyer H, *Changes in citric acid cycle flux and anaplerosis antedate the functional decline in isolated rat hearts utilizing acetoacetate.* J Clin Invest, 1991: **87**(2): p. 384-390.

162. Russell RR, 3rdTaegtmeyer H, *Coenzyme A sequestration in rat hearts oxidizing ketone bodies.* J Clin Invest, 1992: **89**(3): p. 968-973.

163. Sheu KFBlass JP, *The alpha-ketoglutarate dehydrogenase complex.* Ann N Y Acad Sci, 1999: **893**: p. 61-78.

164. Saavedra EMoreno-Sánchez R, *Flux Control Coefficient*, in *Encyclopedia of Systems Biology*, W. Dubitzky, O. Wolkenhauer, K.-H. ChoH. Yokota, Editors. 2013, Springer New York: New York, NY. p. 752-752.

165. Hilz H, Knappe J, Ringelmann ELynen F, *[Methylglutaconase, a new hydrase participating in the metabolism of various carboxylic acids].* Biochem Z, 1958: **329**(6): p. 476-489.

166. Tahiliani AGNeely JR, *A transport system for coenzyme A in isolated rat heart mitochondria.* J Biol Chem, 1987: **262**(24): p. 11607-11610.

167. Huelsmann WC, Siliprandi D, Ciman MSiliprandi N, *Effect of Carnitine on the Oxidation of Alpha-Oxoglutarate to Succinate in the Presence of Acetoacetate or Pyruvate.* Biochim Biophys Acta, 1964: **93**: p. 166-168.

168. Kimura N, Shimada N, Ishijima Y, Fukuda M, Takagi YIshikawa N, *Nucleoside Diphosphate Kinases in Mammalian Signal Transduction Systems: Recent Development and Perspective.* Journal of Bioenergetics and Biomembranes, 2003: **35**(1): p. 41-47.

169. Ohtsuki KYokoyama M, *Direct activation of guanine nucleotide binding proteins through a high-energy phosphate-transfer by nucleoside diphosphate-kinase.* Biochem Biophys Res Commun, 1987: **148**(1): p. 300-307.

170. Thomson M, Lim G, Hall PFKuyznierewicz I, *Overlay blot identification of GTP-binding proteins in mitochondria from human placenta.* Placenta, 1998: **19**(2-3): p. 209-215.

171. Klingenberg MPfaff E, *Metabolic control in mitochondria by adenine nucleotide translocation.* Biochem Soc Symp, 1968: **27**: p. 105-122.

172.   Besse A, Wu P, Bruni F, Donti T, Graham BH, Craigen WJ, McFarland R, Moretti P, Lalani S, Scott KL, Taylor RWBonnen PE, *The GABA transaminase, ABAT, is essential for mitochondrial nucleoside metabolism.* Cell Metab, 2015: **21**(3): p. 417-427.

9. BIBLIOGRAPHY OF THE CANDIDATE'S PUBLICATIONS

Publications related to the present thesis

1. *Catabolism of GABA, succinic semialdehyde or gamma-hydroxybutyrate through the GABA shunt impair mitochondrial substrate-level phosphorylation.*
    Ravasz D, **Kacso G**, Fodor V, Horvath K, Adam-Vizi V, Chinopoulos C.
    Neurochem Int. 2017 Mar 11. pii: S0197-0186(17)30045-1.

    Impact factor: 3.603

2. *Two transgenic mouse models for β-subunit components of succinate-CoA ligase yielding pleiotropic metabolic alterations.*
    Kacso G, Ravasz D, Doczi J, Németh B, Madgar O, Saada A, Ilin P, Miller C, Ostergaard E, Iordanov I, Adams D, Vargedo Z, Araki M, Araki K, Nakahara M, Ito H, Gál A, Molnár MJ, Nagy Z, Patocs A, Adam-Vizi V, Chinopoulos C.
    Biochem J. 2016 Oct 15;473(20):3463-3485.

    Impact factor: 3.797

3. *Abolition of mitochondrial* substrate-level phosphorylation *by itaconic acid produced by LPS-induced Irg1 expression in cells of murine macrophage lineage.*
    Németh B, Doczi J, Csete D, **Kacso G**, Ravasz D, Adams D, Kiss G, Nagy AM, Horvath G, Tretter L, Mócsai A, Csépányi-Kömi R, Iordanov I, Adam-Vizi V, Chinopoulos C. FASEB J. 2016 Jan;30(1):286-300. doi: 10.1096/fj.15-279398.

    Impact factor: 5.498

Publications not related to the present thesis

4. *The total and mitochondrial lipidome of Artemia franciscana encysted embryos.*
    Chen E, Kiebish MA, McDaniel J, Gao F, Narain NR, Sarangarajan R, **Kacso G**, Ravasz D, Seyfried TN, Adam-Vizi V, Chinopoulos C.
    Biochim Biophys Acta. 2016 Nov;1861(11):1727-1735.

    Impact factor: 5.547

5. *Reduction of 2-methoxy-1,4-naphtoquinone by mitochondrially-localized Nqo1 yielding NAD+ supports substrate-level phosphorylation during respiratory inhibition.*
    Ravasz D, **Kacso G**, Fodor V, Horvath K, Adam-Vizi V, Chinopoulos C.
    BBA – Bioenergetics for SI: EBEC 2018
    Biochim Biophys Acta. 2018 May 7. pii: S0005-2728(18)30105-1. doi: 10.1016/j.bbabio.2018.05.002. [Epub ahead of print]

    Impact factor: 4.280

10. ACKNOWLEDGEMENTS

First of all, I would like to express my sincere gratitude to my advisor **Dr. Christos Chinopoulos**. I would like to thank him for supporting me to be able to understand this particular subject and aligned my interest in biochemical field with his endless patience. His guidance during my research was priceless.

I would like to thank **Dr. László Tretter** and the Department of Medical Biochemistry of Semmelweis University for providing me research opportunities for 5 years as a member of the Scientific Student's Associations and later as a PhD student.

I am very thankful to my wonderful colleague **Dr. Dóra Ravasz**, without whom I could not have reached any success. All publications, awards, successes we reached during our TDK and PhD years are the result of our shared work. Thank you Dóri for the joyful moments and for the long discussions we had.

Special thanks to my family. Words cannot express how grateful I am to my parents, to my in-laws for supporting me during my PhD years.

Last but not least, I would like to express my appreciations to my beloved wife **Ágnes Kacsó-Hegedüs** who spent *sleepless* nights with me and was always my support in the moments when there was no one else to answer my queries.

11. SUMMARY

The succinate-CoA ligase (SUCL) is a heterodimer enzyme composed of Suclg1 α-subunit and a substrate-specific Sucla2 or Suclg2 β-subunit yielding ATP or GTP, respectively. In humans, the deficiency of this enzyme leads to severe pathology with or without methylmalonyl aciduria, occasionally also resulting in mitochondrial DNA depletion.

In our study we generated mice lacking either one *Sucla2* and/or *Suclg2* allele. *Sucla2* heterozygote mice exhibited tissue- and age-dependent decrease in Sucla2 expression associated with reductions in ATP-forming activity, but rebound increase in cardiac Suclg2 expression and GTP-forming activity.

Bioenergetic parameters such as substrate-level phosphorylation or oxygen consumption were not different between wild-type and *Sucla2* heterozygote mice, however, a submaximal pharmacological inhibition of succinyl-CoA ligase was concomitantly present.

mtDNA contents were moderately decreased, but blood carnitine esters were significantly higher. *Suclg2* heterozygote mice exhibited decreases in Suclg2 expression but no rebound increases in Sucla2 expression or changes in bioenergetic parameters. Surprisingly the deletion of one *Suclg2* allele in *Sucla2* heterozygote mice still led to a rebound, but the protracted increase in Suclg2 expression. However, in these double heterozygote mice there was no alterations in GTP-forming activity or substrate-level phosphorylation More noticeable changes were identified in mtDNA content and blood carnitine esters, as well as an increase in succinate dehydrogenase activity.

With our study we present a compensatory mechanism of one-allele deletion and conclude that a partial reduction in Sucla2 elicits rebound increases in Suclg2 expression, which is sufficiently dominant to overcome even a concomitant deletion of one *Suclg2* allele, pleiotropically affecting metabolic pathways associated with SUCL.

Our results, as well as the availability of our transgenic mouse colonies contribute the understanding of succinyl-CoA ligase deficiency.

12. ÖSSZEFOGLALÁS

A szukcinil-KoA ligáz egy heterodimer enzim, mely egy invariáns α- Suclg1, és egy ATP-termelő Sucla2 vagy egy GTP-termelő Suclg2 β alegységből épül fel. Az emberi szervezetben az enzim hiánya súlyos mitokondriális DNS-károsodással társuló megbetegedésekhez vezet, amelyek bizonyos esetekben metilmalonsav acidúriával párosulhatnak.

Kutatásunkhoz *Sucla2 +/–*, *Suclg2+/–* és *Sucla2+/–/Suclg2+/–* dupla heterozigóta egértörzseket hoztunk létre. A *Sucla2+/–* egerek szövet- és korspecifikus módon mutattak csökkenést a Sucla2 alegység expressziójában és az ehhez társuló ATP-termelő aktivitásban. A szívizomból származó mitokondriumokban azonban a GTP-termelő alegység mennyiségének és az ehhez tartozó GTP-termelő aktivitásnak a növekedése volt jellemző. A bioenergetikai paraméterekben -a szubsztrát-szintű foszforiláció, illetőleg az oxigénfogyasztás mutatóinak vizsgálatakor- nem tapasztaltunk eltérést a vad típusú egerekhez képest. Ugyanakkor a szukcinil-KoA ligáz szubmaximális farmakológiai gátlásakor már észlelhető különbség jelentkezett. A mitokondriális DNS tartalomban csak enyhe eltéréseket találtunk, míg a vér acil-karnitin szintjeiben már jelentősebb különbségek adódtak.

A *Suclg2* heterozigóta egerekben ugyan a Suclg2 alegység szintje alacsonyabb volt, mint a vad típusú egerek esetében, de nem tapasztaltuk a Sucla2 alegység upregulációját. A bioenergetikai paraméterek ebben az esetben sem mutattak eltérést. Meglepő módon, a kettős Sucla2+/–/Suclg2+/– heterozigóta egerekben továbbra is jelen volt a GTP-termelő alegység upregulációja, annak ellenére, hogy ez nem vezetett változáshoz sem a GTP-termelő aktivitásban, sem a szubsztrát-szintű foszforilációban. A mitokondriális DNS-tartalom, a vér acil-karnitin szintjei nagyobb mértékű eltérést mutattak, a szukcinát dehidrogenáz aktivitásában növekedés volt tapasztalható.

Kutatásunkkal egy kompenzációs mechanizmusra mutattunk példát. Következtetésként levonhatjuk, hogy a részleges Sucla2-szint csökkenés válaszul Suclg2 emelkedéshez vezet. Ez a Suclg2 expresszió emelkedés akár akkora mértékű is lehet, hogy a Sucla2+/–/Suclg2+/– dupla heterozigóta egerekben is képes kompenzálni az ATP-termelő alegység kiesését.

Eredményeink, illetve ezen transzgénikus egerek elérhetősége hozzájárulnak a szukcinil-KoA ligáz enzimhiány okozta betegségek alaposabb megismeréséhez.